CDNA CLONING AND CHARACTERIZATION OF ENZYMES THAT SYNTHESIZE
BILE ACIDS, VITAMIN D AND WAXES

APPROVED BY SUPERVISORY COMMITTEE

David Russell, Ph.D.

Helen Hobbs, M.D.

Elliott Ross, Ph.D.

James Waddle, Ph.D.

CDNA CLONING AND CHARACTERIZATION OF ENZYMES THAT SYNTHESIZE
BILE ACIDS, VITAMIN D AND WAXES

by

JEFFREY BINYAN CHENG

DISSERTATION / THESIS

Presented to the Faculty of the Graduate School of Biomedical Sciences

The University of Texas Southwestern Medical Center at Dallas

In Partial Fulfillment of the Requirements

For the Degree of

DOCTOR OF PHILOSOPHY

The University of Texas Southwestern Medical Center at Dallas

Dallas, Texas

June, 2006

cDNA CLONING AND CHARACTERIZATION OF ENZYMES THAT SYNTHESIZE
BILE ACIDS, VITAMIN D AND WAXES

Publication No. _____

Jeffrey Binyan Cheng, Ph.D.

The University of Texas Southwestern Medical Center at Dallas, 2006

Supervising Professor: David Russell, Ph.D.

Countless enzymes are required for the synthesis of the diverse array of lipids found in nature. The identification and characterization of five different lipid metabolizing enzymes are reported here. The 3β-hydroxy-Δ^5-C_{27}-steroid oxidoreductase (C_{27} 3β-HSD) enzyme catalyzes a step in bile acid synthesis. Subjects with mutations in the encoding gene fail to synthesize bile acids and develop liver disease. Fifteen patients were screened and twelve different mutations were identified in the C_{27} 3β-HSD gene.

Vitamin D is required for normal bone metabolism and maintenance of serum calcium levels. The conversion of vitamin D into an active ligand requires 25-hydroxylation. I report here the identification by expression cloning of a cytochrome P450 (CYP2R1) with

vitamin D 25-hydroxylase activity. A patient with low circulating levels of 25-hydroxyvitamin D and classic symptoms of vitamin D deficiency was identified. Molecular analysis of this individual revealed homozygosity for a transition mutation in the CYP2R1 gene causing the substitution of a proline for a leucine in the protein and eliminating vitamin D 25-hydroxylase enzyme activity. These data identify CYP2R1 as a biologically relevant vitamin D 25-hydroxylase and reveal the molecular basis of a human genetic disease, selective 25-hydroxyvitamin D deficiency.

The reduction of fatty acids to fatty alcohols, by a fatty acyl-CoA reductase enzyme, is required for the synthesis of wax monoesters and ether lipids. Using a bioinformatics approach, the first two mammalian fatty acyl-CoA reductase genes (FAR1 and FAR2) were identified. The two mouse FAR enzymes, which share 57% sequence identity at the amino acid level, have differing substrate specificities and tissue distributions implying unique physiological roles for each.

Wax monoesters are synthesized by the esterification of fatty alcohols and fatty acids. A mammalian enzyme that catalyzes this reaction has not been isolated. Here, I report the identification by expression cloning of a wax synthase gene. Co-expression of cDNAs specifying FAR1 and wax synthase led to the synthesis of wax monoesters. The data suggests that wax monoester synthesis in mammals involves a two step biosynthetic pathway catalyzed by fatty acyl-CoA reductase and wax synthase enzymes.

TABLE OF CONTENTS

PUBLICATIONS

Cheng, J. B., Jacquemin, E., Gerhard, M., Nazer, H., Cresteil, D., Heubi, J.E., Setchell, K.D., and Russell, D. W. (2004). Molecular genetics of 3beta-hydroxy-Delta5-C_{27}-steroid oxidoreductase deficiency in 16 patients with loss of bile acid synthesis and liver disease. J Clin Endocrinol Metab *88*, 1,833-1,841.

Cheng, J. B., Motola, D. L., Mangelsdorf, D. J., and Russell, D. W. (2003). De-orphanization of cytochrome P450 2R1, a microsomal vitamin D 25-hydroxylase. J Biol Chem *278*, 38,084-38,093.

Cheng, J. B., Levine, M.A., Bell, N.H., Mangelsdorf, D.J., and Russell, D. W. (2004). Genetic evidence that the human CYP2R1 enzyme is a key vitamin D 25-hydroxylase. Proc Natl Acad Sci USA *101*, 7,711-7,715.

Cheng, J. B. and Russell, D. W. (2004). Mammalian wax biosynthesis: I. Identification of two fatty acyl-Coenzyme A reductases with different substrate specificities and tissue distributions. J Biol Chem *279*, 37,789-37,797.

Cheng, J. B. and Russell, D. W. (2004). Mammalian wax biosynthesis: II. Expression cloning of wax synthase cDNAs encoding a member of the acyltransferase enzyme family. J Biol Chem *279*, 37,798-37,807.

LIST OF FIGURES AND TABLES

Chapter 6

LIST OF ABBREVIATIONS

25-hydroxycholesterol	[^{3}H]cholest-5-ene-3ß,25-diol
7-dehydrocholesterol	5,7,-cholestadien-3β-ol
ACAT	acyl-CoA:cholesterol acyltransferase
ACC	acetyl-CoA carboxylase
Adx	adrenodoxin
BSA	bovine serum albumin
C_{27} 3ß-HSD	3ß-hydroxy-Δ^5-C_{27}-steroid oxidoreductase
CHAPS	3-[(3-cholamidopropyl)dimethylammonio]-1-propanesulfonic acid
CMV	cytomegalovirus
CoA	acyl-coenzyme A
C_T	threshold value
CYP	cytochrome P450
CYP39A1	24-hydroxycholesterol 7α-hydroxylase
CYP46A1	cholesterol 24-hydroxylase
CYP7A1	cholesterol 7α hydroxylase
CYP7B1	oxysterol 7α-hydroxylase
DGAT	acyl-CoA:diacylglycerol acyltransferase
DHAP	dihydroxyacetone phosphate
DHAPAT	dihydroxyacetone phosphate acyltransferase

DMEM	Dulbecco's modified Eagle's medium
E. coli	*Escherichia coli*
FAR	fatty acyl-coenzyme A reductase
FAS	fatty acid synthase
FXR	farnesoid X receptor
GAL4	galactose 4
h	human
HEK 293	human embryonic kidney 293
His$_6$	hexahistidine
kb	kilobases
LUC	luciferase
LXRα	liver X receptor α
m	mouse
mAdx	mouse adrenodoxin
MGAT	acyl-CoA:monoacylglycerol acyltransferase
OMIM	Online Mendelian Inheritance of Man.
PBS	phosphate-buffered saline
PCR	polymerase chain reaction
PTH	parathyroid hormone
RXR	retinoid x receptor
SEM	standard error of measurement
TK	thymidine kinase

VDR	vitamin D receptor
VDRE	vitamin D response element
Vitamin D_2	$(3\beta,5Z,7E,22E)$-9,10-secoergosta-5,7,10(19),22-tetraen-3-ol
Vitamin D_3	$(3\beta,5Z,7E)$-9,10-secocholesta-5,7,10(19)-trien-3-ol
WS	wax synthase

CHAPTER ONE
Introduction

Lipids are generally defined as nonpolar and hydrophobic molecules that are soluble in organic solvents. Lipids are involved in a wide range of physiological processes including formation of membranes (e.g. glycolipids, phospholipids, and cholesterol), energy storage (e.g. triacylglycerols), solubilization of other lipids (e.g. bile acids), and signaling (e.g. steroids and vitamin D). A diverse set of chemical structures is needed to carry out the varied functions of lipids. Fatty acids are the simplest lipids and consist of a long chain hydrocarbon with a terminal carboxyl group. Other lipids incorporate fatty acids into larger and more complex molecules. For example, triacylglycerols consist of three fatty acids esterified to a glycerol backbone and glycolipids contain a fatty acid, a sugar residue, and a sphingosine backbone. Lipids such as cholesterol, bile acids, and steroids are not derived from fatty acids and share a basic structure composed of four fused carbon rings. Given this diversity of chemical structures and physiological roles for lipids, a myriad of enzymes are responsible for their synthesis. This thesis focuses upon the cDNA cloning and characterization of five different lipid synthesizing enzymes.

The first of these enzymes is 3β-hydroxy-Δ5-C_{27}-steroid oxidoreductase (C_{27} 3β-HSD), a key enzyme in the bile acid biosynthetic pathway. Bile acids are 24 carbon lipids that are synthesized from cholesterol. Their structure is comprised of four fused carbon rings (i.e. a cyclopentanoperhydrophenanthrene steroid nucleus), multiple hydroxyl groups, and a 5 carbon side chain with a terminal carboxyl group. The synthesis of bile acids has several key physiological functions. The body's only catabolic pathway for cholesterol is through

conversion to bile acids. Regulation of cholesterol levels is of great importance as persistently elevated levels of cholesterol can lead to atherosclerosis and cardiovascular disease. Cholesterol cannot be broken down and its hydrophobic nature requires conversion into a more water-soluble form, i.e. the bile acids, before excretion into bile and the small intestine. Cholesterol is also converted into steroids, but these reactions do not consume a significant amount of cholesterol. A second role for bile acids is in the absorption of fats and fat-soluble vitamins in the small intestine. These hydrophobic lipids tend to aggregate in the aqueous environment of the small intestine. Bile acids act as detergents because of their amphipathic nature and solubilize intestinal lipids in mixed micelles so that they can be absorbed by enterocytes. A third role for bile acids is in gene regulation. Bile acids regulate transcription by functioning as ligands for nuclear hormone receptors.

Members of the nuclear hormone receptor superfamily are ligand-dependent transcription factors which have roles in mediating responses to steroids and in lipid homeostasis. There are at least 48 human nuclear hormone receptors, although the ligands for many are still unknown (Chawla et al., 2001). Nuclear hormone receptors have multiple domains which function in ligand binding, receptor dimerization, DNA-binding, and transcription activation. The receptor superfamily can be divided into two subgroups based on their mechanism of action: the classical steroid and the thyroid hormone/nonsteroid receptors. In the unbound state, the steroid (e.g. androgen, mineralocorticoid, and glucocorticoid) receptors typically reside in the cytoplasm in an inactive state and are bound by heat shock proteins. Upon ligand binding, the receptor conformation changes leading to the release of heat shock proteins, receptor homodimerization, translocation to the nucleus,

and binding to DNA response elements in the enhancer region of a target gene. The activated nuclear hormone receptor can now recruit co-activator proteins to increase transcriptional expression of the target gene (McKenna et al., 1999). In contrast, the thyroid hormone/nonsteroid receptors are already in the nucleus bound to their DNA response elements without bound ligand. The free receptors typically repress their target genes and become activated when ligand enters the nucleus and binds to the receptor. Also unique to this subgroup is that the receptors form obligate heterodimers with the retinoid x receptor (RXR) instead of homodimers (McKenna et al., 1999). Members of this subgroup include the liver X receptor α (LXRα), the farnesoid X receptor (FXR), and the vitamin D receptor (VDR) (Chawla et al., 2001; Jones et al., 1998).

There are at least 17 enzymes involved in bile acid synthesis, two of which are regulated by FXR and/or LXRα (Russell, 2003). These bile acid synthetic enzymes are located in the liver, with a few exceptions. Cholesterol is converted into bile acids via three main categories of reactions: 1) hydroxylation of the steroid nucleus, 2) modification of the steroid nucleus, and 3) oxidation and cleavage of the hydrocarbon side chain. Another layer of complexity to bile acid synthesis is that there are three pathways that initiate synthesis of bile acids. The classic pathway begins with the hydroxylation of cholesterol at the 7α carbon position by the cholesterol 7α hydroxylase enzyme (CYP7A1) (figure 1) (Jelinek et al., 1990). In mice, approximately 80% of bile acid synthesis is initiated by this pathway (Schwarz et al., 1996). The CYP7A1 enzymatic reaction is the key regulated step in bile acid synthesis and is controlled by feed-forward and negative feedback mechanisms. When cholesterol substrate levels are high, hydroxylated cholesterols (oxysterols) build up and

activate LXRα leading to transcriptional upregulation of the CYP7A1 gene (Lehmann et al., 1997). Conversely, when bile acid product levels are high, activation of FXR leads to transcriptional downregulation of the CYP7A1 gene (Lu et al., 2000).

The CYP7A1 enzyme is a member of the cytochrome P450 (CYP) superfamily. These heme containing enzymes are named for their unique absorption band at 450 nm when bound to carbon monoxide in their reduced form. CYP enzymes are found in a wide variety of organisms from fungi and bacteria to humans. Different organisms have differing numbers of CYP enzymes, with 57 in humans, 84 in rats, and 87 in mice (Gibbs et al., 2004). In mice and humans, six CYP enzymes are known to be involved in bile acid biosynthesis. CYP enzymes also play a role in the metabolism of steroids, drugs, foreign chemicals, vitamin D, and arachidonic acids; however, the exact role and substrates for many of the CYP enzymes is still unknown. Although these enzymes are capable of other chemical reactions, their principal reaction is substrate hydroxylation. Eukaryotic CYP enzymes utilize molecular oxygen and two electrons from NADPH to carry out the hydroxylation reaction (Omura, 1999). CYP enzymes are described as monooxygenases because one of the two molecular oxygen atoms is added to the substrate as a hydroxyl group while the other atom is incorporated into water. In eukaryotes, CYP enzymes are found either in the membrane of the endoplasmic reticulum or in the inner membrane of mitochondria. CYP enzymes are not able to directly utilize the electrons from NADPH, instead they are transferred through electron donor proteins. Mitochondrial CYP enzymes use adrenodoxin, a flavoprotein, and adrenodoxin reductase, an iron-sulfur protein (Ziegler et al., 1999), to

transfer electrons whereas endoplasmic reticulum CYP enzymes use NADPH-cytochrome P450 reductase, a flavoprotein (Gutierrez et al., 2003).

In addition to the classic pathway of bile acid synthesis, there are two alternative pathways which also utilize cytochrome P450 enzymes. In these pathways, cholesterol is first hydroxylated at the 24, 25, or 27 carbon positions of the hydrocarbon side chain by the cholesterol 24-hydroxylase (CYP46A1) (Lund et al., 1999), cholesterol 25-hydroxylase (Lund et al., 1998), or the sterol 27-hydroxylase (CYP27A1) enzymes (Andersson et al., 1989), respectively (figure 1). The tissue distributions of CYP46A1 and CYP27A1 are notable because of their extra-hepatic expression. CYP46A1 mRNA is most highly expressed in the brain (Lund et al., 1999), whereas CYP27A1 has a relatively ubiquitous expression pattern with highest mRNA expression levels in the liver (Andersson et al., 1989). The CYP27A1 enzyme may also play a role in vitamin D metabolism and will be discussed in more detail (see below). After the initial formation of the 25- and 27-hydroxycholesterol oxysterols, the oxysterol 7α-hydroxylase enzyme (CYP7B1) adds a hydroxyl group at the 7α carbon position (Schwarz et al., 1997). Approximately 20% of total mouse bile acid synthesis is initiated via this pathway. The other oxysterol, 24-hydroxycholesterol, requires another distinct enzyme for hydroxylation at the 7α carbon position, 24-hydroxycholesterol 7α-hydroxylase (CYP39A1) (Li-Hawkins et al., 2000). The 24-hydroxycholesterol initiated pathway does not play much of a role in bile acid biosynthesis and probably leads to formation of approximately 1% of total bile acids (Russell, 2003).

The next step in the pathway is a point of convergence for the classic pathway and the two alternative pathways and leads to the initial modification of the steroid nucleus. The C_{27}

3β-HSD enzyme catalyzes two reactions, the isomerization of the $\Delta 5$ bond to a $\Delta 4$ bond and the oxidation of the 3β-hydroxyl group to an oxo group (figure 1). The cDNA encoding for this enzyme was isolated by an expression cloning approach and the enzyme was determined to specifically utilize 7α-hydroxylated sterol substrates (Schwarz et al., 2000). Enzymes that catalyze a similar reaction in the C_{21} steroid pathway are known; however, these enzymes do not utilize bile acid intermediates. The molecular analysis of 15 cholestatic patients with suspected C27 3β-HSD enzyme deficiency is described in chapter 2. 12 different mutations in the encoding *HSD3B7* gene were identified and 10 of these mutations were studied in detail and shown to cause the complete loss of C_{27} 3β-HSD enzyme activity. We concluded that a diverse spectrum of mutations in the *HSD3B7* gene underlies this rare form of neonatal cholestasis.

Cholestasis is a decrease or stoppage in bile flow leading to a buildup of bile in hepatic cells and an increase in the body of metabolites (e.g. cholesterol and bilirubin) that would normally be excreted in the bile. Cholestasis can be caused by infectious diseases, drugs, bile duct obstruction, and metabolic diseases (e.g. a defect in bile acid synthesis). Defects in the C_{27} 3β-HSD gene, as well as in other bile acid synthetic pathway genes, lead to a progressive neonatal intrahepatic cholestasis (Setchell and O'Connell, 1994). In patients with mutations in the C_{27} 3β-HSD gene, there are two main pathological problems (Clayton et al., 1987). The first problem is progressive injury to the liver due to a buildup of toxic bile acid intermediates prior to the defective enzymatic step, exacerbated by reduced bile acid-dependent bile flow. Patients lack normal bile acids and build up unusual toxic C_{24} bile acids which still maintain the $\Delta 5$ double bond and 3β-hydyroxyl group of the cholesterol

substrate.   Secondly, fats and fat-soluble vitamins are poorly absorbed because of a deficiency of bile acids in the small intestine. In these patients, the reduced bile flow and liver damage leads to giant cell hepatitis, jaundice, hepatomegaly, elevated serum bilirubin levels, and elevated serum liver enzymes (alanine aminotransferase and aspartate aminotransferase). The lack of bile acids in the small intestine leads to steatorrhea (fat in the stools), decreased serum levels of fat-soluble vitamins (A, D, and E), and increased clotting times (indicative of vitamin K deficiency). These patients typically present very early in life, between 3 months and 14 years of age. If left untreated, they will die from cirrhosis and liver failure. Treatment with primary bile acids is quite effective and leads to normalization of liver function and resolution of the cholestasis. Therapy presumably works by increasing bile flow and repressing bile acid synthesis so that there is decreased buildup of toxic intermediates. Additionally, the increase in bile acids in the small intestine leads to increased solubilization and absorption of fats and fat-soluble vitamins.

After the C_{27} 3β-HSD enzymatic reaction, additional modifications to the steroid nucleus of the bile acid intermediates include saturation of the Δ4 double bond, reduction of the 3-oxo group to a 3α-hydroxyl group, and an optional addition of a 12α-hydroxyl group by the FXR regulated CYP8B1 enzyme. If the bile acid intermediate is 12-hydroxylated, its eventual fate is to become cholic acid. After the steroid nucleus modification of the intermediates, the hydrocarbon side chain is oxidized to a carboxylic acid and the three terminal carbons are cleaved to form the primary bile acids, cholic acid and chenodeoxycholic acid. The carboxylic acid of the primary bile acids is then conjugated via an amide linkage to the amino acids, taurine or glycine. These bile salts are then secreted in

the bile from the liver to the gall bladder for storage until their release into the small intestine.

The second lipid synthesizing enzyme that I focused upon was cytochrome P450 2R1 (CYP2R1), a vitamin D 25-hydroxylase. Vitamins are essential organic compounds that are required in trace amounts for normal physiological function. Some of vitamin's diverse functions include serving as hormonal signaling molecules, coenzymes, and electron donors and acceptors. Typically, vitamins cannot be synthesized by the body and are thus required in the diet. Vitamins are classified as being either water-soluble or fat-soluble. Unlike the water-soluble vitamins, the fat-soluble vitamins (A, D, E, and K) are classified as lipids because they are mostly composed of isoprenes. Isoprenes are 5 carbon units which are used in the synthesis of certain lipids, e.g. squalene and cholesterol. Vitamin D is different from the other fat-soluble vitamins because it is directly derived from cholesterol, instead of its isoprene precursors.

The structure of vitamin D is similar to that of the steroids and bile acids because of its cyclopentanoperhydrophenanthrene steroid nucleus; however, one of the four carbon rings has been broken, so it is termed a secosteroid. There are two functionally equivalent forms of vitamin D, vitamin D_3 (cholecalciferol) and vitamin D_2 (ergocalciferol). Vitamin D_2 differs from vitamin D_3 because of the presence of an additional double bond between carbons 22 and 23 and an additional methyl group at the 24 carbon position (figure 2). Vitamin D_2 is synthesized from ergosterol in lower organisms, such as plants, fungi, and molds. Although not very prevalent in natural foods, vitamin D_2 has great dietary significance because of its use in supplementing certain foods, such as milk and grain

products. Vitamin D_3, the form made in animals, is found in high amounts in certain fatty fishes. As discussed earlier, bile acids are required for the intestinal absorption of this fat-soluble vitamin. However, vitamin D is unique among the fat-soluble vitamins because it is not absolutely required in the diet.

In the body, physiologically significant amounts of vitamin D_3 are made when the skin is exposed to sunlight. The cholesterol precursor 7-dehydrocholesterol is prevalent in skin and upon exposure to UV light of sufficient intensity, the B ring of its steroid nucleus is broken between carbons 9 and 10 to form previtamin D. Previtamin D then undergoes spontaneous isomerization to vitamin D_3 (figure 3). Insufficient endogenous vitamin D synthesis is not an infrequent problem. In the winter, the intensity of sunlight in the more northerly latitudes of the United States is not sufficient for vitamin D synthesis. African Americans also have special considerations because their darkly pigmented skin requires longer exposure to sunlight before vitamin D can be made. The elderly also have decreased ability to synthesize vitamin D in the skin and consequently, their vitamin D dietary recommendations are increased (Holick, 1999). Endogenously synthesized vitamin D_3 ends up in the circulation along with vitamin D_3 and D_2 from dietary sources.

Vitamin D actually has very little biological activity as two hydroxylation reactions must occur to form the fully active form of vitamin D, 1, 25-dihydroxyvitamin D (Jones et al., 1998). Interestingly, all the known vitamin D modification enzymes are cytochrome P450 enzymes. The first hydroxylation reaction takes place at carbon 25 of vitamin D and occurs in the liver (figure 4). Initial biochemical characterization of this enzymatic activity gave conflicting data about the subcellular localization of the vitamin D 25-hydroxylase.

Eventually, hepatic extracts were shown to possess 25-hydroxylase activity in both mitochondrial and microsomal fractions (Bhattacharyya and DeLuca, 1974; Bjorkhem and Holmberg, 1978). The mitochondrial enzyme was determined to be CYP27A1, the same sterol 27-hydroxylase enzyme that catalyzes 27-hydroxylation of bile acid intermediates (Guo et al., 1993). The existence of a second, microsomal enzyme was further confirmed through additional biochemical and animal studies. The CYP27A1 enzyme was shown to only 25-hydroxylate vitamin D_3 and not D_2, indicating the existence of another enzyme which can 25-hydroxylate vitamin D_2 (Holmberg et al., 1986). Also, mice with a disrupted *Cyp27a1* gene and humans who have a mutation in this gene have reduced levels of bile acid synthesis but no changes in 25-hydroxyvitamin D levels (Bjorkhem et al., 2001; Rosen et al., 1998). Either the microsomal 25-hydroxylase compensates for the missing mitochondrial enzyme or the mitochondrial enzyme is of little importance in vitamin D metabolism.

The identity of the microsomal 25-hydroxylase enzyme has been unclear. Several enzymes from different species, CYP2C11 (Andersson et al., 1983), CYP2D25 (Hosseinpour and Wikvall, 2000), CYP3A4 (Gupta et al., 2004), and CYP2J3 (Yamasaki et al., 2004a), have been demonstrated to have in vitro 25-hydroxylase activity but there is substantial doubt as to whether any of these enzymes actually play a role in human vitamin D metabolism. The rat CYP2C11 enzyme is only expressed in males (Andersson and Jornvall, 1986). There is no evidence of sexual dimorphism in vitamin D metabolism. CYP2D6, the closest human homologue to porcine CYP2D25, does not have 25-hydroxylase activity. Under our assay conditions, human CYP3A4 has negligible 25-hydroxylase activity (Cheng et al., 2003). It is unlikely that human CYP2J2, the closest human homologue to rat CYP2J3, has 25-

hydroxylase activity because there is only 55% amino acid sequence identity between the two enzymes. As it appeared that the bona fide microsomal enzyme had not been identified, an expression cloning approach was used to identify CYP2R1, an evolutionarily conserved microsomal vitamin D 25-hydroxylase. The identification and characterization of CYP2R1 is described in chapter 3. Ligand activation assays, thin layer chromatography, and radioimmunoassays showed that expression of CYP2R1 in cultured mammalian cells led to the 25-hydroxylation of vitamin D_2 or D_3. Real time PCR experiments showed that CYP2R1 mRNA is abundant in the liver where it is presumed to catalyze the 25-hydroxylation reaction. From this data, we conclude that CYP2R1 is a strong candidate for the microsomal vitamin D 25-hydroxylase.

The second vitamin D activation step occurs in the kidney where 25-hydroxyvitamin D is hydroxylated at the 1α-position (figure 4). The 25-hydoxyvitamin D 1α-hydroxylase was determined to be the mitochdondrial CYP27B1 enzyme, which shares significant homology with the CYP27A1 mitochondrial 25-hydroxylase enzyme (Takeyama et al., 1997). 1,25-dihydroxyvitamin D acts as a hormone and serves as a high-affinity ligand for the vitamin D receptor (Jones et al., 1998). The activated vitamin D receptor then leads to transcriptional regulation of its target genes.

In order for the body to maintain appropriate levels of 1,25-dihydroxyvitamin D, there is an inactivation pathway in addition to the vitamin D activation pathway. The mitochondrial CYP24A1 enzyme inactivates vitamin D metabolites in the kidney by initially adding a hydroxyl group at the 24 carbon position of 1,25-dihydroxyvitamin D and 25-hydroxyvitamin D (figure 4). Subsequently, the multicatalytic CYP24A1 enzyme catalyzes a

further oxidation at the 24 carbon position to form a keto group, a hydroxylation at the 23 carbon, and a cleavage between the 23 and 24 carbons to form a side chain that ends in an alcohol group (Beckman et al., 1996). It is unclear if CYP24A1 or another enzyme further oxidizes the alcohol group to a carboxylic acid to form calcitroic acid, the excretable fully catabolized end-product of vitamin D.

The main physiological function of vitamin D is the maintenance of normal plasma levels of calcium and phosphate. Vitamin D may also have possible roles in immunoregulation, cellular differentiation, and anti-proliferation. Vitamin D, through the vitamin D receptor, leads to an increase in the intestinal and renal absorption of calcium and phosphate and can stimulate mobilization of calcium from the bone. Bone growth and mineralization is also dependent upon vitamin D-dependent maintenance of normal calcium and phosphorus levels. Parathyroid hormone (PTH) is another calcium regulatory molecule which is released in response to and functions to counter low plasma calcium levels. One action of PTH is to co-regulate, with 1,25 dihydroxyvitamin D, the expression of the CYP27B1 and CYP24A1 genes. When plasma calcium levels are low, increased levels of PTH lead to upregulation of CYP27B1 expression and a decrease in CYP24A1 expression (Omdahl et al., 2002). The consequent increase in 1,25 dihydroxyvitamin D helps to correct the low calcium levels. 1,25 dihydroxyvitamin D regulates its own levels via negative feedback transcriptional repression of CYP27B1 and feed-forward transcriptional regulation of CYP24A1 (Omdahl et al., 2002).

Vitamin D deficiency can occur due to inadequate dietary intake, insufficient sunlight exposure, or hereditary defects in vitamin D metabolism. Vitamin D deficient patients will

present with muscle weakness, bone pain and deformity, and fractures.   In adults, vitamin D deficiency will lead to osteomalacia which is characterized by inadequate mineralization of the bone matrix (Rosen, 1999). In addition to osteomalacia, children also have rickets where bone growth is abnormal because there is disordered cartilage formation and incomplete mineralization of the cartilage growth plates leading to the characteristic bowing of the lower extremities (Garabedian and Ben-Mekhbi, 1999).

Hereditary causes for vitamin D deficiency include mutations in the vitamin D 1α-hydroxylase, the vitamin D receptor, or the vitamin D 25-hydroxylase. Patients with a mutation in the CYP27B1 1α-hydroxylase gene have vitamin D dependent rickets type I. These patients have normal or elevated levels of vitamin D and 25-hydroxyvitamin D but low or undetectable levels of 1,25 dihydroxyvitamin D.   Patients are treated with 1α-hydroxyvitamin D_3 which can serve as a substrate for the 25-hydroxylase and eliminates the need for 1α-hydroxylase activity or alternatively, can be treated with 1,25 dihydroxyvitamin D (Demay, 1999).

Patients with a mutation in the vitamin D receptor have vitamin D-dependent rickets type II. There is a lack of vitamin D receptor mediated action including feedback repression of the 1α-hydroxylase and upregulation of CYP24A1 expression, leading to elevated levels of 1,25 dihydroxyvitamin D. Depending on the severity of receptor dysfunction, some patients can be treated with high levels of vitamin D, 25-hydroxyvitamin D, or 1,25-dihydroxyvitamin D. Other patients must be given infusions of calcium (Demay, 1999).

The molecular analysis of a patient with low circulating levels of 25-hydroxyvitamin D and classic symptoms of vitamin D deficiency is described in chapter 4.   Genomic

sequencing revealed a transition mutation in exon 2 of the CYP2R1 vitamin D 25-hydroxylase gene. The inherited mutation caused the substitution of a proline for an evolutionarily conserved leucine at amino acid 99 in the CYP2R1 protein and eliminated vitamin D 25-hydroxylase enzyme activity. These data identify CYP2R1 as a biologically relevant vitamin D 25-hydroxylase and reveal the molecular basis of a new human genetic disease, 25-hydroxyvitamin D deficiency. The low levels of 25-hydroxyvitamin D in the patient were effectively treated with pharmacological doses of 25-hydroxyvitamin D.

The last three lipid synthesizing enzymes that I characterized utilize activated fatty acids as substrates. Before fatty acids are used in biosynthetic reactions, they are typically converted into bioactive fatty acyl-coenzyme A (CoA). The ATP-driven conjugation of fatty acids with coenzyme A through a high energy thioester bond is catalyzed by an acetyl-CoA synthetase enzyme (Luong et al., 2000). Coenzyme A, which functions as a carrier of acyl and acetyl groups, is derived from the water-soluble vitamin pantothenic acid and contains a terminal sulfhydryl group which is used to form the thioester bond.

Although the major source for fatty acids in the body is through the diet, the body also synthesizes a significant amount through de novo synthesis. In eukaryotes, two cytosolic multifunctional enzymes are able to convert eight molecules of acetyl-CoA into the saturated fatty acid, palmitic acid. Like the fatty acids, its two carbon acetate precursor also needs to be in the activated coenzyme A conjugated form. The first enzyme, acetyl-CoA carboxylase (ACC), catalyzes the rate limiting step of fatty acid synthesis which is the carboxylation of acetyl-CoA to form three carbon malonyl-CoA. The second enzyme, fatty acid synthase (FAS), transfers a 2 carbon unit from malonyl-CoA to acetyl-CoA to form a

four carbon acyl chain intermediate. FAS then sequentially repeats this reaction six more times with 2 carbon units from malonyl-CoA being transferred to the growing FAS enzyme-linked acyl chain intermediate until the 16 carbon fatty acid, palmitic acid, is formed (Wakil et al., 1983).

The palmitic acid product specificity of the fatty acid synthase enzyme is determined by its thioesterase domain (Wakil et al., 1983). It preferentially cleaves and releases the growing enzyme-linked acyl chain when it reaches 16 carbons in length. In the body, there are substantial amounts of fatty acids that have different carbon chain lengths and also contain one or more double bonds. In order for the fatty acid synthase to produce fatty acids of less than 16 carbons, a soluble thioesterase enzyme is used. This discrete enzyme gains access to and preferentially cleaves the growing FAS enzyme-linked acyl chain when it contains between 8 to14 carbons (Tai et al., 1993). Palmitic acid can be elongated into fatty acids of up to 26 carbons in length by a number of microsomal fatty acyl elongase and reductase enzymes (Moon and Horton, 2003; Moon et al., 2001; Tvrdik et al., 2000). These enzymes work together to catalyze a fatty acid synthase-like three step reaction which sequentially elongates palmitoyl-CoA by the addition of 2 carbon units from malonyl-CoA.

The shorthand description of fatty acids numbers the carbons beginning with the carboxyl group carbon as number one. An example of the shorthand nomenclature for fatty acids is given for the most prevalent unsaturated fatty acid, oleic acid (18:1 Δ9). 18 refers to the number of carbons, 1 refers to the number of double bonds, and Δ9 refers to the position of the double bond between carbons 9 and 10. At least six mammalian enzymes have the ability to desaturate fatty acids through the formation of a double bond in the cis

configuration (Cho et al., 1999a; Cho et al., 1999b; Miyazaki et al., 2003; Miyazaki and Ntambi, 2003). These enzymes are located in the endoplasmic reticulum membrane and require molecular oxygen and NADH to desaturate fatty acyl-CoAs. In animals, double bonds are added to fatty acids specifically at the $\Delta 5$, $\Delta 6$, and $\Delta 9$ positions. Almost all animal monounsaturated fatty acids have a double bond at the $\Delta 9$ position. This $\Delta 9$ desaturation reaction is catalyzed by one of the four stearoyl-CoA desaturase (SCD) isozymes (Miyazaki et al., 2003; Miyazaki and Ntambi, 2003) .

Animals can also make polyunsaturated fatty acids with multiple double bonds. These fatty acids are utilized as precursors for prostaglandins and also make up a significant proportion of the fatty acid content in phospholipids. The additional double bond is typically added three carbons away from the existing double bond, with an intervening methylene group. Double bonds cannot be added to fatty acids beyond the $\Delta 9$ position in animals because of a lack of $\Delta 12$ and $\Delta 15$ desaturase activity. The fatty acids linoleic acid (18:2 $\Delta 9,12$) and linolenic acid (18:3 $\Delta 9,12,15$) are thus considered essential and are required from dietary plant sources. A variety of physiologically important polyunsaturated fatty acids are derived from further desaturation and elongation of linoleic acid and linolenic acid (Wallis et al., 2002). For example, arachidonic acid (20:4 $\Delta 5,8,11,14$) is synthesized from linoleic acid by desaturation at the $\Delta 6$ position, elongation by two carbons, and desaturation at the $\Delta 5$ position which is now 3 carbons away from the former $\Delta 6$ position. Arachidonic acid is the precursor of signaling molecules, such as the prostaglandins, leukotrienes, and thromboxanes.

Fatty acids have many other fates in the body other than conversion into signaling molecules. Fatty acids can be oxidized and broken down to provide a source of energy. Three fatty acids can be linked to glycerol through ester bonds to form triacylglycerol, a major energy storage molecule in animals. Fatty acids can also be incorporated into phospholipids and glycolipids through ester linkages to a glycerol based molecule or amide linkages to a sphingosine based molecule. These molecules are major components of cell membranes. Fatty acids can also be converted into fatty alcohols by the reduction of the terminal carboxyl group.

The third and fourth lipid synthesizing enzymes that I worked upon were the two fatty acyl-CoA reductase isozymes (FAR1 and FAR2). These enzymes convert activated fatty acids (fatty acyl-CoAs) into fatty alcohols using the reducing equivalents of NADPH (figure 5). The identification of cDNAs encoding for two mammalian FAR isozymes through a bioinformatics approach is described in chapter 5. FAR enzymes had been identified in the jojoba plant and the silkworm moth but not in mammals. The fatty acid substrate specificity of the two isozymes differed as FAR1 preferred saturated, monounsaturated, and polyunsaturated fatty acids ranging in size from 16 to 20 carbons as substrates whereas FAR2 preferred saturated fatty acids with 16 or 18 carbons. Confocal light microscopy indicated that FAR1 and FAR2 were localized in the peroxisome. The FAR1 mRNA was detected in many mouse tissues with the highest levels found in the preputial gland, a modified sebaceous gland. The FAR2 mRNA was more restricted in distribution and most abundant in the eyelid where the meibomian glands, another type of modified sebaceous glands, are located. Both FAR mRNAs were present in the brain, a tissue rich in ether lipids.

One of the two main metabolic fates for fatty alcohols is incorporation into ether lipids, a unique type of phospholipid. The typical glycerol-based phospholipid is composed of a glycerol backbone with two fatty acids linked through ester bonds and an alcohol group (e.g. serine or ethanolamine) linked through a phosphodiester linkage (figure 6A). Ether lipids have an ether-linked alkyl group at the glycerol carbon 1 position instead of the ester-linked fatty acyl group of glycerophopholipids (figure 6B). Most ether lipids are actually plasmalogens, a subset which has a vinyl ether-linked alkyl group at the glycerol C1 position so that there is a double bond adjacent to the oxygen atom (figure 6C).

The ether lipid biosynthetic pathway consists of two initial reactions in the peroxisomes followed by a series of reactions in the endoplasmic reticulum membrane (Nagan and Zoeller, 2001). The first peroxisomal reaction, catalyzed by dihydroxyacetone phosphate acyltransferase (DHAPAT), is the formation of an ester bond between dihydroxyacetone phosphate (DHAP) and an acyl group derived from fatty acyl-CoA (Thai et al., 1997). The second peroxisomal reaction, catalyzed by alkyl-dihydroxyacetone phosphate synthase, is the formation of the ether bond through replacement of the acyl group with an alkyl group derived from a fatty alcohol (de Vet et al., 1997). The ether lipid intermediates are transported to the endoplasmic reticulum membrane where ether lipid synthesis is completed by reduction of the keto group, addition of a fatty acyl group, and addition of an alcohol group (ethanolamine or choline) through a phosphodiester linkage. Plasmalogen synthesis requires an extra reaction where the ether linked alkyl group is desaturated to form a double bond adjacent to the ether linkage.

Despite making up 15-18% of phospholipids in humans, the physiological roles of ether lipids are not well understood. They have been proposed to modulate membrane dynamics, act as antioxidants, and function as signaling molecules (Nagan and Zoeller, 2001). It is clear that at least one ether lipid, platelet activating factor, mediates cell signaling and leads to inflammatory and allergic responses (Prescott et al., 1990). Despite the lack of clarity about the functions of most ether lipids, their importance in human physiology is clearly demonstrated in patients with rhizomelic chondrodysplasia punctata type II or III. These patients have defects in the DHAPAT and alkyl DHAP synthase ether lipid synthetic enzymes which leads to rhizomelic shortening of the limbs, joint contractures, dysmorphic facial appearance, severe mental retardation, and cataracts (de Vet et al., 1998; Ofman et al., 1998) It is unclear how a deficiency of ether lipids leads to this phenotype.

The high levels of FAR1 and FAR2 mRNA expression in sebaceous glands is consistent with the second metabolic fate of the fatty alcohols, the wax monoesters. The wax monoesters are neutral lipids whose presence in humans has only been reported in the sebum (sebaceous gland secretions) and meibum (meibomian gland secretions). In these lipid-rich secretions, wax monoesters make up 25-35% of total lipids (Downing and Strauss, 1974; Nicolaides et al., 1981). Like the ether lipids, the exact physiological role of wax esters in humans is unclear. Sebum is believed to play a role in lubricating the skin and/or development of the water barrier and it is likely that wax esters are involved in these functions. Meibum forms the outer layer of the tear film and is important for proper spreading of and preventing evaporation from the tear film (Driver and Lemp, 1996). Loss of the wax ester component in meibum will likely disrupt these processes.

Wax monoesters are formed by the conjugation of a long chain fatty alcohol with a long chain fatty acyl-CoA via an ester linkage; this reaction is catalyzed by a wax synthase enzyme (figure 5). The last of the lipid synthesizing enzymes that I focused upon was the wax synthase enzyme. Wax synthases are known in the jojoba plant (Lardizabal et al., 2000) and bacteria (Kalscheuer and Steinbuchel, 2003), but not in mammals. These two proteins are not related to each other or to any mammalian proteins in the database. Mammalian wax synthase activity has been isolated in a number of tissue extracts but the enzymes responsible for this activity have never been identified. An expression cloning approach was used to identify a cDNA encoding for a mammalian wax synthase enzyme that is a member of the acyltransferase family of enzymes that synthesize neutral lipids. The identification and characterization of this enzyme is described in chapter 6. Expression of wax synthase in cultured cells led to the formation of wax monoesters from saturated, unsaturated, and polyunsaturated fatty alcohols and acids. The wax synthase had little or no ability to synthesize diacylglycerols or triacylglycerols, whereas other acyltransferases, including the acyl-CoA:monoacylglyercaol acylteransferase 1 and 2 enzymes and the acyl-CoA:diacylglycerol acyltransferase 2 enzyme, exhibited modest ability to catalyze wax monoester formation. As expected, the mouse wax synthase mRNA is abundant in tissues rich in sebaceous glands, such as the preputial gland, eyelid, and skin.

Figure 1. Biochemical steps involved in conversion of cholesterol to bile acids

Cholesterol

| CYP7A1, Cholesterol 7α-Hydroxylase | CYP46A1, Cholesterol 24-Hydroxylase | Cholesterol 25-Hydroxylase | CYP27A1, Sterol 27-Hydroxylase |

CYP39A1, Oxysterol 7α-Hydroxylase   CYP7B1, Oxysterol 7α-Hydroxylase

3β-Hydroxy-Δ^5-C_{27} Steroid Oxidoreductase

Δ^4-3-Oxosteroid 5β-Reductase

3α-Hydroxysteroid Dehydrogenase

CYP27A1, Sterol 27-Hydroxylase

Bile Acid-CoA Ligase

2-Methylacyl-CoA Racemase

Branched-Chain Acyl-CoA Oxidase

D-Bifunctional Protein

Peroxisomal Thiolase 2

Bile Acid CoA: Amino Acid N-Acyltransferase

Conjugated Bile Acids

Figure 2. Two different forms of vitamin D

Vitamin D$_2$
(Ergocalciferol)

Vitamin D$_3$
(Cholecalciferol)

Figure 3. Steps involved in endogenous synthesis of vitamin D

7-Dehydrocholesterol   Previtamin D   Vitamin D
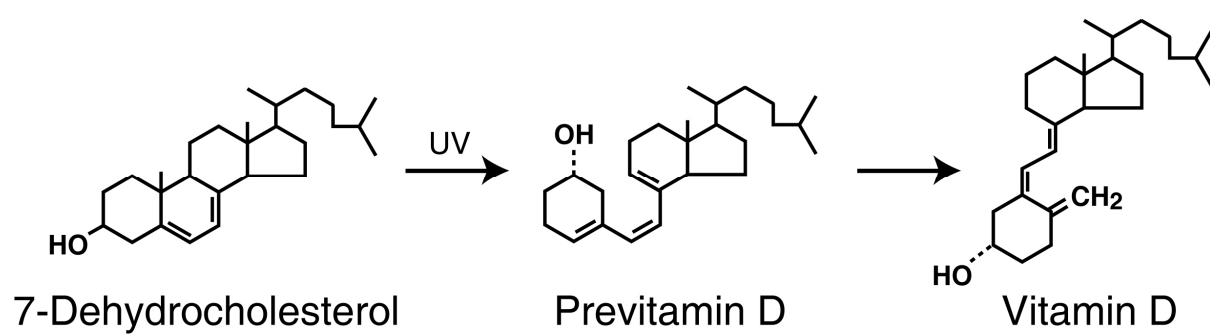
Figure 4. Activation and inactivation pathways of vitamin D

Activation

Cholecalciferol (D₃) → 25-Hydroxylase CYP27A1 CYP2R1 → 25-Hydroxycholecalciferol → 1α-Hydroxylase CYP27B1 → 1α,25-Dihydroxycholecalciferol

Inactivation

1α,25-Dihydroxycholecalciferol → 24-Hydroxylase CYP24A1 → 1α,24,25,-Trihydroxy-cholecalciferol
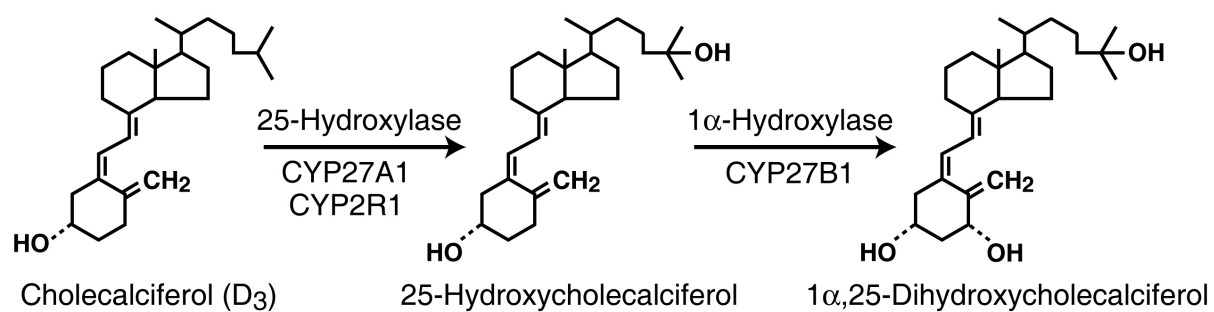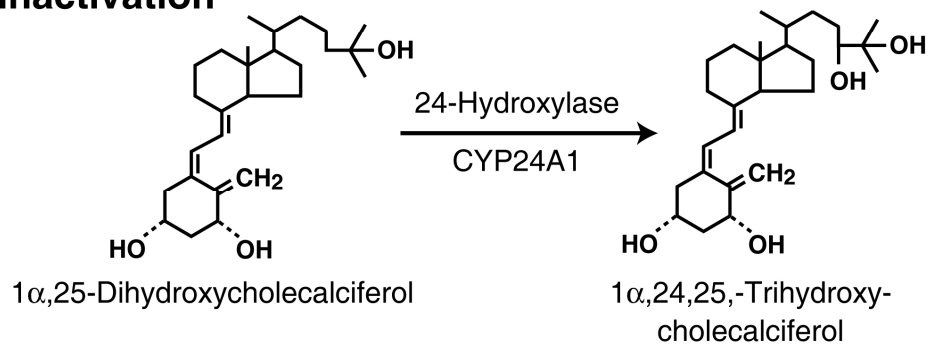
Figure 5. The biochemical steps of mammalian wax biosynthesis

$$\underset{\text{Fatty}\atop\text{acyl-CoA}}{\overset{\overset{\displaystyle O}{\|}}{\text{RCSCoA}}} \xrightarrow[\text{NAD(P)H}]{\overset{\text{Fatty acyl-}}{\text{CoA reductase}}} \underset{\substack{\text{Fatty}\\\text{alcohol}}}{\text{RCH}_2\text{OH}} + \underset{\substack{\text{Fatty}\\\text{acyl-CoA}}}{\overset{\overset{\displaystyle O}{\|}}{\text{RCSCoA}}} \xrightarrow{\overset{\text{Wax}}{\text{synthase}}} \underset{\substack{\text{Wax}\\\text{monoester}}}{\overset{\overset{\displaystyle O}{\|}}{\text{RCH}_2\text{OCR}'}}$$

Ether lipids → Platelet activating factor
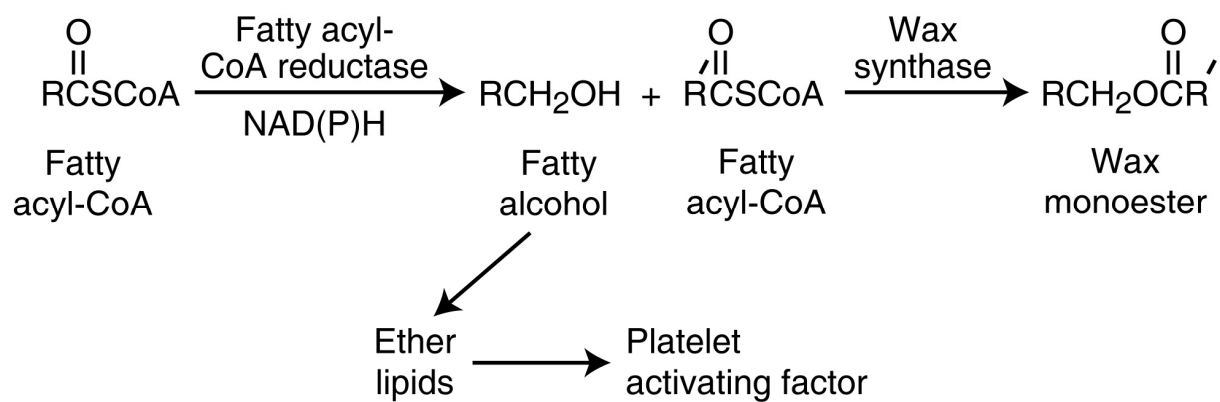
Figure 6. Subclasses of Phospholipids

A

O
‖
O−C−R

O
‖
O−C−R

Ⓟ−ethanolamine

Glycerophospholipid

B

O−C−C−R

O
‖
O−C−R

Ⓟ−ethanolamine

Ether Lipid

C

O−C=C−R

O
‖
O−C−R

Ⓟ−ethanolamine
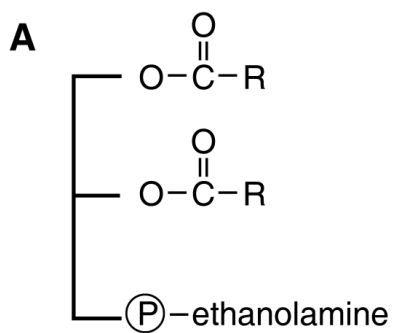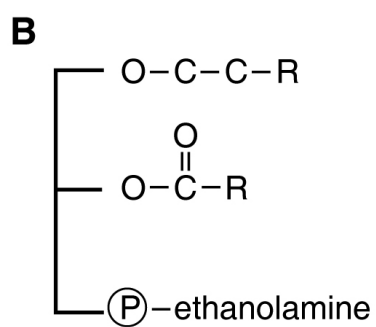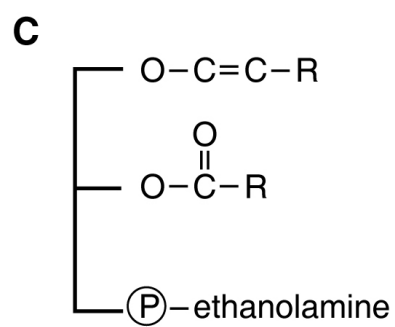
Plasmalogen

CHAPTER TWO
MOLECULAR GENETICS OF 3β-HYDROXY-Δ^5-C_{27}-STEROID OXIDOREDUCTASE DEFICIENCY IN 16 PATIENTS WITH LOSS OF BILE ACID SYNTHESIS AND LIVER DISEASE

INTRODUCTION

The conversion of cholesterol into bile acids is essential for the maintenance of cholesterol homeostasis, the regulation of hepatic function, and the absorption of fats and fat-soluble vitamins from the gastrointestinal tract. Inherited mutations that decrease the synthesis of bile acids or their transport cause a disorder beginning in infants and consisting of impairment of liver function due to decreased bile flow (cholestasis) and lipid and vitamin malabsorption.

The genetic basis of neonatal cholestasis is heterogeneous. Mutations in three genes encoding primary bile acid biosynthetic enzymes have so far been identified as causes of this disease. These include the oxysterol 7α-hydroxylase gene (*CYP7B1*, (Setchell et al., 1998)) located on chromosome 8q21.3, the 3-oxo-Δ^4-steroid 5β-reductase gene (*AKR1D1*, (Setchell et al., 1988)) on chromosome 7q32-33, and the 3β-hydroxy-Δ^5-C_{27}-steroid oxidoreductase (C_{27} 3β-HSD) gene (*HSD3B7,* (Clayton et al., 1987; Schwarz et al., 2000)) on chromosome 16p11.2-12. Each of the encoded enzymes catalyzes an early step in the biosynthetic pathway and, consequently, their loss prevents the synthesis of adequate levels of primary bile acids required for the promotion of bile secretion and intralumenal fat absorption.

Deficiencies in bile acid transport causing neonatal cholestasis also have been traced to mutations in three genes, including *FIC1* on chromosome 18q21 (Bull et al., 1998), *ABCB11* on chromosome 2q24 (Strautnieks et al., 1998), and *ABCB4* on chromosome 7q21.1 (de Vree et al., 1998). The product of *FIC1* is a P-type ATPase expressed on the apical membranes of enterocytes in the small intestine and to a lesser extent in liver parenchyma. The *ABCB11* gene product often is referred to as the bile salt export protein and is expressed on the hepatocyte canalicular membrane. The protein specified by the *ABCB4* gene, originally designated the multidrug resistance 3 protein, is located on the canalicular membrane of the hepatocyte and is active in the transport of phospholipids. Both ABCB11 and ABCB4 are members of a large family of proteins that transport small molecules out of cells (Borst and Elferink, 2002; Dean et al., 2001).

Although neonatal cholestasis is genetically heterogeneous, the manifestations of loss of either a biosynthetic enzyme or a transport protein are similar. Affected individuals present at birth or in early childhood with cholestatic jaundice, fat-soluble vitamin deficiency, and acholic or fatty stools (steatorrhea). Serum transaminases are usually elevated, and a conjugated hyperbilirubinemia is present often. Liver biopsies may reveal non-specific changes, but giant cell transformation of hepatocytes, inflammation, fibrosis, and canalicular and hepatocyte cholestasis are usual (Bove et al., 2000; Daugherty et al., 1993; Witzleben et al., 1992). Chemical analysis of body fluids reveals an accumulation of atypical bile acids and sterol intermediates. Bile acid biosynthetic defects, in particular C_{27} 3β-HSD deficiency, may also cause late onset chronic cholestasis, and in these individuals the clinical history generally reveals a pattern of mildly elevated transaminases in infancy

that often resolves only to reemerge later and an early onset of vitamin D deficient rickets (Setchell and O'Connell, 2001).

Despite a shared clinical presentation, the various genetic forms of neonatal cholestasis require different treatments. Loss of either the C_{27} 3β-HSD or the 3-oxo-Δ^4-steroid 5β-reductase enzyme is treated by oral administration of bile acids (Daugherty et al., 1993; Ichimaya et al., 1990; Jacquemin et al., 2001; Setchell et al., 1990), a therapy that is both effective and relatively free of side effects. In contrast, loss of the oxysterol 7α-hydroxylase enzyme (Setchell et al., 1998), or of the various bile acid transporters (Trauner et al., 1998), requires liver transplantation. The marked differences in the treatment regimens for the various forms of inherited neonatal cholestasis underscore the importance of defining the molecular basis of the disease in individual patients (Jacquemin, 2000).

In this study, we describe the molecular basis of neonatal cholestasis due to C_{27} 3β-HSD deficiency in a cohort of patients diagnosed by mass spectrometric analyses in Paris and Cincinnati (Jacquemin et al., 1994). Affected individuals in this cohort are either homozygous or compound heterozygous carriers of twelve different mutations in the *HSD3B7* gene, many of which are shown to inactivates the encoded enzyme. Notwithstanding this molecular heterogeneity, diagnosis of the disease and subsequent treatment with bile acids led to favorable outcomes in most patients.

MATERIALS AND METHODS

Genomic DNA Extraction and Sequencing – Human genomic DNA was isolated from white blood cells or cultured fibroblasts using Puregene DNA isolation kits (Gentra Systems). Exons of the *HSD3B7* gene were amplified by PCR using the Advantage–GC Genomic PCR kit (Clontech). DNA products were purified by centrifugation through Centricon YM-100 filter devices (Millipore) and subjected to sequence analysis using a thermostable DNA polymerase and fluorescently-labeled nucleoside terminators (Applied Biosystems). Data were collected on an automated DNA sequencer (Applied Biosystems).

Biochemical Analysis of HSD3B7 alleles – A fragment of DNA corresponding to nucleotides 181,011 through 178,216 of the *Homo sapiens* chromosome 16 working draft sequence (accession number NT_024826.3) that encompassed exons 1 through 6 of the *HSD3B7* gene was amplified from each proband's genomic DNA. The primers were designed to introduce a *Sal*I site at the 5'-end of the amplified DNA and a *Not*I site at the 3'-end. Amplification reactions contained 2.5 units of *Pfu* Turbo DNA polymerase (Stratagene) and 5% (v/v) dimethylsulfoxide. The resulting DNA fragment was ligated into the pCMV6 expression vector (GenBank Accession #239250), and the presence of the appropriate mutation was confirmed by DNA sequence analysis. A small fragment of DNA containing each mutation was then substituted for the corresponding segment of the normal gene harbored in pCMV6.

Human embryonic kidney 293 cells (American Type Culture Collection CRL 1573) were plated at a density of 4×10^5 cells per 60 mm dish in 2.5 ml Dulbecco's modified

Eagle's (DMEM) medium containing 1 g/l glucose, 10 % (v/v) fetal calf serum, 100 units/ml penicillin and 100 μg/ml streptomycin sulfate. Two days after plating, cells were transfected using the FuGENE6 reagent (Roche Diagnostics) with a mixture of plasmid DNAs. The mixture included 1.8 μg of pCMV6-hCYP7B1, encoding the human oxysterol 7α-hydroxylase enzyme (Setchell et al., 1998), 1.8 μg of pCMV6-*HSD3B7* (mutant or normal), and 0.4 μg of pVA-1, a vector expressing the adenovirus type 5 VA1 gene (Schneider and Shenk, 1987). At 16 h post-transfection, the FuGENE6-containing medium was replaced with fresh DMEM medium supplemented with 0.0152 μM [^{3}H]cholest-5-ene-3β,25-diol (25-hydroxycholesterol, 78.5 Ci/mmol, NEN Life Sciences Products), and 1.0 μM 25-hydroxycholesterol. The medium was harvested 8 h later and lipids were extracted using 8 ml Folch reagent (chloroform:methanol; 2:1, v/v) per dish. The organic extract was lyophilized and lipids were dissolved in 50 μl acetone and resolved by thin layer chromatography on pre-scored LK5DF silica gel plates (Whatman) in a solvent system of toluene:ethyl acetate (2:3, v/v). Radioactive sterols were detected by phosphorimaging on a BAS1000 machine (Fuji Medical Systems), or by autoradiography using Kodak X-OMAT AR film. The detection limit for this enzymatic assay was 0.05-0.2 pmol C_{27} 3β-HSD product/min/mg cell protein.

Analysis of HSD3B7 RNA – 293 cells were transfected as described above with pCMV6 constructs harboring either a normal C_{27} 3β-HSD gene fragment or a variant allele. At 24 h after transfection, total cellular RNA was isolated using RNA STAT-60 (Tel-Test "B" Inc.) and poly(A)$^+$-enriched mRNA was isolated by oligo(dT)-cellulose chromatography (mRNA

Purification kit, Amersham Pharmacia Biotech). Aliquots of purified mRNA (5 μg) were separated by electrophoresis through 1.4% (w/v) agarose gels and subjected to blot hybridization using standard procedures (Sambrook and Russell, 2000). Radiolabeled probes were derived from a human C_{27} 3β-HSD cDNA, GenBank Accession #AF277719 (Schwarz et al., 2000) and a β–actin cDNA, GenBank Accession #NM_001101 (Gunning et al., 1983).

Database Access – Accession numbers and URLs for data in this article are as follows:
GenBank, http://www.ncbi.nih.gov/Genbank/ (for human *CYP7B1* cDNA [accession number AF029403], for pCMV6 [accession number AF029403], for C_{27} 3β-HSD cDNA [accession number AF277719], for human C_{27} 3β-HSD gene [accession number NT_024826.3], for human β–actin [accession number NM_001101])

Online Mendelian Inheritance of Man (OMIM), http://www.ncbi.nlm.nih.gov/omim/ (for giant cell hepatitis, neonatal [MIM231100], for oxysterol 7α-hydroxylase 1, CYP7B1 [MIM603711], for 3-oxo-Δ^4-steroid 5β-reductase [MIM235555], for *FIC1* [MIM602397], for *ABCB11* [MIM603201], for *MDR3* [MIM602347])

Experimental Subjects – Institutional Review Board approvals were obtained from the University of Texas Southwestern Medical Center, Bicêtre University Hospital, King Faisal Specialist Hospital, St. Joseph Hospital, and the Cincinnati Children's Hospital. Informed consent was obtained from all subjects, and consent forms are maintained at the above institutions. Oral bile acid therapy with cholic acid was provided as an Investigational New Drug approved by the Food and Drug Administration. An preliminary medical history of probands from Families A-E has been reported (Jacquemin et al., 1994). Salient clinical

features of these and other affected individuals in the cohort analyzed here are summarized in

Table 1.

RESULTS

The diagnosis of C_{27} 3β-HSD deficiency in probands was based on clinical presentation and mass spectrometric identification in urine of the signature 3β-hydroxy-Δ^5 bile acids characteristic of the biochemical defect (Fig. 1). To confirm the diagnosis and establish the molecular basis of the disorder, genomic DNA was isolated from the white blood cells of probands, and when possible, other affected and unaffected family members. The data of Figures 2A and 2B show two extended Arabic pedigrees in which C_{27} 3β-HSD deficiency segregated as an apparent autosomal recessive trait. This inheritance pattern was confirmed in Family J by DNA sequence analysis of exon 6 in which a two base pair deletion (1057, ΔCT) was detected in heterozygous form in the parents and unaffected carrier offspring, and in homozygous form in the proband and an affected sibling (Fig. 2B).

Amplifying a 3-kilobase segment that encompassed the six exons and five introns of the gene and subjecting this DNA to sequence analysis identified additional mutations in HSD3B7. These experiments revealed twelve different mutations segregating in the 13 kindreds analyzed (Fig. 3). In ten of the twelve families, including all of those with confirmed or suspected consanguinity, a single mutation was found in homozygous form. The probands in the remaining three kindreds were compound heterozygotes who inherited two different mutations in the *HSD3B7* gene. The molecular genetic features of this cohort are summarized in Table 2.

Individual mutations mapped to four exons and two introns of *HSD3B7* and included one nonsense mutation, two missense mutations, five small deletions of one to three base

pairs, two small insertions of one to two base pairs, and two mutations that altered consensus splice junction sequences (Fig. 4).

The effects of ten of these mutations on the size and amount of mRNA transcribed from the mutant *HSD3B7* alleles were determined. Individual mutations were recreated by site-directed mutagenesis in a pCMV expression vector containing a 3-kilobase segment of genomic DNA encompassing the gene. Transcription from these minigene constructs is initiated within a cytomegalovirus promoter and is terminated within sequences of the human growth hormone gene, while splicing signals are supplied by the introns of the *HSD3B7* gene. Individual plasmid DNAs were introduced into 293 cells by transfection and levels of mature C_{27} 3β-HSD mRNA were determined by blot hybridization.

The data of Figure 5 show that cells transfected with the pCMV vector alone do not produce a C_{27} 3β-HSD mRNA (lane 1), whereas those transfected with a construct containing the normal gene synthesize a mRNA that is approximately 1.5 kilobases in length(lane 2). All but two of the eight mutant genes analyzed in this experiment produced a similarly sized mRNA in approximately the same amount. The two exceptions were genes containing the 132, iCC mutation in exon 1 (lane 5), and the 713-1, G→A mutation in the splice acceptor site of intron 5 (lane 9). Little or no mature C_{27} 3β-HSD mRNA was detected in cells transfected with the 132, iCC mutation, presumably because this lesion leads to rapid turnover of the transcribed mRNA. The 713-1, G→A mutation gave rise to a small amount of normal sized mRNA and a larger RNA of ~2.7 kilobases. Although not tested directly, the size of the larger RNA suggested that it might contain sequences corresponding to the unspliced intron 5 in addition to those derived from exons 1 through 5. Constructs

containing two additional *HSD3B7* mutations, 63, ΔAG and 1057, ΔCT, were analyzed in a separate experiment and found to produce mRNAs that were similar in size and amount to those derived from the normal gene (data not shown). The effects of the G19S and 140, ΔTC mutations on steady state mRNA levels were not determined.

The C_{27} 3β-HSD enzyme catalyzes the isomerization and oxidation of 7α-hydroxylated sterol intermediates that arise in the pathways of bile acid synthesis. These substrates are neither commercially available nor readily synthesized in radiolabeled form. To overcome these challenges, an assay was employed in which 7α-hydroxylated substrates are produced in situ by incubating cells transfected with cDNAs encoding sterol 7α-hydroxylase enzymes with radiolabeled sterol precursors (Schwarz et al., 2000). For example, incubation of 293 cells transfected with the CYP7B1 oxysterol 7α-hydroxylase cDNA with [^{3}H]cholest-5-ene-3β,25-diol (25-hydroxycholesterol), resulted in the production of [^{3}H]cholest-5-ene-3β,7α,25-triol (Fig. 6, lane 2), a 7α-hydroxylated substrate of the C_{27} 3β-HSD enzyme. Monitoring the conversion of this sterol into 7α,25-dihydroxycholest-4-ene-3-one, in cells cotransfected with cDNA expression vectors encoding both CYP7B1 and C_{27} 3β-HSD, allowed measurement of C_{27} 3β-HSD enzyme activity (lane 3).

When expression plasmids containing eight of the mutant *HSD3B7* genes were transfected into 293 cells together with the CYP7B1 cDNA, little or no conversion of [^{3}H]cholest-5-ene-3β,7α,25-triol into the C_{27} 3β-HSD product was observed (Fig. 6, lanes 4-11). In separate experiments, minigenes harboring the 63, ΔAG and 1057, ΔCT mutations also failed to encode an active enzyme when introduced into 293 cells (data not shown).

These results indicated that ten of the twelve mutations identified in the *HSD3B7* gene were null alleles at least as judged at the level of sensitivity (0.05-0.2 pmol C_{27} 3β-HSD product/min/mg cell protein) of the biochemical assay employed. The effects of the two remaining mutations (G19S and 140, ΔTC) were not determined. Antibodies directed against the human C_{27} 3β-HSD were not available, and thus we were unable to determine which of the mutant alleles directed the synthesis of a stable protein.

DISCUSSION

We describe a genetic and molecular analysis in 16 patients from 13 families with a form of neonatal cholestasis arising from C_{27} 3β-HSD deficiency. A diverse spectrum of point mutations, small insertions and deletions in the *HSD3B7* genes of affected individuals are present in homozygous and compound heterozygous form. These lesions variably affect the steady state levels of mRNA transcribed from the mutant genes and in every case tested impair synthesis of an active C_{27} 3β-HSD enzyme. In turn, this loss prevents the synthesis of bile acids and disrupts liver function.

It has been recognized since 1987 that this disorder is the result of a defect in an early step of bile acid synthesis (Clayton et al., 1987). We previously showed that the molecular basis of this genetic disease in one well studied patient from Saudi Arabia was due to a mutation in the *HSD3B7* gene (Schwarz et al., 2000). The present study reveals that C_{27} 3β-HSD deficiency is molecularly heterogeneous but genetically and therapeutically homogeneous. Molecular heterogeneity is indicated by the identification of 12 different mutations in the gene. The existence of so many different mutations does not complicate the molecular diagnosis of the disease since the *HSD3B7* gene spans only ~3 kilobases of DNA and is thus readily amplified and sequenced in its entirety. Genetic homogeneity is evident from the findings that all patients presenting with documented or suspected (see below) urinary accumulations of 3β,7α-dihydroxy-5-cholenoic acid and 3β,7α,12α–trihydroxy-5-cholenoic acid inherited mutations in the *HSD3B7* gene. Thus, unlike other bile acid biosynthetic enzymes, which exist in multiple isoforms (Schwarz et al., 1998), there appears

to be only one human gene that encodes C_{27} 3β-HSD enzyme activity. A positive response to oral bile acids in all but two of the patients harboring different mutations shows the therapeutic homogeneity in C_{27} 3β-HSD deficiency (Table 1).

Mutations in *HSD3B7* are rare and account for only a small percentage of neonatal cholestasis. In agreement with this low frequency, the probands from 10 of the 12 families studied here are true homozygotes who inherited identical mutations from both parents (Table 2). The remaining three probands are compound heterozygotes. The 310, iC, E147K, 1057, ΔCT, and 63, ΔAG mutations were each present in two families, although there were no known shared histories between family pairs with the same mutation. This outcome suggests that these four mutations have been present for extended periods of time in the population, presumably existing in heterozygous form, as prior to the advent of bile acid therapy in the twentieth century, individuals inheriting two mutations in the gene would have almost certainly perished prior to sexual maturation.

The Online Mendelian Inheritance in Man classifies C_{27} 3β-HSD deficiency under the general heading of "giant cell hepatitis, neonatal" (OMIM #231100), together with various forms of neonatal hemochromatosis due to mutations in the steroid 5β-reductase (*AKR1D1*) and oxysterol 7α-hydroxylase (*CYP7B1*) genes of bile acid biosynthesis. The detailed clinical descriptions published in the literature together with the isolation of the encoding gene and the molecular analyses presented in this study and elsewhere (Schwarz et al., 2000) clearly indicate that C_{27} 3β-HSD deficiency is a distinct disease entity.

The mutations identified here shed little light on the biochemistry of C_{27} 3β-HSD, a 369 amino acid enzyme that is located in the endoplasmic reticulum membrane and that has

an unknown topology (Furster et al., 1996; Schwarz et al., 2000). Six of the twelve mutations map to the first two exons of the gene and are predicted to encode severely truncated proteins (Fig. 4). As expected, these fragments do not possess enzyme activity (Fig. 6). Similarly, the loss of one (1042, ΔT) or two (1057, ΔCT) base pairs from the last exon of the gene shifts the translational reading frame and eliminates enzyme activity. The protein encoded by the 1042, ΔT mutation is composed of 341 amino acids from the normal protein fused to a 74 residue extension at the C-terminus, whereas the 1057, ΔCT mutation encodes a protein with the first 346 amino acids of the normal protein fused to a five residue extension. In these cases, we do not know whether inactivation of the enzyme results from elimination of the normal C-terminal sequences or from the addition of spurious amino acids at this end.

Only two potentially informative substitution mutations were identified in this survey. A G19S mutation in exon 1 was detected in the proband of Family M while the manuscript was being reviewed and was not analyzed further. The proband of Family F inherited a G to A transition mutation in exon 4 that results in the substitution of a lysine residue for glutamate at position 147 (E147K). Although an apparently stable mRNA of normal abundance is transcribed from the mutant gene (Fig. 5), no enzyme activity is detected in the transfected cells (Fig. 6). The C_{27} 3β-HSD is a member of a small family of enzymes that metabolize steroids and share sequence identity (Schwarz et al., 2000). In sequence alignments of the seven known family members, the glutamate 147 residue of C_{27} 3β-HSD is conserved in all of them, and this residue is shared also between the human, mouse, and rat C_{27} 3β-HSD enzymes (Schwarz et al., 2000). The preservation of this glutamate is

suggestive of an important catalytic or structural role in these isomerase/dehydrogenases and may explain why substitution with lysine inactivates the C_{27} 3β-HSD enzyme in the proband. The glycine residue at position 19 also is conserved in all members of the 3β-HSD enzyme family, and its loss may inactivate the C_{27} 3β-HSD in the patient from family M.

Because all of the mutations analyzed in detail here were null alleles, we are unable to deduce any phenotype-genotype correlations in this cohort of C_{27} 3β-HSD deficient patients.

The availability of chemical and molecular methods to diagnose C_{27} 3β-HSD deficiency raises questions concerning the relative merits of each procedure and whether there are cases in which one or the other method, or both, are needed for an unambiguous assignment? Ascertainment by chemical procedures requires sophisticated mass spectrometry that is only available in a small number of medical centers. Diagnosis by molecular methods is more widely possible but still requires access to appropriate facilities and expertise. While this manuscript was in review, we encountered a case in which both methods were required to make an accurate diagnosis of C_{27} 3β-HSD deficiency. The mass spectra of samples obtained from the proband of family M were suggestive of the disorder but not definitive as a consequence of the advanced liver disease in this patient and the presence of obscuring ions arising from the ursodeoxycholic acid that was prescribed at the first signs of cholestasis. Analysis of the proband's DNA, which revealed two mutations in exon 1 of the gene (G19S and 140, ΔTC), was required to make an unambiguous assignment of the deficiency.

We conclude that mutations in the *HSD3B7* gene underlie C_{27} 3β-HSD deficiency, an autosomal recessive form of neonatal cholestasis. Preliminary data on long term cholic acid

therapy in children with this disorder show that it is an adequate and very effective treatment (Daugherty et al., 1993; Ichimaya et al., 1990; Jacquemin et al., 2001; Setchell et al., 1990). The identification of disease causing mutations will allow prenatal diagnosis within affected families and the initiation of cholic acid therapy in the immediate neonatal period.

Table 1. Summary of clinical data from 16 patients with C_{27} 3β-HSD deficiency

Family	Subject	Sex	Age at Diagnosis (yr)	Family History	MS Diagnosis[a]	Symptoms	Treatment	Outcome
A	1	M	4	Yes	Cincinnati	Jaundice, hepatomegaly, discolored stools, rickets	Ursodeoxycholate, then cholate	Favorable
B	1	F	4	No	Cincinnati	Hepatomegaly, fatty stools	Ursodeoxycholate, then cholate	Favorable
C	1	F	7.8	Yes	Cincinnati	Jaundice, hepatomegaly	Ursodeoxycholate, then cholate	Favorable
D	1	F	4.3	Yes	Cincinnati	Jaundice, hepatomegaly	Ursodeoxycholate, then cholate	Favorable
E	E1	M	4.8	Yes	Cincinnati	Hepatomegaly, fatty stools	Ursodeoxycholate, then cholate	Favorable
	E2	F	13			Fatty stools, rickets, hepatosplenomegaly		
F	1	M	2	No	Paris	Jaundice, hepatomegaly, Fatty and discolored stools	Ursodeoxycholate, then cholate	Favorable
G	G1	F	2.3	Yes	Paris	Hepatomegaly	Cholate	Favorable
	G2	F	11.5			Hepatomegaly, fatty stools		
H	1	F	0.3	No	Paris	Jaundice, hepatomegaly, fatty stools	Cholate	Favorable
I	I1[b]	M	0.3	Yes	Cincinnati	Cholestasis, rickets	Chenodeoxycholate, then cholate	Favorable
	I2	M	11		ND	Cholestasis, rickets		

Table 1. cont.

						Progressive liver disease	Cholate	Favorable
J	1	M	NA	Yes	NA	Progressive liver disease	Cholate	Favorable
K	1	M	4.2	No	Cincinnati	Discolored stools, dark urine, coagulopathy, developmental delay, rickets	Cholate	Favorable
L	1	F	13.5	No	Cincinnati	Jaundice, cirrhosis, hepatosplenomegaly	Cholate	Transplanted[c]
M	1	M	0.6	No	Cincinnati	Jaundice, cirrhosis, coagulopathy, hepatosplenomegaly	Ursodeoxycholate	Transplanted[c]

ND, not determined.
NA, not available.
[a]City in which analysis by mass spectrometry was performed.
[b]This is Patient MU1, the index case in whom C_{27} 3β-HSD deficiency was first described (3).
[c]Liver damage (cirrhosis) prior to diagnosis was extensive in these patients and bile acid therapy was unsuccessful. Both underwent orthotopic liver transplantation.

Table 2. Molecular genetics of C_{27} 3β-HSD deficiency

Designation	Ethnic background	Consanguinity	Molecular lesion		
			Type	Location	Mutation
Family A	Portuguese	Yes	Deletion	Exon 2	1042, ΔT
Family B	Chilean	No	Insertion	Exon 2	310, iC
Family C	Portuguese	Yes	Nonsense	Exon 1	Q6*
Family D	Italian	Yes	Insertion	Exon 2	310, iC
Family E	French	No			
Patient E1			Splice junction	Intron 2	340+1, G → T
Patient E2			Splice junction	Intron 5	713-1, G → A
Family F	French	Yes	Missense	Exon 4	E147K
Family G	French	Yes	Missense	Exon 4	E147K
Patient G1					
Patient G2					
Family H	French	No	Insertion	Exon 1	132, iCC
			Deletion	Exon 1	91, ΔGTG
Family I	Saudi Arabian	Yes	Deletion	Exon 6	1057, ΔCT
Patient I1					
Patient I2					
Family J	Saudi Arabian	Yes	Deletion	Exon 6	1057, ΔCT

Table 2. cont.

Family K	British	No	Deletion	Exon 1	60, ΔAG
Family L	Canadian	No	Deletion	Exon 1	60, ΔAG
Family M	African-American	No	Missense	Exon 1	G19S
			Deletion	Exon 1	140, ΔTC

NA, not available.

Figure 1. Reaction catalyzed by the C_{27} 3β-HSD enzyme. A generic 7α-hydroxylated intermediate in the bile acid biosynthetic pathway is shown at left. The C_{27} 3β-HSD reaction involves isomerization of the Δ^5 bond to Δ^4 bond and the oxidation of the 3β-hydroxyl group to an oxo group. The actions of an additional nine or ten enzymes produce primary bile acids. Mutations in the C_{27} 3β-HSD enzyme cause the accumulation in the plasma and urine of 7α-hydroxylated intermediates with 3β-hydroxyl, Δ^5 structures.

HSD3B7,
3β-Hydroxy-Δ⁵-C₂₇
Steroid Oxidoreductase

R = OH

Bile Acids
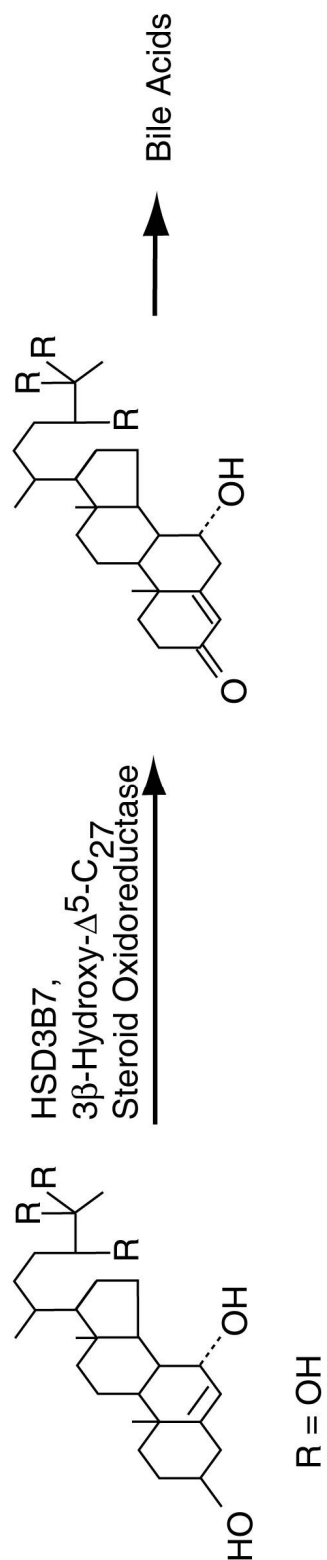
Figure 2. Pedigrees of two families with C_{27} 3β-HSD deficiency. The two kindreds are designated by a capital letter (I, J) with generations designated by a Roman numeral and each individual within a generation by an Arabic number. An arrow designates the proband in each family. Question marks designate individuals of unknown *HSD3B7* genotype. The DNA sequence of a small segment of exon 6 from the *HSD3B7* genes of seven Family J individuals is shown below the pedigree in B. The 1057, ΔCT mutation segregates in an autosomal recessive manner in this family.

A. Family I
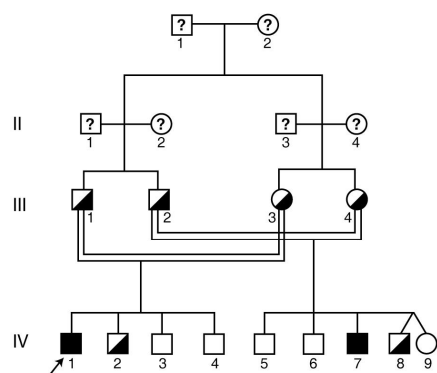
B. Family J
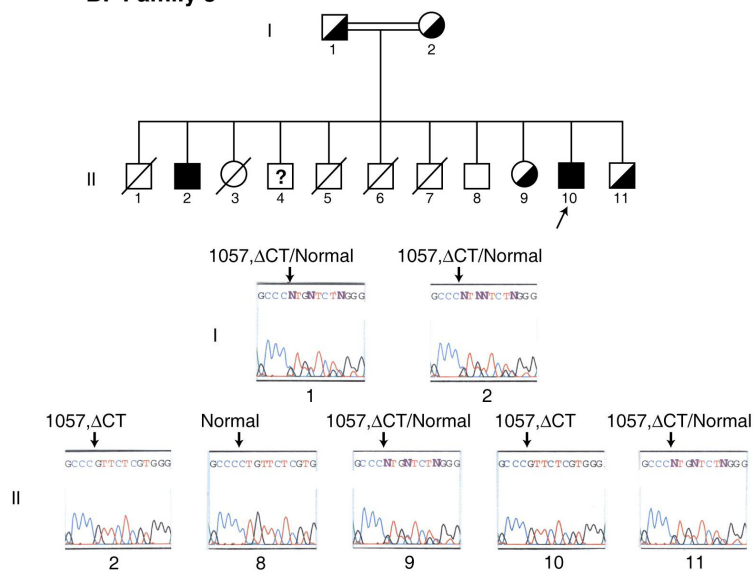
Figure 3. DNA sequence analyses of mutations in the *HSD3B7* gene. The sequences of small segments of the gene are shown together with the locations of ten mutations identified in twelve families.

60
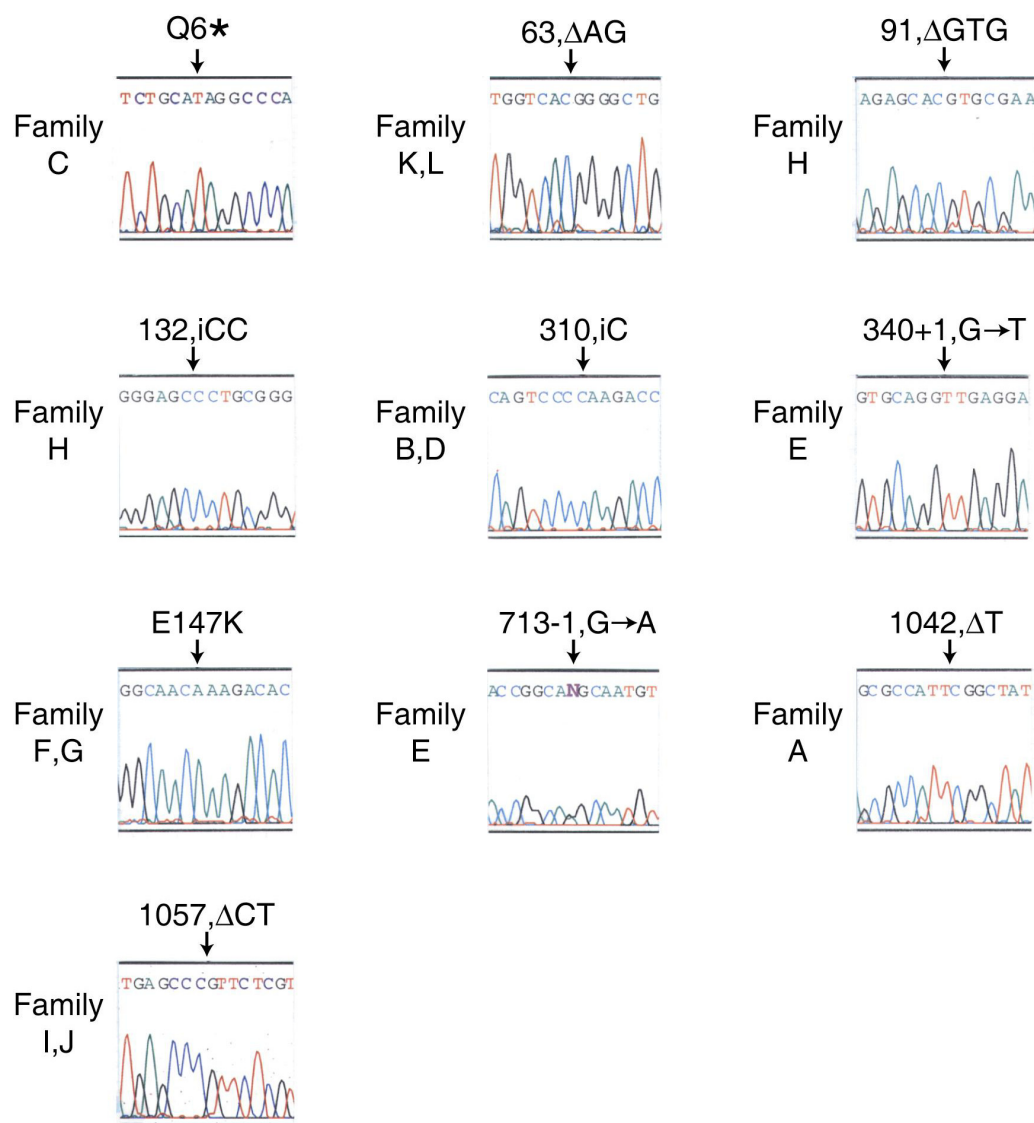
Figure 4. Structure of the *HSD3B7* gene and locations of mutations identified in subjects with neonatal cholestasis. The structure of the gene is drawn to scale with exons indicated by boxes and introns by interconnecting lines. Amino acids occurring at exon/intron boundaries are indicated in single letter code above the gene schematic. The locations of twelve mutations identified in 16 patients are shown below the schematic together with the chromosomal assignment of the *HSD3B7* gene. The nucleotide numbers indicating the positions of individual mutations refer to those of the human C_{27} 3β-HSD cDNA (GenBank Accession number AF277719).
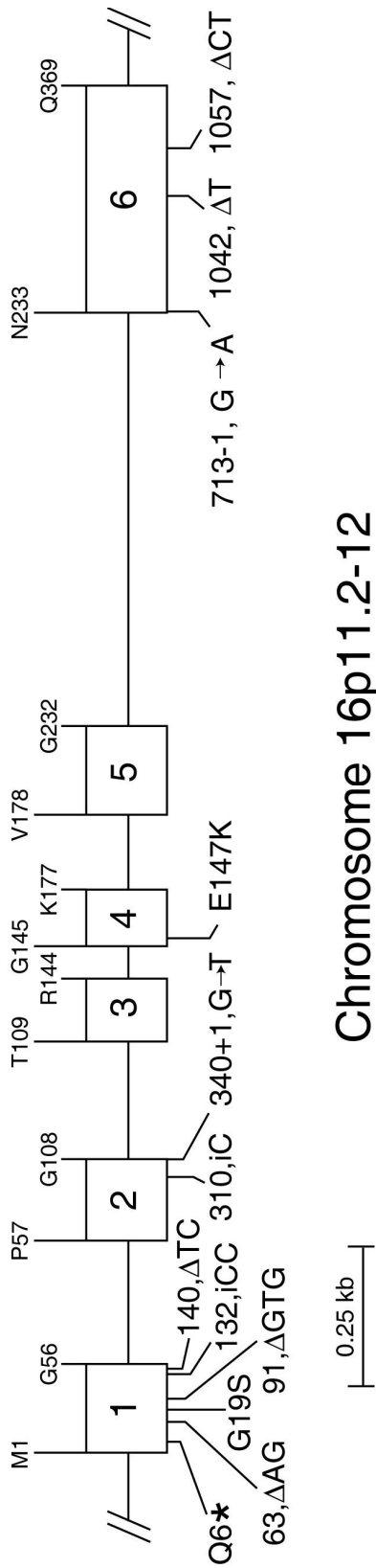
Chromosome 16p11.2-12

Figure 5. RNA blotting analysis of *HSD3B7* mutations. A segment of genomic DNA spanning exons 1 through 6 of the C_{27} 3β-HSD gene and containing either the normal sequence or the indicated mutation was ligated into the pCMV6 expression vector. The resulting plasmids were introduced into cultured human embryonic kidney 293 cells by transfection. After a 16 hour period of expression, poly(A)$^+$ RNA was isolated from the transfected cells and analyzed by blot hybridization with a radiolabeled probe derived from the C_{27} 3β-HSD cDNA (upper panel). The filter was stripped of radioactivity and hybridized again with a radiolabeled probe derived from a β-actin cDNA (lower panel). The positions to which RNAs of known size migrated to in the gel are indicated on the left of the autoradiograms.

C_{27} 3β-HSD

β-Actin

kb

2.4 —
1.4 —

2.4 —
1.4 —

Vector Normal Q6★ 91, ΔGTG 132, iCC 310, iC 340+1, G→T E147 K 713-1, G→A 1042, ΔT

1 2 3 4 5 6 7 8 9 10
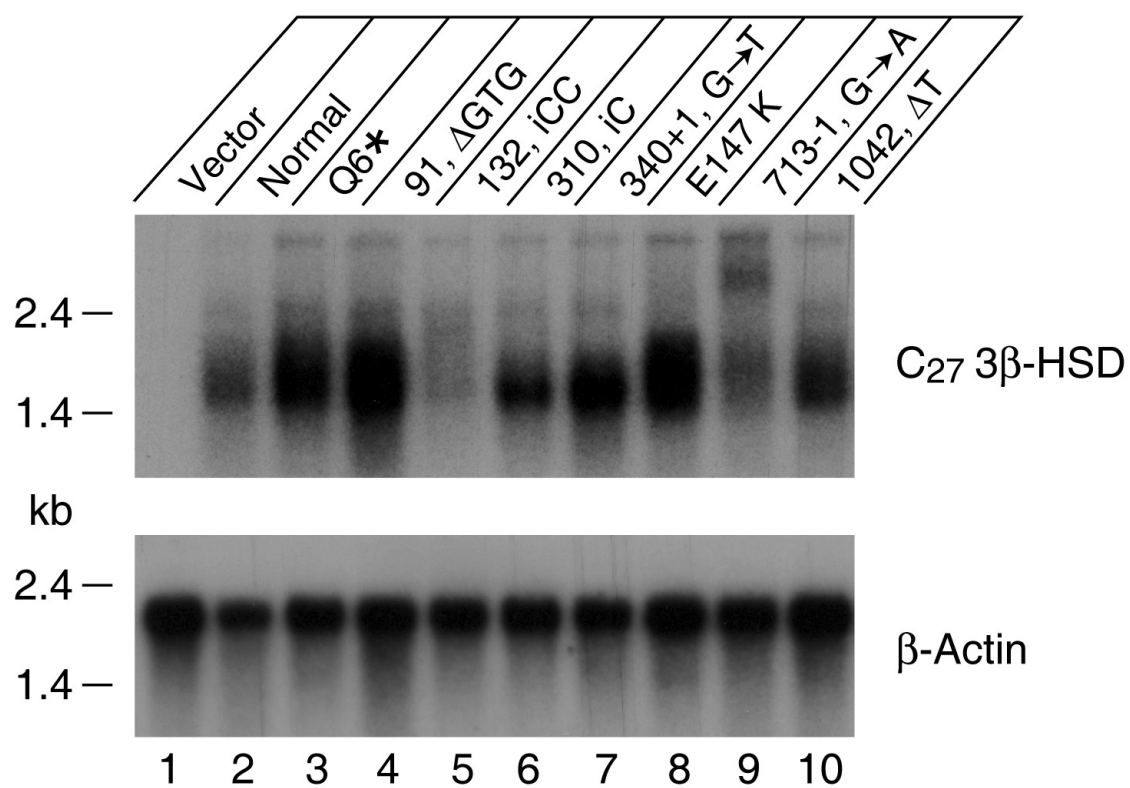
Figure 6. Effects of *HSD3B7* mutations on C_{27} 3β-HSD enzyme activity. Expression vectors harboring genomic DNAs bearing the indicated normal or mutant alleles of the *HSD3B7* gene were introduced into cultured human embryonic 293 cells by transfection. Subsequent enzyme activity measurements in whole cells were performed as described in Materials and Methods. A phosphorimage arising from a scan of a thin layer chromatography plate is shown. The positions to which sterols of known structure migrated to on the plate are shown on the right of the image. Only cells transfected with the normal *HSD3B7* gene (lane 3) expressed an enzyme capable of converting cholest-5-ene-3β,7α,25-triol into 7α,25-dihydroxy-cholest-4-ene-3-one. Approximately five-times more of the starting substrate (cholest-5-ene-3β,25-diol) was chromatographed in lane 1 versus the other lanes.

66

Cholest-5-ene-3β,25-diol

7α,25-Dihydroxy-cholest-4-ene-3-one

Cholest-5-ene-3β,7α,25-triol
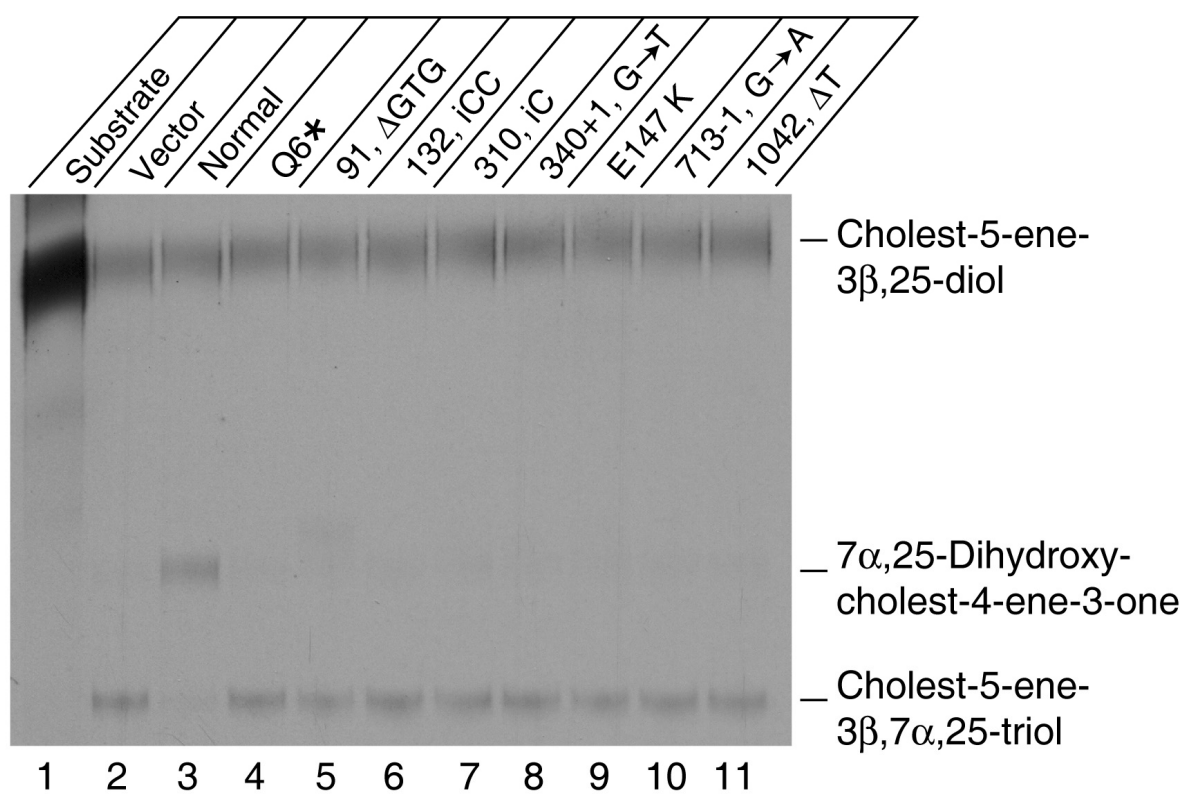
CHAPTER THREE
DE-ORPHANIZATION OF CYTOCHROME P450 2R1: A MICROSOMAL VITAMIN D 25-HYDROXYLASE

INTRODUCTION

Vitamin D regulates calcium and phosphate metabolism by activating the vitamin D receptor, a transcription factor and member of the nuclear receptor family. In the 1920s, McCollum, Mellanby, and Pappenheimer showed that deficiency of vitamin D caused rickets in experimental animals (Simoni et al., 2002). Subsequently, the structure of vitamin D and its origins from plant and animal steroids were determined, and the roles of the vitamin in the mobilization of minerals from the diet and in bone were defined. The liver was shown to be required for the activation of vitamin D by 25-hydroxylation (Ponchon and DeLuca, 1969; Ponchon et al., 1969). While 25-hydroxyvitamin D was more active than vitamin D in many bioassays (Blunt et al., 1968), the most potent hormone was 1α,25-dihydroxyvitamin D (Haussler et al., 1968; Holick et al., 1971), which was synthesized from 25-hydroxyvitamin D by the kidney (Fraser and Kodicek, 1970). The molecular mechanism of vitamin D action were manifest with the identification (Haussler and Norman, 1969) and cDNA cloning (McDonnell et al., 1987) of the vitamin D receptor.

Hydroxylation reactions catalyzed by cytochrome P450s activate and inactivate vitamin D as a ligand for the receptor. 25-Hydroxylation is performed in the liver by two different enzymes, one located in the mitochondria (Bjorkhem and Holmberg, 1978), identified as the CYP27A1[1] sterol 27-hydroxylase (Dahlback and Wikvall, 1988; Guo et al.,

1993; Masumoto et al., 1988; Su et al., 1990; Usui et al., 1990), and a second in microsomes (Bhattacharyya and DeLuca, 1974; Madhok and DeLuca, 1979), whose identity in most species has not been determined. A second mitochondrial P450 (CYP27B1), for which an encoding cDNA was isolated by expression cloning (Takeyama et al., 1997), catalyzes 1α-hydroxylation of 25-hydroxyvitamin D in the kidney, while a third mitochondrial P450, vitamin D 24-hydroxylase (CYP24A1), inactivates the vitamin in this tissue (Chen et al., 1993; Itoh et al., 1995; Ohyama et al., 1991). Together, these enzymes regulate the systemic and local levels of vitamin D through complex feedback mechanisms mediated in part by the vitamin D receptor (Jones et al., 1998).

The existence and physiological importance of the two hepatic vitamin D 25-hydroxylase enzymes is demonstrated in humans (Bjorkhem et al., 2001; Cali et al., 1991) and mice (Repa et al., 2000; Rosen et al., 1998) by mutations in the mitochondrial CYP27A1 vitamin D 25-hydroxylase gene. Loss of this enzyme has profound effects on cholesterol metabolism as CYP27A1 catalyzes an essential reaction in bile acid synthesis. In contrast, vitamin D metabolism is normal in individuals and mice with no functional CYP27A1. These findings indicate that the microsomal vitamin D 25-hydroxylase can compensate for loss of the mitochondrial activity.

In the current study, a cDNA library made from hepatic mRNA of mice deficient in the gene encoding the mitochondrial CYP27A1 enzyme was screened using a vitamin D receptor based, ligand activation assay (Takeyama et al., 1997). A single cDNA specifying a microsomal P450 enzyme termed CYP2R1 with previously unknown substrate specificity

was identified. The biochemical properties and tissue distribution of CYP2R1 are consistent with this enzyme being the microsomal vitamin D 25-hydroxylase.

MATERIALS AND METHODS

Expression Plasmids – A mouse adrenodoxin cDNA (mAdx, nucleotides 41-772 of GenBank™/EBI Data Bank accession number L29123) was amplified by the polymerase chain reaction (PCR) from random hexamer primed mouse hepatic cDNAs using the following oligonucleotide primers: Forward: 5'-GCCTATGTCGACTCAGCACTGCGCAGGACTCC-3', and Reverse: 5'-GCGGGATCCGACAGCACAGCTACTCACAC-3'. The amplified DNA was digested with the enzymes *Sal*I and *Bam*HI, and ligated into pCMV6 (GenBank™/EBI Data Bank accession number AF239250). The adrenodoxin expression vector encoded the expected electron transport enzyme activity in transfected cells as judged by the protein's ability to stimulate the vitamin D 25-hydroxylase activity of sterol 27-hydroxylase.

A mouse vitamin D 24-hydroxylase cDNA (mCYP24A1, nucleotides 281 to 2200 of GenBank™/EBI Data Bank accession number D89669) was amplified by PCR from random hexamer primed kidney cDNA. The RNA for this cDNA synthesis reaction was isolated from a mouse injected intraperitoneally with 36 pmol/g body weight 1α,25-dihydroxyvitamin D for five h prior to tissue harvest. Oligonucleotide primers for the amplification reaction were: Forward: 5'-GCCTATGTCGACACTTCAGAACCCAACAGCAC-3', and Reverse: 5'-ATTATGCGGCCGCAGTGACATCAGGCTCTTGAG-3'. The amplified DNA was digested with the restriction enzymes *Sal*I and *Not*I, and ligated into the pCMV6 vector.

Human cytochrome P450 subfamily 3A, polypeptide 4 (hCYP3A4, nucleotides 98-1617 of GenBank™/EBI Data Bank accession number NM_017460) and cytochrome P450

2R1 (hCYP2R1) cDNAs were amplified by PCR from liver QUICK-clone cDNA (Clontech). Oligonucleotide primers for the hCYP3A4 cDNA were: Forward: 5'-GCCTATGTCGACAGTGATGGCTCTCATCCCAG-3', and Reverse: 5'-ATTATGCGGCCGCTTCAGGCTCCACTTACGGTG-3'. The amplified DNA was digested with the restriction enzymes *Sal*I and *Not*I, and then ligated into the pCMV6-SPORT vector (Invitrogen). The CYP3A4 expression vector encoded testosterone 6β-hydroxylase enzyme activity in HEK 293 cells as judged by thin layer chromatography. Oligonucleotide primers for the hCYP2R1 cDNA were: Forward: 5'-GCCTATGTCGACTGTGGAGTTCGCACCTCCAG-3', and Reverse: 5'-ATTATGCGGCCGCAACCAAGTTCAGGGATAAGG-3'. The amplified DNA was digested with the enzymes *Sal*I and *Not*I, and then ligated into the pCMV6 vector.

A DNA fragment encompassing the 5'-flanking region of the mouse osteopontin gene (nucleotides 1-862 of GenBank™/EBI Data Bank accession number D14816) was amplified via PCR from mixed strain C57Bl/6J;129S6/SvEv mouse genomic DNA. Oligonucleotide primers were: Forward: 5'-ATTATGCGGCCGCTTCAGGCTCCACTTACGGTG-3', and Reverse: 5'-CCGCTCGAGCTTGGCTGGTTTCCTCCGAGAATG-3'. The amplified DNA product was digested with the restriction enzymes *Hind*III and *Xho*I, and then ligated into the pTK-LUC reporter plasmid (Willy et al., 1995).

A mouse 25-hydroxyvitamin D_3 1α-hydroxylase cDNA (mCYP27B1, **GenBank™/EBI Data Bank accession number** AB006034) was a kind gift of Professor Shigeaki Kato, University of Tokyo, Tokyo, Japan. The mouse sterol 27-hydroxylase cDNA (mCYP27A1) used in these studies was generated previously (Lund et al., 1998).

Expression Cloning – A cDNA library was made from 3 µg of poly(A)$^+$ hepatic RNA isolated from mice deficient in sterol 27-hydroxylase (Rosen et al., 1998) using the SUPERSCRIPT plasmid system for cDNA synthesis (Invitrogen Life Technologies). cDNA synthesis was initiated by *Not*I oligo(dT) primer-adapters, the cDNA products were ligated to *Sal*I adapters, digested with the restriction enzyme *Not*I, size-fractionated by gel filtration chromatography, and then ligated into *Not*I and *Sal*I digested pCMV-SPORT 6 vector. Nucleic acids in the ligation mixture were precipitated with ethanol and resuspended in 5-µl of deionized-distilled H$_2$O. *Escherichia coli* (*E. coli*) Electromax DH10B cells (Invitrogen) were transformed with 1-µl of the resuspended DNAs. The transformation mixture was diluted into 500-ml of Luria-Bertani medium supplemented with ampicillin (50 µg/ml). An aliquot (1.25-ml) of the diluted culture (containing approximately 100 transformants) was added to each well of a 96-well block (Qiagen) and incubated with shaking for 20-24 hours at 37°C. Plasmid DNA was isolated from the bacterial cultures using the QIAprep96 Turbo Miniprep kit (Qiagen).

Human embryonic kidney (HEK) 293 cells (American Type Culture Collection CRL number 1573) were transfected with pools of ~100 cDNAs using the FuGENE6 reagent (Roche). The cells were maintained in monolayer culture at 37ºC in an atmosphere of 8.8% CO$_2$/91.2% air in low glucose Dulbecco's modified Eagle's medium (DMEM) supplemented with 10% (v/v) fetal calf serum, 100 units/ml of penicillin, and 100 µg/ml streptomycin sulfate. On day 0 of an expression cloning experiment, 25,000 cells per well were plated in 96-well plates (Corning Costar, #3595) in a volume of 100-µl of high glucose DMEM

supplemented with 10% (v/v) dextran-charcoal-stripped fetal calf serum. On day 1, cells were transfected with a mixture containing 0.45-µl FuGENE6 and 150 ng of plasmid DNA comprised of: 20 ng of pCMX-β-galactosidase (Lu et al., 2000), 20 ng of TK-MH100X4-LUC (Willy et al., 1995), 20 ng of pCMX/GAL4-VDR (see below), 10 ng of pVA1 (Schneider and Shenk, 1987), 5 ng of pCMV6/mAdx, and 75 ng of cDNA pool. Cells were returned to the incubator for 8-10 hours, and then vehicle (ethanol) or 1α-hydroxyvitamin D$_3$ (Sigma Chem. Co.) substrate was added to a final concentration of 10 nM. After a further 16-20 h incubation, cells were lysed by the addition of 100-µl per well of Lysis Buffer (2% (v/v) 3-[(3-cholamidopropyl)dimethylammonio]-1-propanesulfonate, 0.6% (w/v) phosphatidylcholine, 2.5 mM Tris-phosphate, pH 7.8, 0.6% (w/v) bovine serum albumin, 15% (v/v) glycerol, 4 mM ethylene glycol-bis(2-aminoethylether)-N,N,N',N'-tetraacetic acid, 8 mM MgCl$_2$, 1 mM DL-dithiothreitol, and 1% (w/v) Pefabloc SC (Centerchem). The 96-well plates were shaken for 5 min at 23°C, and then 20-µl of cell lysate from each well were transferred to a fresh 96-well assay plate (Corning Costar #3922). Thereafter, 100-µl of Luciferase Assay Buffer (4 mM ATP (Roche), 20 mM MgCl$_2$, and 0.1 M KPO$_4$) was added to each well, and luciferase activity was measured in a Dynex MLX Microtiter Plate Luminometer running the Revelation MLX Version 4.25 software after the addition of 100-µl of Luciferin Solution (1 mM D-luciferin (Molecular Probes) in 0.1 M KPO$_4$). β-Galactosidase enzyme activity was determined in cell lysates using a Dynex Opsys MR machine running the Revelation Quicklink software; an aliquot (40-µl) of cell lysate was transferred to each well of a fresh 96-well plate (Corning Costar #3598), followed by the addition of 125-µl of β-Galactosidase Assay Buffer (60 mM Na$_2$HPO$_4$, 40 mM NaH$_2$PO$_4$, 8

mM KCl, 8 mM $MgCl_2$, 0.4 % (w/v) 2-nitrophenyl-β-D-galactopyranoside (Boehringer Manheim), and 3 mM β-mercaptoethanol), and an incubation of 10 min at 37^oC prior to measuring the absorbance at A_{405}. Relative Luciferase Units were calculated by dividing the measured luciferase activities by the absorbance values per min determined in the β-galactosidase assay. All values are expressed as means ± standard error of measurement (SEM) derived from triplicate wells.

Vitamin D Receptor Activation Assay and Ligands – The GAL4-VDR/GAL4-Luciferase receptor-reporter system was composed of the pTK-MH100X4-LUC plasmid (Willy et al., 1995)**,** and pCMX/GAL4-VDR, which specifies a fusion protein consisting of amino acids 1-147 of the *Saccharomyces cerevisiae* galactose 4 (GAL4) transcription factor (encoded by nucleotides 2901 to 3353 of GenBank™/EBI Data Bank accession number X85976) and amino acid 90 to 427 of the human vitamin D receptor (hVDR, encoded by nucleotides 383 to 1397 of GenBank™/EBI Data Bank accession number 44507882). The VDR/vitamin D response element (VDRE)-Luciferase system used here consisted of the SPPX3-TK-LUC plasmid (Choi et al., 2003) and a plasmid expressing the full-length mouse vitamin D receptor (pCMX/mVDR, nucleotides 109-1377 of GenBank™/EBI Data Bank accession number D31969) (Makishima et al., 2002)**.** The VDR/Osteopontin-Luciferase system was composed of the Osteopontin-LUC plasmid (0.862 kb DNA fragment encompassing the mouse osteopontin gene promoter ligated into the pTK-LUC vector (Willy et al., 1995)), and the pCMX/mVDR DNA described above. Transfection experiments with the GAL4-VDR/GAL4-luciferase receptor-reporter systems were carried out as described under

"Expression Cloning". For the VDR/VDRE-Luciferase and VDR/Osteopontin-Luciferase systems, the plasmid DNA mixtures (150 ng DNA total) contained 5 ng of pCMX/mVDR, 20 ng of SPPX3-TK-LUC or pOsteopontin-LUC, 20 ng of pCMX-β-galactosidase, 10 ng of pVA1, and 95 ng of CYP expression vector or pCMV6 plasmid DNA.

Secosteroids used in the experiments reported here (vitamin D_2, vitamin D_3, 1α-hydroxyvitamin D_3, 25-hydroxy vitamin D_3, and 1α,25-dihydroxy vitamin D_3) were obtained from Sigma and added to the culture medium in ethanol (1-μl per ml medium). Stock solutions of these compounds ranged in concentration from 10^{-2} to 5 x 10^{-7} M and were stored at -20ºC.

Thin Layer Chromatography – HEK 293 cells were plated at a density of 4 x 10^5 cells per 60-mm dish in 2.5-ml of high glucose DMEM medium supplemented with 10% (v/v) dextran-charcoal-stripped fetal calf serum, 100 units/ml of penicillin, and 100 μg/ml streptomycin sulfate. On day 2, cells were transfected with FuGENE6 reagent and a mixture of plasmid DNAs (3.5 μg total) containing 0.5 μg pVA1, and either 3 μg of pCMV6, 3 μg of pCMV6-h2R1, 1.5 μg of pCMV6 and 1.5 μg of pCMV6-mAdx, or 1.5 μg of pCMV6-mCYP27A1 and 1.5 μg of pCMV6-mAdx. After 18 h, the transfection medium was removed from the dish and replaced with 2-ml of fresh medium supplemented as above and containing 4.6 x 10^{-7} M [4-^{14}C] Vitamin D_3 (Amersham). For cells transfected with the pCMV6-mCYP27A1 plasmid, the medium was brought to a final concentration of 10^{-6} M vitamin D_3 by the addition of unlabeled secosteroid. Cells and medium were harvested 96 h later, and vitamin D metabolites were extracted with 8-ml chloroform:methanol (2:1, v/v), and then dried under

a stream of N_2. The extracted metabolites were resuspended in 50-µl acetone and resolved by thin layer chromatography on pre-scored LD5DF silica gel 150 Å plates (Whatman). Solvent systems of cylohexane:ethyl acetate (3:2, v/v), chloroform:ethyl acetate (3:1, v/v), and 2,2,4-trimethylpentane:ethyl acetate: acetic acid (50:50:17, v/v) were used. Radiolabeled vitamin D metabolites were detected by phosphorimage analysis on a BAS1000 machine (Fuji Medical Systems, Tokyo, Japan). Aliquots (5-µl) of 10^{-2} M stock solutions of unlabeled standards (vitamin D_3, 25-hydroxyvitamin D_3, 1α-hydroxyvitamin D_3, and 1α,25-dihydroxyvitamin D_3) dissolved in ethanol were chromatographed in adjacent lanes on the plates and visualized by iodine staining (Touchstone, 1992).

Radioimmunoassays – The Gamma-B 25 Hydroxy Vitamin D RIA kit (Alpco Diagnostics) was used for the quantitative determination of 25-hydroxyvitamin D in medium from HEK 293 cells cultured in the 96-well plate format described above. Cells were transfected via the FuGENE6 reagent with 150 ng of total plasmid DNA comprised of 5 ng pCMX/mVDR, 20 ng SPPX3-TK-LUC, 20 ng pCMX-β-galactosidase, 10 ng pVA1, and either 95 ng of pCMV6, pCMV6-h2R1, pCMV6 SPORT-m2R1, or 45 ng pCMV6-mCYP27A1 and 45 ng pCMV6-mAdx. After 10 h, ethanol vehicle, or vitamin D_3 at final concentrations of 0.5 or 1 µM, were added to the medium. Radioimmunoassays were performed 44 h later on 50-µl aliquots of pooled medium from triplicate wells following directions provided by the manufacturer. The correlation coefficient of accuracy for the radioimmunoassay kit was r = 0.95. Sensitivity was < 3 nmol/l. Luciferase and β-galactosidase assays also were performed on cell lysates to ensure that transfected plasmids were expressed.

Real Time PCR – Total RNA was prepared from mouse tissues using RNA STAT-60 (Tel-Test, Friendswood, TX). Aliquots (100 μg) of total RNA were treated with deoxyribonuclease I (DNA-free; Ambion). cDNA synthesis was initiated from 2 μg of deoxyribonuclease I-treated RNA using random hexamer primers and Taqman Reverse Transcription Reagents (Applied Biosystems, ABI). For each real time PCR reaction, which was carried out in triplicate, cDNA synthesized from 20 ng of deoxyribonuclease I-treated RNA was mixed with 2X SYBR Green PCR Master Mix (ABI). Samples were analyzed on an ABI PRISM 7900HT Sequence Detection System.

Oligonucleotide primer sequences used in these experiments were: CYP2R1 mRNA – 5'-CAGAAAGACGCTGAAAGTGCAA-3' and 5'-CAGTGTATTTGTGTTTACTTGGCTTTATAA-3'; CYP24A1 mRNA – 5'-CTCCCTATGGATGCAGTATGTATAGTG-3' and 5'-TTTAAAAACGTTGTCAGTAGGTCATAACT-3'; CYP27A1 mRNA – 5'-GGAGGGCAAGTACCCAATAAGA-3' and 5'-TGCGATGAAGATCCCATAGGT-3'; CYP27B1 mRNA – 5'-TCAGCAGGCATCGCAGAAC-3' and 5'-GCATTGGATCCTGAGGAATGA-3'; cyclophilin mRNA – 5'-TGGAGAGCACCAAGACAGACA-3' and 5'-TGCCGGAGTCGACAATGAT-3'.

RESULTS

An expression cloning assay was established in cultured cells and optimized to isolate cDNAs encoding enzymes capable of activating vitamin D_3 by 25-hydroxylation. The vitamin D-responsive reporter system consisted of a plasmid encoding a chimeric protein composed of the DNA binding domain of the yeast GAL4 transcription factor fused to the ligand binding domain of the human vitamin D receptor, and a reporter plasmid in which luciferase expression was directed by a heterologous promoter consisting of four GAL4 DNA response elements linked to basal expression elements from the herpes simplex 1 thymidine kinase (TK) gene; this receptor-reporter system is referred to as GAL4-VDR/GAL4-Luciferase. The introduction of these plasmids into HEK 293 cells followed by the addition of saturating levels of $1\alpha,25$-dihydroxyvitamin D_3 to the culture medium led to a >700-fold increase over background of luciferase enzyme activity versus that observed in the absence of ligand (data not shown).

To determine the maximum number of cDNAs that could be assayed at one time in the expression screen, dilution experiments were performed with the sterol 27-hydroxylase (CYP27A1) expression plasmid, the receptor-reporter system, and the precursor substrate, 1α-hydroxyvitamin D_3. A luciferase enzyme activity that was three-fold over background was observed when the sterol 27-hydroxylase plasmid was diluted 190-fold with a control plasmid lacking a cDNA insert. These results indicated that a cDNA pool size of approximately 100-200 could be reliably screened in the expression cloning assay when 1α-hydroxyvitamin D_3 was used as the precursor. They also confirmed that the sterol 27-

hydroxylase enzyme is capable of 25-hydroxylating both vitamin D_3 and 1α-hydroxyvitamin D_3 (Guo et al., 1993; Holmberg et al., 1986; Saarem and Pedersen, 1985).

To avoid isolating cDNAs encoding the sterol 27-hydroxylase, the cDNA library used in these studies was constructed using poly(A)$^+$ mRNA isolated from livers of mice lacking sterol 27-hydroxylase (Rosen et al., 1998). The resulting library was estimated to contain 7.9 x 10^6 independent transformants with an average cDNA insert size of 1.5 kilobases (kb). Aliquots of the library containing ~100 cDNAs were transfected together with the GAL4-VDR/GAL4-Luciferase receptor-reporter plasmids into HEK 293 cells. The data generated from one such experiment is shown in Fig. 1. One cDNA pool (A11) produced a luciferase enzyme activity that was approximately two-fold over that generated in mock transfected cells. Subsequent cycles of cDNA purification and screening were performed on the A11 pool to identify a single cDNA that encoded the vitamin D activating activity.

A total of ~110,000 cDNAs in 1056 pools were screened. Seven positive cDNA pools were identified, revealing four different encoded proteins. cDNAs for the retinoid X receptor α, hypoxia induction factor 1α, and the SEC14-related protein (GenBank^{TM}/EBI Data Bank accession number NM_144520) produced a luciferase signal over background. Stimulation by the retinoid X receptor α protein may reflect a shortage of this vitamin D receptor heterodimerization partner in the HEK 293 cells. Similarly, enhancement by the hypoxia induction factor 1α is most likely due to synergism between the receptor and this transcription factor. The mechanism by which the SEC14-related protein stimulated expression remains unknown but the effect was modest (≤ two-fold).

The cDNA in the A11 pool that stimulated vitamin D receptor activity encoded cytochrome P450 2R1 (CYP2R1) based on sequence comparisons among gene family members (http://drnelson.utmem.edu/CytochromeP450.html). The amino acid sequence of the CYP2R1 protein was deduced from the isolated mouse cDNA (GenBank™/EBI Data Bank accession number AY323818), and the amino acid sequence of the human enzyme (GenBank™/EBI Data Bank accession number AY323817) was generated from a cDNA isolated from liver mRNA using PCR (Fig. 2*A*). The two enzymes share 89% sequence identity at the amino acid level (Fig. 2*A*), and the coding regions of the two cDNAs share 89% identity at the nucleic acid level. The human *CYP2R1* gene is located on chromosome 11, band p15.2, and contains five exons distributed over approximately 15.5 kb (Fig. 2*B*). The mouse *Cyp2r1* gene occupies a syntenic location on chromosome 7, band 7E3. The mouse CYP2R1 mRNAs are ~1.6 and 1.1 kb in length, with the larger form being more abundant than the smaller form (data not shown).

The high degree of sequence conservation between mouse and human CYP2R1 protein sequences, and the ability of this enzyme to activate 1α-hydroxyvitamin D_3, suggested that it might be a vitamin D 25-hydroxylase. This hypothesis was tested further in a series of transfection experiments with different cytochrome P450 cDNAs, vitamin D receptor constructs, and reporter genes. Vitamin D_3 rather than 1α-hydroxyvitamin D_3 was utilized as a precursor since 25-hydroxyvitamin D_3 also activates the vitamin D receptor, albeit with decreased potency compared to the 1α,25-dihydroxy compound (Takeyama et al., 1997). Transfection of the mouse or human CYP2R1 cDNA increased luciferase expression approximately 7-10-fold in the GAL4-VDR/GAL4-luciferase reporter system (Fig. 3*A*). A

similar stimulation was observed when a plasmid encoding the mouse sterol 27-hydroxylase (mCYP27A1) was introduced into the HEK 293 cells. As negative controls, neither the expression vector alone (pCMV6), nor a vector expressing the human cytochrome P450 3A4 cDNA (hCYP3A4), stimulated the expression of luciferase enzyme activity (Fig. 3*A*).

Similar responses were ascertained when the receptor-reporter system was switched to one composed of the intact vitamin D receptor and a luciferase reporter gene driven by three copies of a vitamin D response element from the mouse osteopontin gene linked to a basal TK promoter (Fig. 3*B*). Plasmids expressing these genes are referred to as the VDR/VDRE-Luciferase system. Here, expression of the human or mouse CYP2R1 cDNAs led to marked stimulation of luciferase enzyme activity (16- and 17-fold, respectively), as did expression of the mCYP27A1 cDNA (18-fold).

The final receptor-reporter system tested was composed of the intact vitamin D receptor and a 0.862 kb DNA fragment encompassing the promoter of the mouse osteopontin gene linked to the luciferase reporter gene (VDR/Osteopontin-Luciferase). Previous studies showed that the osteopontin regulatory sequences contain a bona-fide vitamin D responsive element (Barletta et al., 2002). The basal luciferase expression level observed in this system in the presence of the control CMV or hCYP3A4 plasmids was substantial (Fig. 3*C*). Nevertheless, transfection of the human or mouse CYP2R1 cDNAs consistently produced a 2-3-fold stimulation of luciferase activity. This level of stimulation by vitamin D$_3$ is similar to that reported in other studies with the osteopontin promoter (Barletta et al., 2002).

We next tested the ability of the CYP2R1 enzymes to work in concert with the CYP27B1 vitamin D 1α-hydroxylase to activate vitamin D precursors. These experiments

proved challenging for three reasons. First, 1α-hydroxyvitamin D_3 generated by the CYP27B1 enzyme has some agonist activity on the vitamin D receptor (Takeyama et al., 1997). Second, 25-hydroxyvitamin D_3 generated by the CYP2R1 or CYP27A1 enzymes also has significant agonist activity (Fig. 3); and third, there is a low level of endogenous CYP2R1 enzyme activity expressed in the HEK 293 cells, which is very active against 1α-hydroxyvitamin D_3 generated in situ following transfection with the CYP27B1 cDNA.

Despite these challenges, informative data were generated in transfection experiments with the various P450 expression vectors. As shown in Fig. 4*A*, when the GAL4-VDR/GAL4-Luciferase system was employed using vitamin D_3 as a substrate, transfection of the CYP27B1 1α-hydroxylase cDNA alone led to a 470-fold stimulation of luciferase enzyme activity. This increase presumably represents the synthesis and activation of the receptor by both the 1α-hydroxylated form of vitamin D_3 produced by CYP27B1 and the further 25-hydroxylation of this product by the endogenous CYP2R1. Co-transfection with the CYP27B1 and the human CYP2R1 cDNA increased the level of stimulation to 670-fold, and similar responses were observed when the CYP27B1 and CYP27A1 cDNAs were co-transfected. The latter fold-stimulations were roughly equivalent to those measured when cells transfected with the receptor-reporter system alone were incubated with 10 nM 1α,25-dihydroxyvitamin D_3 (Fig. 4*A*). Similar increases were observed when the VDR/VDRE-Luciferase and VDR/Osteopontin-Luciferase systems were used to monitor vitamin D activation (Figs. 4*B*, 4*C*). The stimuli ascertained upon co-transfection of the vitamin D 1α-hydroxylase and 25-hydroxylase cDNAs were modestly but reproducibly higher than those determined with the vitamin D 1α-hydroxylase cDNA alone.

To determine the specificity of CYP2R1, the capacity of the encoded protein to activate or inactivate ligands for other nuclear receptors was determined. Expression of human CYP2R1 cDNA was found to have no effect on the abilities of the following receptor/ligand pairs to stimulate luciferase reporter genes: human thyroid hormone receptor β/triiodothyronine, mouse liver X receptor α/T0901317, human farnesoid X receptor/GW4064, human retinoic acid receptor α/(E)-4-[2-(5,6,7,8-tetrahydro-5,5,8,8-tetramethyl-2-naphthylenyl)-1-propenyl]benzoic acid, and mouse peroxisomal proliferator receptor γ/rosiglitazone (data not shown).

The experiments reported in Figs. 3 and 4 used single amounts of CYP expression plasmids and single concentrations of vitamin D_3 precursor to demonstrate activation of the receptor-reporter systems. To assess the effects of changing the concentrations of these components, dose-response curves were generated in two different ways. In the first, which utilized the VDR/VDRE-Luciferase system, the amount of P450 or control expression plasmid was varied and the level of 1α-hydroxyvitamin D_3 substrate was held constant. The data from this experiment showed an increase in luciferase enzyme expression with increasing amounts of human or mouse CYP2R1 expression plasmid added to the dish (Fig. 5A). Saturation of the response system was reached when 10 ng of P450 expression plasmid was added to the cells. A similar hyperbolic curve was observed when the mouse CYP27A1 expression plasmid was used but the relative level of enzyme activity measured at saturation was 50% less, which may be a consequence of an intrinsically lower activity of the CYP27A1 enzyme against 1α-hydroxyvitamin D_3 (Guo et al., 1993). No increase in

luciferase enzyme activity was observed when mouse adrenodoxin or human CYP3A4 were expressed in these cells (Fig. 5A).

In the second experiment, levels of vitamin D_3 were varied and the amounts of the P450 expression plasmids were held constant (Fig. 5B). In these experiments, CYP2R1 was more robust than CYP27A1 in generating an active receptor at low levels of vitamin D_3, but this difference was lost at higher concentrations of the precursor. Expression of the CYP27B1 1α-hydroxylase led to an even higher level of luciferase enzyme activity for the reasons noted above. The most potent combination of plasmids was composed of the human CYP2R1 and mouse CYP27B1, which generated a measurable luciferase signal at the lowest concentration (50 nM) of vitamin D_3 assayed (Fig. 5B).

Mitochondrial vitamin D 25-hydroxylase shows a preference for vitamin D_3 over vitamin D_2 as a substrate (Guo et al., 1993; Holmberg et al., 1986). This preference, and the well known ability of both secosteroids to fulfill the physiological roles of the vitamin, supports the existence of additional mammalian vitamin D 25-hydroxylases (Jones et al., 1998). To determine the substrate preference of the CYP2R1 enzyme, activation of both vitamin D precursors was assessed using the VDR/VDRE-Luciferase receptor-reporter system. These experiments revealed that the human CYP2R1 activated vitamin D_3 and D_2 equally well, and that as expected, CYP27A1 showed a preference for vitamin D_3 (Fig. 6). This difference in substrate preference also was observed when the 25-hydroxylases were used in combination with the CYP27B1 1α-hydroxylase. No activation of either vitamin D precursor was observed when the cells were transfected with a CMV vector alone (Fig. 6).

The inactivation of vitamin D is mediated by the vitamin D 24-hydroxylase enzyme, a microsomal P450 (CYP24A1) that is highly selective for this substrate (Jones et al., 1998). If the activation of vitamin D mediated by the CYP2R1 enzyme was due to 25-hydroxylation, then co-transfection of a 24-hydroxylase cDNA with the CYP2R1 cDNA should lead to inactivation of the ligand, and a consequent reduction in luciferase enzyme activity. As shown in Fig. 7, co-transfection of HEK 293 cells with the VDR/VDRE-Luciferase receptor-reporter system and the 24-hydroxylase cDNA reduced luciferase activity in response to ligand generated from vitamin D_3 by the human CYP2R1 enzyme (presumably 25-hydroxyvitamin D_3), and by a combination of the CYP2R1 and vitamin D 1α-hydroxylase enzyme (presumably 1α,25-dihydroxyvitamin D_3).

The experiments with the vitamin D 24-hydroxylase expression plasmid suggested that the active vitamin D ligand generated by the CYP2R1 enzyme was 25-hydroxyvitamin D. This interpretation was confirmed in chemical and immunological experiments (Fig. 8*A*). Transfection of a CYP2R1 cDNA into HEK 293 cells followed by incubation with ^{14}C vitamin D_3 led to the synthesis of a radiolabeled product that migrated on a thin layer chromatography plate at the same position as 25-hydroxyvitamin D_3. Similarly, expression of the sterol 27-hydroxylase, a known vitamin D_3 25-hydroxylase, produced an apparently identical product (lane 4). Transfection with the vector alone (lane 1) or with a cDNA encoding mouse adrenodoxin (lane 3) did not lead to synthesis of this product. Similar results were observed when three different solvent systems were used to develop the thin layer chromatography plates (data not shown).

A radioimmunoassay was used to measure the production of 25-hydroxyvitamin D_3 (Fig. 8*B*). Expression of mouse or human CYP2R1 cDNAs in the presence of 0.5 μM vitamin D_3 led to the synthesis of ~25 nM of 25-hydroxyvitamin D_3. A comparable level of synthesis was measured after expression of the sterol 27-hydroxylase cDNA (Fig. 8*B*). Doubling the level of vitamin D_3 substrate to 1 μM led to a corresponding two-fold increase in 25-hydroxyvitamin D_3 production (to approximately 50 nmol/l) with all three cDNAs. In this experiment, the sterol 27-hydroxylase enzyme was more active at higher substrate concentrations than was CYP2R1. Similar results were obtained when the synthesis of 1α,25-dihydroxyvitamin D_3 from 1α-hydroxyvitamin D_3 was assessed in transfected cells. When the concentration of this substrate added to the medium was 1 nM, cells expressing CYP2R1 produced 0.26 nM of 1α,25-dihydroxyvitamin D_3 versus 0.13 nM for CYP27A1 expressing cells. Taken together, the data shown in Figs 1-8 indicated that CYP2R1 is a vitamin D 25-hydroxylase.

The tissue distribution of the CYP2R1 mRNA was determined in the mouse by real time PCR and compared to those of the CYP27A1 sterol 27-hydroxylase, CYP27B1 vitamin D 1α-hydroxylase, and CYP24A1 vitamin D 24-hydroxylase mRNAs (Fig. 9). These experiments revealed that CYP2R1 mRNA was most abundant in the liver and testis[2] and present in lower levels in numerous other tissues and cell types. The CYP27A1 mRNA was present at high levels in liver and muscle, and detectable in all other tissues tested. As expected, the CYP27B1 and CYP24A1 mRNAs were most abundant in the kidney and present in much lower amounts in other tissues. Inasmuch as threshold values (C_T) determined for different mRNAs with different primer pairs can be compared, it is interesting

to note that the C_Ts for the CYP2R1, CYP27B1, and CYP24A1 mRNAs in the liver and kidney are in the same range (C_T = 25-26), whereas that for the hepatic CYP27A1 mRNA is far higher (C_T = ~18). In separate experiments for which the data are not shown, the C_T values determined for the CYP2R1 mRNA in male and female mouse liver were 24.7 and 24.6, respectively, indicating the absence of sexual dimorphism in the expression of this gene.

DISCUSSION

We report the isolation and characterization of a cDNA encoding a vitamin D 25-hydroxylase. Expression cloning using a vitamin D receptor ligand activation assay identified one cDNA from among ~110,000 in a mouse liver library that specified this enzyme activity. DNA sequence analysis revealed a highly conserved orphan cytochrome P450 enzyme, termed CYP2R1, which is predicted to reside in the microsomal membrane. The product of the CYP2R1 enzyme co-migrated with authentic 25-hydroxyvitamin D_3 on thin layer chromatography, and was detected in a radioimmunoassay using antibodies directed against 25-hydroxylated forms of vitamin D_3. Expression of the CYP2R1 enzyme in cultured cells stimulated the transcriptional activity of the vitamin D receptor in three different reporter gene systems, acted synergistically with the CYP27B1 vitamin D 1α-hydroxylase to produce a more potent ligand, and was antagonized by co-expression of the CYP24A1 vitamin D 24-hydroxylase. Unlike the CYP27A1 sterol 27-hydroxylase, which showed specificity for vitamin D_3, the CYP2R1 enzyme hydroxylated both vitamin D_2 and vitamin D_3. CYP2R1 mRNA is present in the liver where it is predicted to play an important role in the activation of vitamin D.

Studies over the last thirty years identified vitamin D 25-hydroxylase activities in both microsomal (Bhattacharyya and DeLuca, 1974; Madhok and DeLuca, 1979) and mitochondrial membranes (Bjorkhem and Holmberg, 1978) that were associated with cytochrome P450 enzymes. Purification of the mitochondrial protein (Dahlback and Wikvall, 1988; Masumoto et al., 1988), and subsequent cDNA cloning (Andersson et al.,

1989; Su et al., 1990; Usui et al., 1990), yielded the CYP27A1 sterol 27-hydroxylase, which in addition to hydroxylating vitamin D, catalyzed 27-hydroxylation of sterol intermediates in the bile acid biosynthetic pathway (Russell, 2003). Anomalies of cholesterol catabolism are a characteristic feature of sterol 27-hydroxylase deficiency in humans and mice, but affected individuals (Bjorkhem et al., 2001) and animals (Rosen et al., 1998) do not exhibit signs of vitamin D insufficiency suggesting that another enzyme, presumably the microsomal activity, compensates for the loss of CYP27A1-mediated vitamin D 25-hydroxylation.

Several lines of evidence are consistent with the notion that the CYP2R1 enzyme identified here is the microsomal vitamin D 25-hydroxylase. First, CYP2R1 has characteristic sequence features associated with a P450 of the endoplasmic reticulum, including a hydrophobic amino terminus (Fig. 2), and sequences involved in the interaction with the cytochrome P450 reductase cofactor (Peterson and Graham, 1998). CYP2R1 does not contain a signature sequence associated with mitochondrial P450 proteins, CXX(R/K)(R/K), which is located towards the carboxyl-terminus and includes the cysteine ligand of the heme co-factor (Graham and Peterson, 2002). The mouse CYP2R1 is 89% identical in sequence to the human enzyme (Fig. 2*A*), and is conserved through evolution at least through the bony fish *Takifugu rubripes* (Nelson, 2003). Highly conserved P450 enzymes are often those with endogenous substrates, such as sterols, fatty acids, and vitamins, and CYP2R1 fits this pattern. In addition, vitamin D receptor orthologues are reported for several different species of fish, including *Takifugu rubripes* (GenBank Accession numbers AF164512, BAA95016, AJ243956, Ensemble Gene ID

SINFRUG00000063876), suggesting that CYP2R1 may perform a similar activation function in teleosts.

A second line of evidence is that the substrate specificity of CYP2R1 closely resembles that of the microsomal vitamin D 25-hydroxylase. Experiments in cultured cells with different receptor-reporter systems show that CYP2R1 activates vitamin D_2, vitamin D_3, and 1α-hydroxyvitamin D_3 (Figs. 3-6). The ability to 25-hydroxylate both ergocalciferol (D_2) and cholecalciferol (D_3) is a characteristic of the microsomal vitamin D 25-hydroxylase but not the mitochondrial CYP27A1 sterol 27-hydroxylase (Guo et al., 1993). Although the typical order of vitamin D hydroxylation events is thought to be 25-hydroxylation in the liver followed by 1α-hydroxylation in the kidney or other target tissues (Jones et al., 1998), biochemical data show that the microsomal 25-hydroxylase also is capable of utilizing the 1α-form of the vitamin as a substrate (Saarem and Pedersen, 1985).

In several experiments (e.g., Fig. 5*B*, 8*B*), the mitochondrial CYP27A1 enzyme was more active at higher concentrations of vitamin D_3 substrate than was CYP2R1. This behavior represents a third line of evidence in support of CYP2R1 being the microsomal vitamin D 25-hydroxylase since in vivo data (Fukushima et al., 1976) and in vitro data (Bjorkhem and Holmberg, 1978; Bjorkhem et al., 1980; Madhoc and DeLuca, 1979) suggest that the mitochondrial hydroxylase is a low-affinity, high capacity enzyme whereas the microsomal hydroxylase is a high-affinity, low capacity enzyme. While the reasons for these apparently different kinetic properties were not determined here, future experiments with the recombinant CYP27A1 and CYP2R1 enzymes should reveal whether they are related to

transport of the vitamin into the mitochondrion or microsome, differences in the biochemical characteristics of the two enzymes, or other parameters.

The tissue distribution of the encoding mRNA represents a fourth line of evidence that CYP2R1 is the microsomal 25-hydroxylase (Fig. 7). In the rat, and presumably the mouse, the liver is the major site of vitamin D 25-hydroxylation as judged by the failure of hepatectomized animals to synthesize this intermediate following intravenous injection of radiolabeled vitamin D (Ponchon and DeLuca, 1969; Ponchon et al., 1969). In agreement with this tissue selectivity, CYP2R1 mRNA is most abundant in the liver ($C_T \sim 24.9$, Fig. 7). The mRNA is present also in the testis at similar levels ($C_T \sim 25.0$)[2], and in lower amounts in other organs and cell types. Not all mRNAs present in the testis are translated (Kleene, 2001), and we have not been successful in raising antibodies directed against the CYP2R1 protein to determine whether the enzyme is present in this tissue. Furthermore, the experimental design used to detect hepatic 25-hydroxyvitamin D synthesis noted above may have missed inter-conversion in the testis due to the blood-testis barrier (Setchell and Waites, 1975). For these reasons it is not clear whether CYP2R1 enzyme activity is expressed in the testis, or if it is, what the physiological significance of this expression might be.

Several microsomal P450 enzymes with vitamin D 25-hydroxylase activity have been identified in other species. For example, rat CYP2C11 is a male-specific enzyme with this activity but is unique to this species and does not act on vitamin D_2 (Andersson et al., 1983; Andersson and Jornvall, 1986). Pig CYP2D25 25-hydroxylates both vitamin D_2 and D_3 but there is no corresponding orthologue for this P450 in humans (Hosseinpour and Wikvall, 2000). The human CYP2D6 protein shares the greatest sequence identity (77%) with the pig

CYP2D25 but the CYP2D6 enzyme does not possess vitamin D 25-hydroxylase activity (Hosseinpour and Wikvall, 2000). In contrast to these findings, the CYP2R1 enzyme reported here is not sexually dimorphic, is conserved from fish to humans, and acts on both forms of vitamin D. Sequence identity between the human CYP2R1 and the other rat, pig and human vitamin D 25-hydroxylase enzymes varies between 33 and 39%, as would be expected from their inclusion in the CYP2 family (Nelson et al., 1996). In addition, the human CYP2R1 sequence shares little identity with a P450 enzyme isolated from the bacterium *Amycolata autotrophica* that has vitamin D 25-hydroxylase activity (Kawauchi et al., 1994). Whether the limited sequence identity between these enzymes can be used to reveal important features of the substrate binding domain remains to be determined in structure-function studies.

The existence of two enzymes in humans and mice capable of 25-hydroxylating vitamin D raises the question of what are the relative contributions of CYP2R1 and CYP27A1 to activation? In attempting to answer this question, it is partially instructive to compare the specific activities of 25-hydroxylation in the microsomal and mitochondrial fractions. Values for these activities were reported by Bjorkhem and Holmberg (Bjorkhem and Holmberg, 1978), who used a quantitative mass spectrometry-based assay to determine a specific activity ranging from 48-157 pmol 25-hydroxyvitamin D_3 formed per 45 min for the microsomal enzyme, and 95-270 pmol/45 min for the mitochondrial enzyme. Assuming a one-to-one correspondence between these activities and the production of 25-hydroxyvitamin D in vivo suggests that the microsomal enzyme is responsible for ~30% of total activity and the mitochondrial enzyme 70%. A comparison of CYP2R1 and CYP27A1 mRNA levels

provides further insight into this question. As determined in real time PCR experiments, the C_T value for CYP2R1 mRNA in liver was ~24.9, while that for the CYP27A1 mRNA was ~17.8 (Fig. 7). This result indicates that CYP27A1 is the more abundant enzyme in the liver.

Extrapolation of these data, which suggest that CYP27A1 synthesizes a majority of 25-hydroxyvitamin D, to the in vivo production of the transformed vitamin must be done with caution. The biochemical measurements assume the absence of inhibitors in the crude membrane fractions used in the assay, equal accessibility to an otherwise hydrophobic substrate, and similar stabilities of the two enzymes following subcellular fractionation. The mRNA measurements assume the absence of post-transcriptional and translational control, equal amplification efficiencies of the primer pairs used in the PCR assay, and that both mRNAs are targeted to their respective membrane compartments with parity. Although these caveats prevent a definitive answer to the question of the relative contributions of CYP2R1 and CYP27A1 to vitamin D 25-hydroxylation, it is clear from analysis of humans (Bjorkhem et al., 2001; Rosen et al., 1998) and mice (Rosen et al., 1998) deficient in sterol 27-hydroxylase that the microsomal activity, which the current data suggest is CYP2R1, is able to fulfill this biological role. We are in the process of constructing mice with mutations in the CYP2R1 gene to gain further insight into the role of this P450 in vitamin D activation.

Figure 1. Expression cloning of vitamin D 25-hydroxylase cDNA. A cDNA library was constructed from hepatic mRNA purified from sterol 27-hydroxylase deficient mice and divided into pools of ~100 cDNAs each. Plasmid DNA (75 ng) from individual pools was combined with 20 ng of a GAL4-vitamin D receptor expression plasmid, 20 ng of a GAL4-responsive luciferase reporter gene plasmid, 20 ng of a CMV-β-galactosidase plasmid (for normalization purposes), 5 ng of a mouse adrenodoxin expression plasmid (to boost the activity of mitochondrial P450s encoded by the cDNA pools), and 10 ng of the VA1 plasmid (to increase expression from the receptor and reporter gene plasmids, (Schneider and Shenk, 1987)), and introduced via the FuGENE6 reagent (Roche) into HEK 293 cells cultured in microtiter plates. 1α-Hydroxyvitamin D_3 (10 nM) was added to the medium 8-10 h later. After a further incubation of 16-20 h in an atmosphere of 91.2 % air and 8.8 % CO_2, the cells were disrupted in the microtiter plate by the addition of 100-µl of Lysis Buffer, and aliquots of 20-µl and 40-µl were assayed by luminometry and spectroscopy, respectively, for luciferase and β–galactosidase enzyme activity. Relative luciferase activity was calculated for each well by dividing luciferase enzyme activity by the amount of β–galactosidase activity per unit of time. One pool of cDNAs (A11, marked by *asterisk*) produced a modest activation of the vitamin D receptor-reporter system compared to that obtained with the pCMV vector alone (-) and a positive control (+) consisting of a plasmid encoding the mouse CYP27A1 vitamin D 25-hydroxylase.
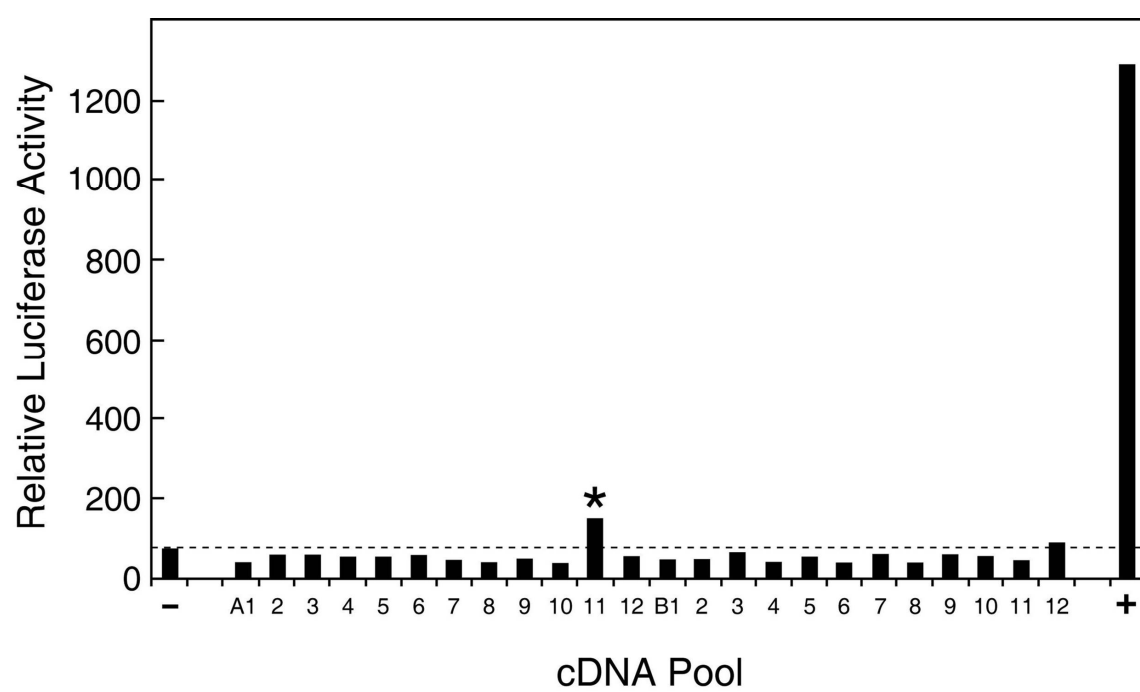
Figure 2. Amino acid sequences and gene structure of cytochrome P450 2R1. *A*, The deduced sequences of the human (*h*) and mouse (*m*) CYP2R1 proteins are aligned with identities between the two enzymes indicated by *black boxes*. Amino acids are numbered on the *left*. *Arrowheads* above the alignment indicate the positions of introns in the encoding genes. An *asterisk* indicates the cysteine residue that is predicted to ligand with the heme cofactor. The GenBank™/EBI Data Bank accession numbers for the human and mouse CYP2R1 cDNA sequences are AY323817 and AY323818, respectively. *B*, Structure of the human *CYP2R1* gene. Exons are indicated by *boxes* and introns by *connecting lines*. Amino acids encoded at the beginning and end of the protein are indicated *above* the gene schematic together with those at exon-intron junctions. The structure of the gene and its indicated chromosomal location were deduced by comparing the sequences of the cloned cDNA to those of the genomic DNA (GenBank™/EBI Data Bank accession number NT_009237.15).

A. Protein

```
1   M W K L W R A E E G A A A L G G A L F L L L F A L G V R Q L L K Q R R P M G F P h
1   M L E L P G A R A C A G A L A G A L L L L L F V L V V R Q L L R Q R R P A G F P m

41  P G P P G L P F I G N I Y S L A A S S E L P H V Y M R K Q S Q V Y G E I F S L D
41  P G P P R L P F V G N I C S L A L S A D L P H V Y M R K Q S R V Y G E I F S L D

81  L G G I S T V V L N G Y D V V K E C L V H Q S E I F A D R P C L P L F M K M T K
81  L G G I S T V V L N G Y D V V K E C L V H Q S E I F A D R P C L P L F M K M T K

121 M G G L L N S R Y G R G W V D H R R L A V N S F R Y F G Y G Q K S F E S K I L E
121 M G G L L N S R Y G R G W I D H R R L A V N S F H Y F G S G Q K S F E S K I L E

161 E T K F F N D A I E T Y K G R P F D F K Q L I T N A V S N I T N L I I F G E R F
161 E T W S L I D A I E T Y K G G P F D L K Q L I T N A V S N I T N L I L F G E R F

201 T Y E D T D F Q H M I E L F S E N V E L A A S A S V F L Y N A F P W I G I L P F
201 T Y E D T D F Q H M I E L F S E N V E L A A S A P V F L Y N A F P W I G I L P F

241 G K H Q Q L F R N A A V V Y D F L S R L I E K A S V N R K P Q L P Q H F V D A Y
241 G K H Q R L F R N A D V V Y D F L S R L I E K A A V N R K P H L P H H F V D A Y

281 L D E M D Q G K N D P S S T F S K E N L I F S V G E L I I A G T E T T T N V L R
281 L D E M D Q G Q N D P L S T F S K E N L I F S V G E L I I A G T E T T T N V L R

321 W A I L F M A L Y P N I Q G Q V Q K E I D L I M G P N G K P S W D D K C K M P Y
321 W A I L F M A L Y P N I Q G Q V H K E I D L I V G H N R R P S W E Y K C K M P Y

361 T E A V L H E V L R F C N I V P L G I F H A T S E D A V V R G Y S I P K G T T V
361 T E A V L H E V L R F C N I V P L G I F H A T S E D A V V R G Y S I P K G T T V

401 I T N L Y S V H F D E K Y W R D P E V F H P E R F L D S S G Y F A K K E A L V P
401 I T N L Y S V H F D E K Y W K D P D M F Y P E R F L D S N G Y F T K K E A L I P

441 F S L G R R H C L G E H L A R M E M F L F F T A L L Q R F H L H F P H E L V P D
441 F S L G R R H C L G E Q L A R M E M F L F F T S L L Q Q F H L H F P H E L V P N

481 L K P R L G M T L Q P Q P Y L I C A E R R 501
481 L K P R L G M T L Q P Q P Y L I C A E R R 501
```

B. Human Gene

Chromosome 11p15.2
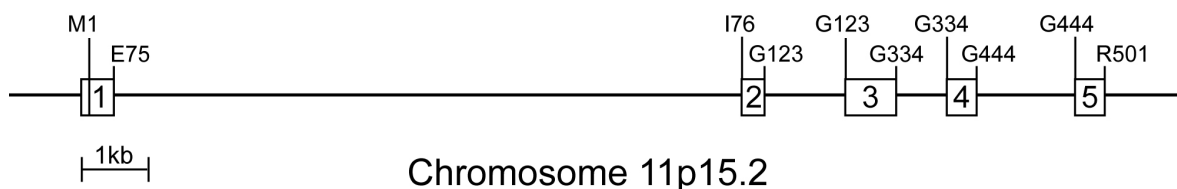
Figure 3. Activation of vitamin D$_3$ by CYP2R1. The indicated vitamin D receptor-reporter systems were introduced into HEK 293 cells grown in 60 mm dishes together with the expression plasmids designated at the *bottom* of the figure. Relative luciferase enzyme activity was determined 16-20 h later as indicated in "Experimental Procedures", and the means ± SEM for experiments carried out in triplicate were plotted as histograms. The amounts of vitamin D$_3$ added to the medium were 0.5 μM (*A, B*), and 1 μM (*C*).
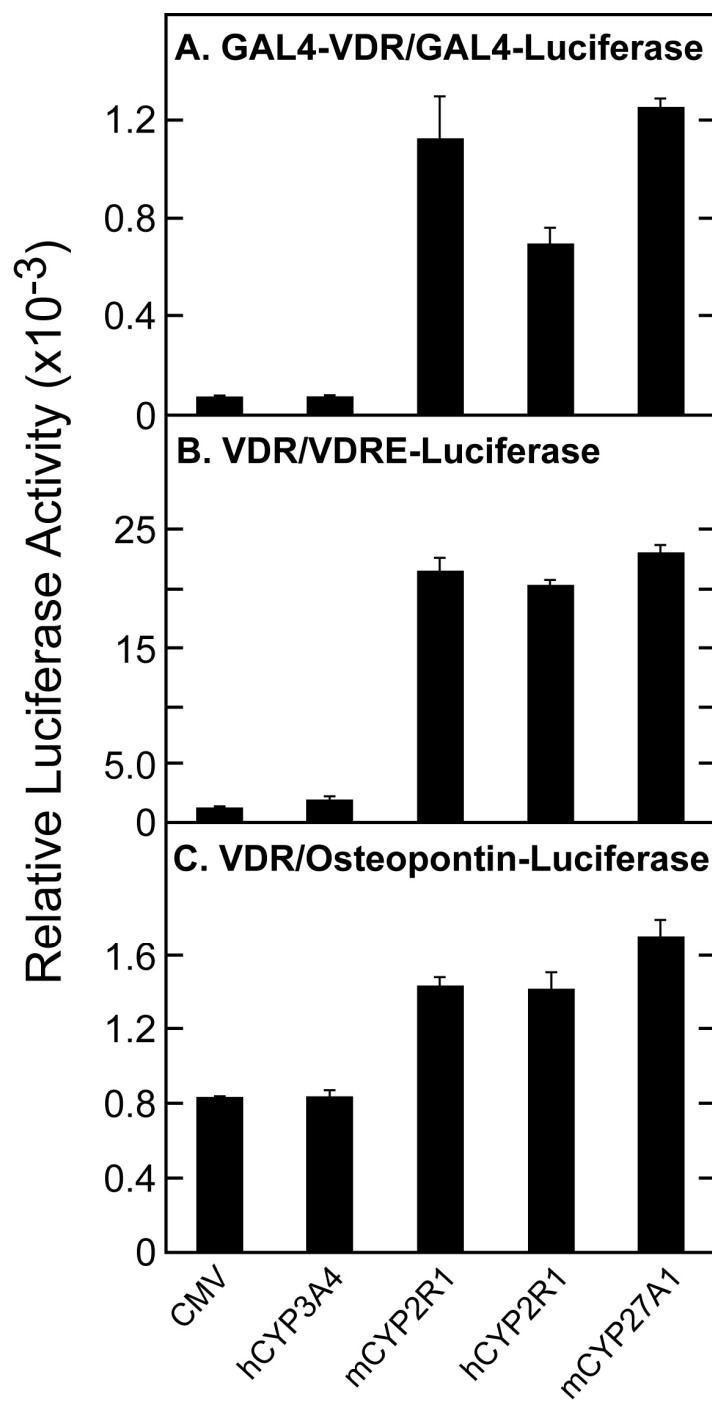
Figure 4. Activation of vitamin D_3 by cytochrome P450 enzymes. Plasmids encoding the indicated vitamin D receptor-reporter systems were transfected into HEK 293 cells grown in 60 mm dishes together with DNAs encoding the hydroxylase enzymes shown at the *bottom* of the figure. Relative luciferase enzyme activity was measured 16-20 h later and the means ± SEM of values derived from experiments performed in triplicate were calculated. The amounts of vitamin D_3 added to the culture medium were 0.5 μM (*A*), 0.25 μM (*B*), and 5 μM (*C*). 1α,25-dihydroxyvitamin D_3 (0.01 μM) was added in the absence of hydroxylase expression plasmids to control wells for the receptor-reporter systems to generate the data shown by the histogram bars on the *right* of each panel.

A. GAL4-VDR/GAL4-Luciferase

B. VDR/VDRE-Luciferase

C. VDR/Osteopontin-Luciferase

Relative Luciferase Activity ($\times 10^{-3}$)

CMV
mCYP27B1
mCYP27B1 hCYP2R1
mCYP27B1 mCYP27A1
1,25 Vitamin D_3
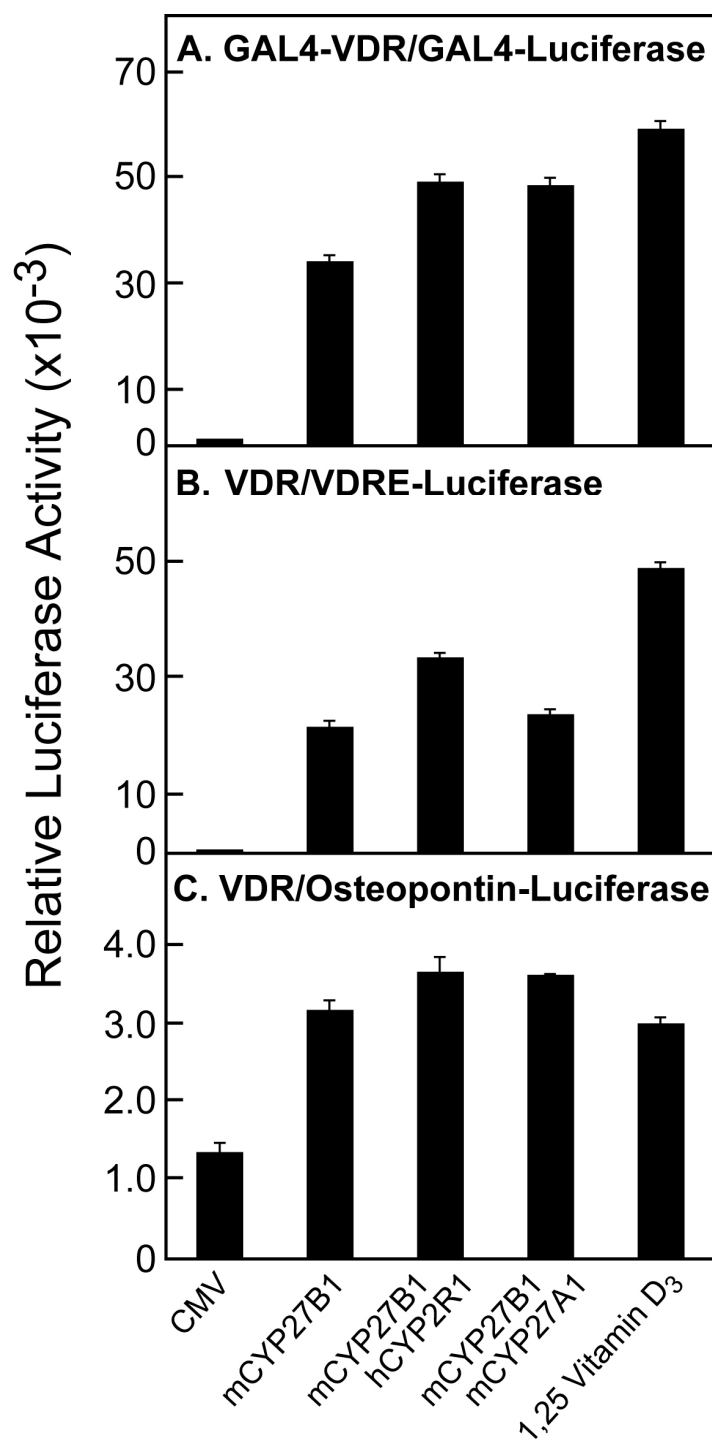
Figure 5. Response of VDR/VDRE-Luciferase reporter system to P450 expression vectors and vitamin D$_3$. *A,* The indicated amounts of P450 expression plasmids were introduced by transfection with the FuGENE6 reagent into HEK 293 cells grown in 60 mm dishes. Relative luciferase enzyme activities were measured 16-20 h later and means ± SEM calculated from individual experiments performed in triplicate. The concentration of 1α-hydroxyvitamin D$_3$ added to the culture medium was 1 nM. *B,* P450 expression vectors (5 to 20 ng plasmid DNA) were transfected into HEK 293 cells grown in 60 mm dishes in medium containing the indicated concentrations of vitamin D$_3$. Relative luciferase enzyme activities were determined 16-20 h later. Mean values based on data from triplicate dishes for each concentration of vitamin D$_3$ were plotted.

A.
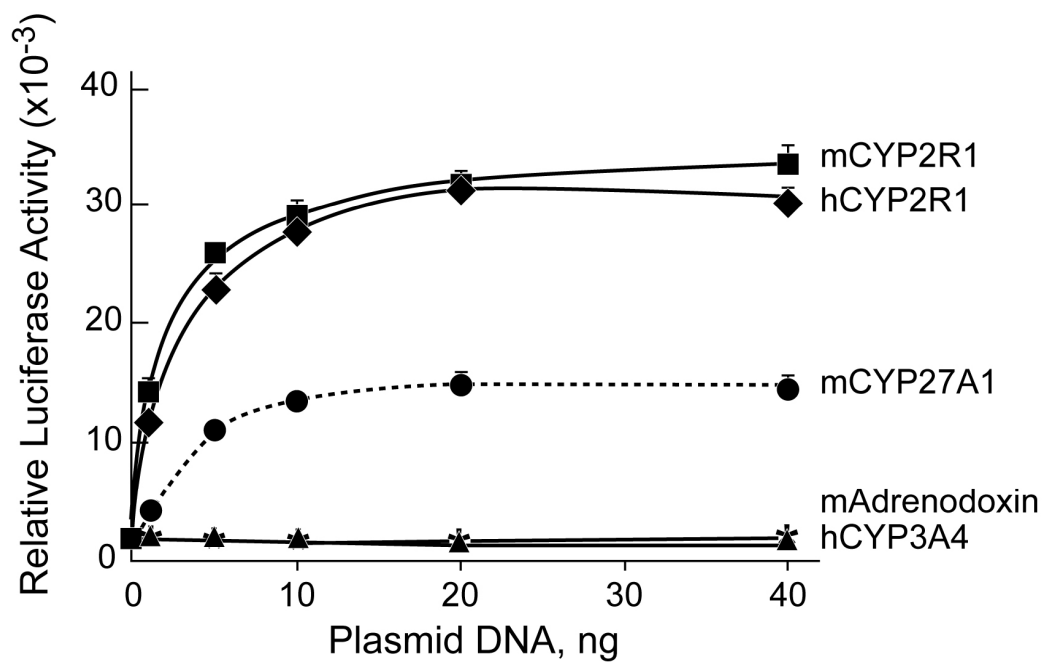
B.
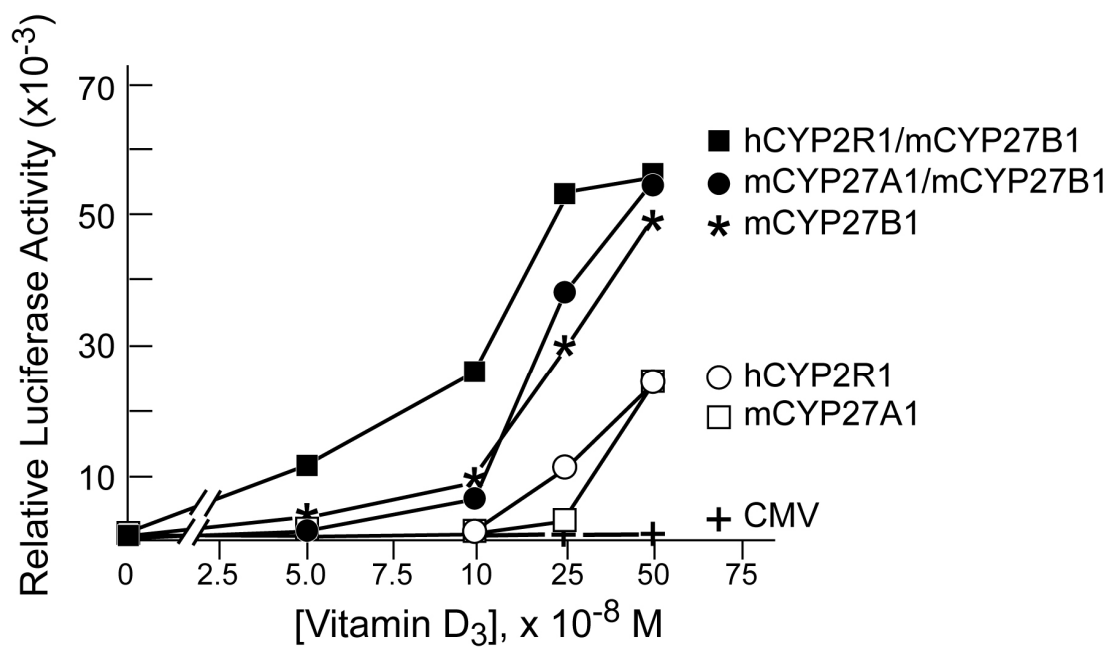
Figure 6. Activation of vitamin D_3 and vitamin D_2 by microsomal versus mitochondrial P450 enzymes. Vectors specifying the VDR/VDRE-Luciferase repoter system were introduced into HEK 293 cells grown in 60 mm dishes together with the indicated expression plasmids encoding no protein (CMV) or various vitamin D hydroxylases. Relative luciferase enzyme activities were measured 16-20 h later. The means ± SEM were calculated for each plasmid or combination of plasmids analyzed in triplicate. *A*, the concentration of vitamin D_3 in the medium of dishes transfected with the CMV, hCYP2R1, and mCYP27A1 plasmids (*left* three histogram bars) was 0.5 μM, and the concentration in the medium of dishes transfected with CMV, hCYP2R1 + mCYP27B1, and mCYP27A1 + mCYP27B1 plasmids (*right* three histogram bars) was 0.25 μM. *B*, the concentration of vitamin D_2 in the medium of dishes transfected with the CMV, hCYP2R1, and mCYP27A1 plasmids (*left* three histogram bars) was 0.5 μM, and that in the medium of dishes transfected with CMV, hCYP2R1 + mCYP27B1, and mCYP27A1 + mCYP27B1 plasmids (*right* three histogram bars) was 0.1 μM.
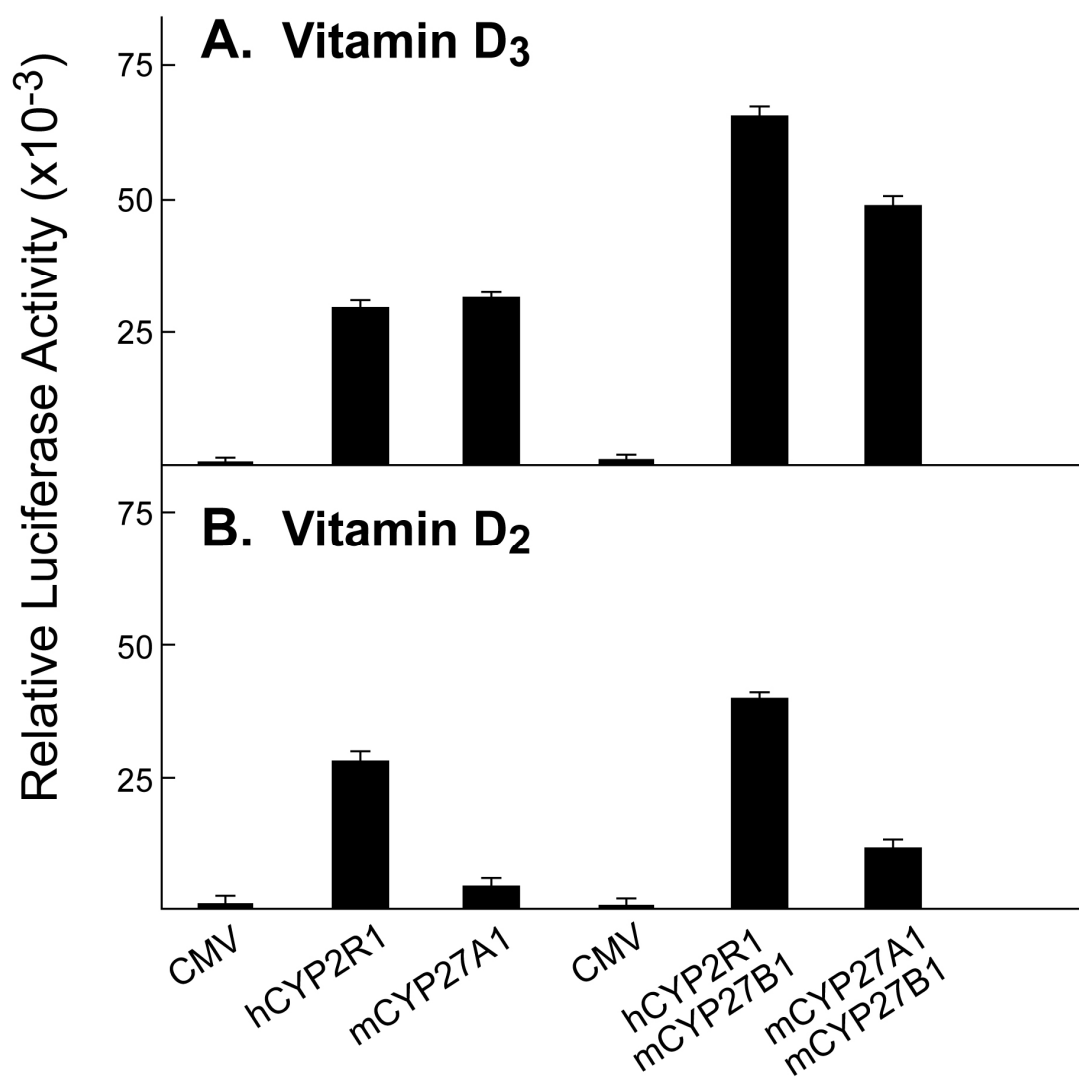
Figure 7. Inactivation of vitamin D metabolites by expression of CYP24A1 vitamin D 24-hydroxylase. The indicated plasmid or combinations of plasmid DNAs were introduced into HEK 293 cells cultured in 60 mm dishes together with vectors specifying the VDR/VDRE-Luciferase reporter system. Vitamin D_3 was added to the medium at a final concentration of 0.25 μM, and relative luciferase activity was measured in triplicate dishes 16-20 h later as described in "Experimental Procedures". Means ± SEM were calculated and plotted as histograms. Co-expression of the CYP24A1 vitamin D 24-hydroxylase with either the CYP2R1 25-hydroxylase, or a combination of CYP2R1 and the CYP27B1 1α-hydroxylase, led to a reduction of vitamin D receptor activation and lower luciferase enzyme activity.
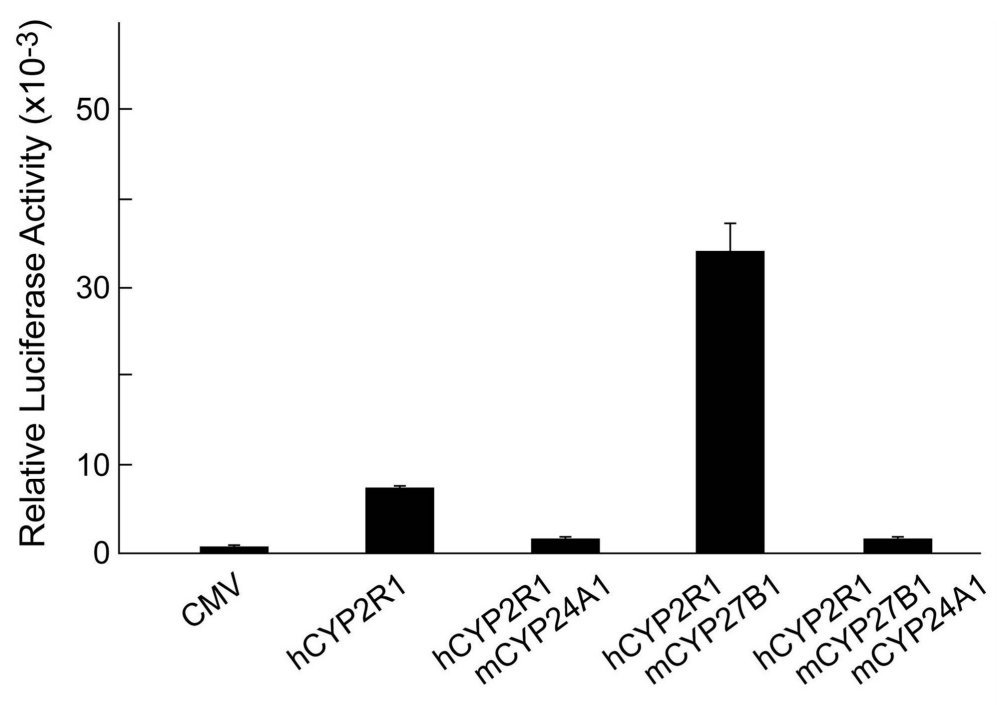
Figure 8. Biochemical and immunological identification of CYP2R1 vitamin D metabolites. *A,* The indicated expression plasmids were introduced into HEK 293 cells cultured in 60 mm dishes. 18 h later, ^{14}C labeled vitamin D_3 was added to the medium, and the incubation continued for an additional 96 h. Vitamin D metabolites were extracted from the medium into 8-ml of chloroform:methanol (2:1), dried under a stream of N_2, resuspended in 50-μl of acetone, and separated by thin layer chromatography on silica plates. The plates were dried and subjected to phosphorimage analysis to reveal the locations of radioactivity. The identities of the radiolabeled compounds were determined based on their co-migration with authentic vitamin D_3 and 25-hydroxyvitamin D_3 standards chromatographed in adjacent lanes on the plate. The mAdx plasmid expresses mouse adrenodoxin. *B*, Radioimmunoassay of vitamin D metabolites produced in transfected cells. The indicated plasmid expression vectors were introduced by transfection into HEK 293 cells grown in 96-well microtiter plates. 10 h later, 0.5 or 1 μM vitamin D_3 was added to the medium and the incubation continued for an additional 44 h. Thereafter, the medium from replicate wells was pooled and subjected to radioimmunoassay using a kit containing antibodies directed against 25-hydroxyvitamin D_3. The values obtained were compared to those of a standard curve to estimate the amount of 25-hydroxyvitamin D produced in duplicate dishes. A background value corresponding to the amount of 25-hydroxyvitamin D detected in the medium from cells transfected with the CMV vector plasmid (17.2 nM) was subtracted from the experimental values and the resulting number plotted as a histogram.

A.

B.
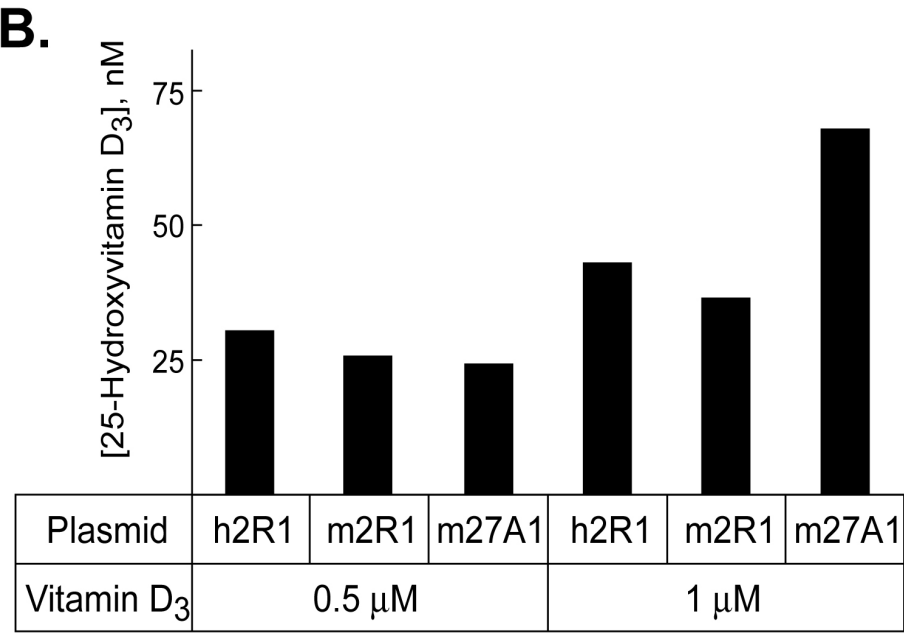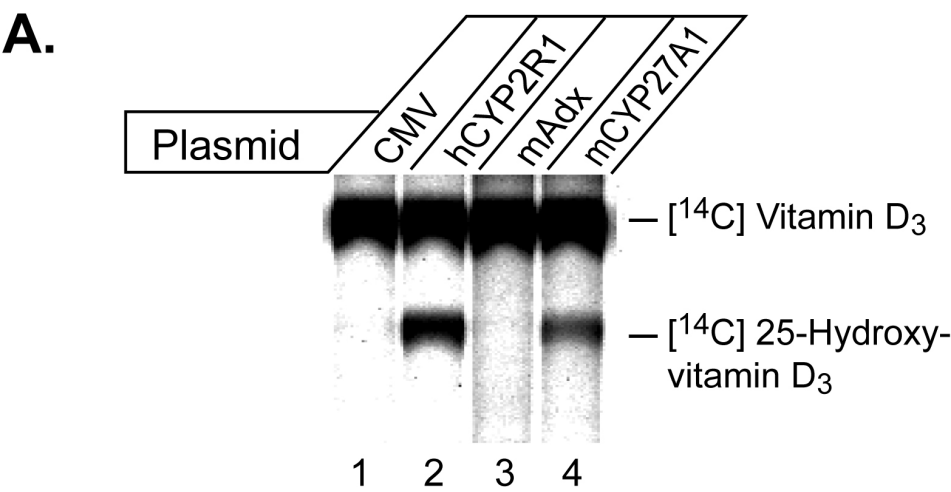
Figure 9. Tissue distributions of mouse vitamin D hydroxylase mRNAs. The relative levels of the vitamin D hydroxylase mRNAs were determined by real time PCR in the tissues and cell types indicated at the *bottom* of the figure using cyclophilin mRNA levels as a reference standard. The data for a given hydroxylase mRNA were normalized to the threshold (C_T) values determined in the liver for the CYP2R1 and CYP27A1 mRNAs (*top* two panels), and to the kidney C_T values for the CYP27B1 and CYP24A1 mRNAs (*bottom* two panels). WT liver, wild type liver; *Cyp27a1*$^{-/-}$ Liver, liver of CYP27A1 sterol 27-hydroxylase deficient mice; Sem. Vesicle, seminal vesicle; Per. Macrophage, peritoneal macrophages elicited by a thioglycolate challenge (Edelson et al., 1975); J774 Macrophage, transformed mouse macrophage cells (ATCC #TIB-67); S. Intestine, small intestine.
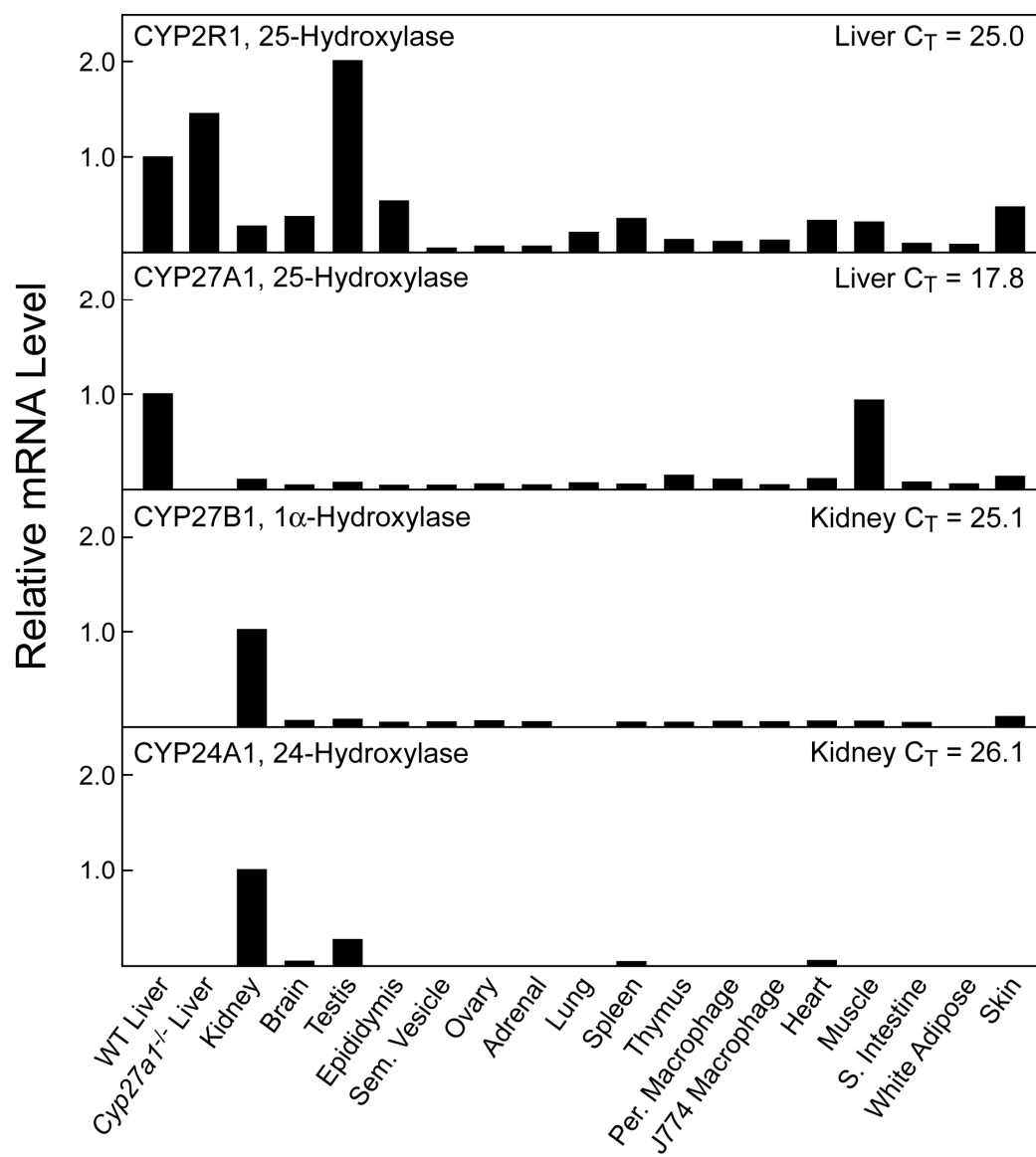
CHAPTER FOUR
GENETIC EVIDENCE THAT THE HUMAN CYP2R1 ENZYME IS A KEY VITAMIN D 25-HYDROXYLASE

INTRODUCTION

The metabolic pathway leading to the synthesis of active vitamin D[*] involves three reactions that occur in different tissues (Jones et al., 1998). The pathway is initiated in the skin with the ultraviolet light-mediated cleavage of 7-dehydrocholesterol to produce the secosteroid vitamin D_3. The second step occurs in the liver and is catalyzed by a cytochrome P450 enzyme that hydroxylates carbon 25, producing the intermediate 25-hydroxyvitamin D_3, which is the major circulatory form of the vitamin. The third and final step takes place in the kidney and involves 1α-hydroxylation by another cytochrome P450, producing $1\alpha,25$-dihydroxyvitamin D_3. This product is a potent ligand of the vitamin D receptor and mediates most of the physiological actions of the vitamin (Jones et al., 1998).

Although the chemical and enzymatic steps in the vitamin D_3 biosynthetic pathway have been known for 30 years (Jones et al., 1998), the enzyme catalyzing the 25-hydroxylation step in the liver has never been identified. At least six cytochrome P450s can catalyze this reaction in vitro, including CYP2C11, CYP2D25, CYP3A4, CYP2J1, CYP27A1, and CYP2R1 (Cheng et al., 2003; Gupta et al., 2004; Yamasaki et al., 2004b). Of these, the two most viable candidates for the vitamin D 25-hydroxylase are CYP27A1 and CYP2R1 (Cheng et al., 2003). Both enzymes are expressed in the liver and are conserved among species known to have an active vitamin D signaling pathway. However, mutations

in the human and mouse genes encoding the mitochondrial CYP27A1 protein impair bile acid synthesis but have no consequences for vitamin D metabolism (Bjorkhem et al., 2001; Cali et al., 1991; Repa et al., 2000; Rosen et al., 1998; Skrede et al., 1986). It is thus not clear whether the two vitamin D_3 25-hydroxylases represent an example of biological redundancy in an important biosynthetic pathway or whether CYP2R1 alone or some unidentified enzyme fulfills this essential role.

In contrast to the uncertainty surrounding vitamin D_3 25-hydroxylase, the renal enzyme responsible for 1α-hydroxylation of the vitamin is the cytochrome P450 CYP27B1 (Takeyama et al., 1997). This mitochondrial protein is expressed in the proximal renal tubules where activation of vitamin D_3 takes place (Nykjaer et al., 1999; Zehnder et al., 1999; Zhang et al., 2002). As predicted from the biosynthetic pathway, mutations in the gene encoding CYP27B1 cause selective $1\alpha,25$-dihydroxyvitamin D_3 deficiency (also referred to as vitamin D dependent rickets type I) in both humans (Kitanaka et al., 1998) and mice (Kato, 2001), in which 25-hydroxyvitamin D_3 accumulates in plasma and levels of $1\alpha,25$-dihydroxyvitamin D_3 are low (Liberman and Marx, 2001).

In the present study, we describe the molecular analysis of a patient with abnormally low plasma levels of 25-hydroxyvitamin D_3 and classic symptoms of vitamin D deficiency, including skeletal abnormalities, hypocalcemia and hypophosphatemia (Casella et al., 1994; Zerwekh et al., 1979). This individual is homozygous for a substitution mutation in exon 2 of the CYP2R1 gene on chromosome 11p15.2. The CYP2R1 mutation changes a leucine residue at position 99 to a proline and eliminates the vitamin D_3 25-hydroxylase activity of CYP2R1.

MATERIALS AND METHODS

Patient Description – This young man is from Nigeria and was evaluated for bone abnormalities of the lower extremities appearing between ages 2 to 7 years (Casella et al., 1994). Prior to treatment, he had low normal serum calcium levels (2.00-2.32 mM; normal range 2.12-2.62 mM), low serum phosphate levels (0.84-0.87 mM; normal range 0.97-1.45 mM), elevated serum alkaline phosphatase levels (2360-3000 U/l; normal range 100-320 U/L), serum 1α,25-dihydroxyvitamin D levels (137-142 pM) that were in the normal range (48-182 pM), and low 25-hydroxyvitamin D levels (10-12 nM; normal 25-137 nM). Lymphocytes from this individual were immortalized and stored for future study when he was first seen in the clinic. He and his family have since been lost to follow-up.

DNA sequencing - Genomic DNA was extracted from Epstein Barr virus-transformed lymphocytes using standard techniques (Sambrook and Russell, 2001). Exons 2, 3, and 5 of the human CYP2R1 gene were amplified separately by the polymerase chain reaction (PCR) using Platinum® *Taq* DNA Polymerase (Invitrogen). Exon 4 was amplified by PCR using *PfuTurbo*® Hotstart polymerase (Stratagene). The thermocycler program for exons 2 - 5 consisted of one cycle at 94ºC for 60 s, 35 cycles at 94ºC for 30 s, 55ºC for 30 s, and 72ºC for 150 s, followed by one cycle at 72ºC for 600 s. Exon 1 of the CYP2R1 gene was amplified by using the Advantage™ GC Genomic PCR kit (BD Biosciences). The thermocycler program consisted of one cycle at 95ºC for 60 s, 35 cycles at 94ºC for 30 s, and 68ºC for 180 s, followed by one cycle at 68ºC for 180 s. The nine exons of the CYP27A1 gene were amplified by the PCR as described previously (Leitersdorf et al., 1993). PCR products from

all amplification reactions were purified by low-speed centrifugation through a Centricon YM-100 filter device (Millipore) prior to DNA sequence analysis using fluorescently labeled dye-terminators and a thermostable DNA polymerase on an ABI Prism 3100 Genetic Analyzer (Perkin-Elmer).

Genomic DNA also was extracted from white blood cells of 50 unaffected African-American subjects (Mooser et al., 1997) and fifty Nigerian subjects (Cooper et al., 2002) using standard techniques. Exon 2 of the CYP2R1 gene was amplified from each of these control DNAs by the PCR and subjected to sequence analysis as described above.

Site Directed Mutagenesis - A plasmid containing a full-length human CYP2R1 cDNA (GenBank™/EBI Databank accession number AY323817) in the pCMV6 expression vector (GenBank™/EBI Databank accession number AF239250) was the starting template DNA for mutagenesis, which was performed using the QuikChange® kit (Stratagene). Nucleotide 296 of the CYP2R1 cDNA was mutated from thymine to cytosine using the sense oligonucleotide, 5'-TATGATGTAGTAAAGGAATGCCCTGTTCATCAAAGCGAAATTTTTG-3', and its complement. The cDNA insert of the engineered expression vector was sequenced to confirm the presence of the desired base pair change and to ensure the absence of spurious mutations. The insert was then excised by digestion with the restriction enzymes *Sal*I and *Not*I, and subcloned into an untreated pCMV6 expression vector.

Thin layer chromatography - Transfection of human embryonic kidney 293 cells (HEK 293, American Type Culture Collection CRL no. 1573), incubation with 4.6×10^{-7} M [4-^{14}C]vitamin D_3, extraction of lipids from cells and medium, and resolution of vitamin D

metabolites by thin layer chromatography were performed as described (Cheng et al., 2003).

A solvent system of cyclohexane:ethyl acetate (3:2, v/v) was used for thin layer

chromatography. Radiolabeled vitamin D metabolites were detected by phosphorimaging of

thin layer chromatography plates using Fuji BAS-TR2040 imaging plates (Fuji Medical

Systems, Tokyo, Japan) and a Storm 820 imaging system (Amersham Biosciences).

Vitamin D Receptor Activation Assay - Receptor activation assays were performed as

described (Cheng et al., 2003). Briefly, HEK 293 cells were grown in 96-well plates and

transfected with the indicated plasmid DNAs for a period of 8-10 hours. Vitamin D ligands

were then added to the medium in ethanol, and the cells cultured for an additional 16-20 h.

Experiments were terminated by cell lysis and measurements of β-galactosidase and

luciferase enzyme activities using appropriate substrates were performed (Cheng et al.,

2003).

Three different vitamin D receptor-(VDR)-luciferase (LUC) reporter gene systems

were used (Cheng et al., 2003). The Galactose 4 (GAL4)-VDR/GAL4-luciferase reporter

gene system consisted of the pCMX/GAL4-VDR and pTK-MH100X4-LUC plasmids.

pCMX/GAL4-VDR encodes a fusion protein composed of the GAL4 DNA binding domain

linked to the human vitamin D receptor ligand binding domain. pTK-MH100X4-LUC is a

reporter plasmid with four GAL4 DNA response elements linked to a viral thymidine kinase

(TK) promoter segment and the firefly luciferase gene. The VDR/vitamin D response

element (VDRE)-luciferase reporter gene system consisted of an expression plasmid

encoding a full length human VDR, and the pSPPX3-TK-LUC plasmid, which is a reporter

plasmid with three copies of the VDRE sequence from the mouse osteopontin gene linked to

a viral TK promoter element and the luciferase gene. The VDR/osteopontin-LUC reporter gene system consisted of the above human VDR expression plasmid coupled with the osteopontin-LUC plasmid, a reporter DNA containing 0.862 kb of the mouse osteopontin enhancer and promoter region linked to the luciferase gene.

RESULTS

We first defined the exon-intron structure of the human CYP2R1 gene. As shown in Fig. 1, computer-assisted comparison of the cDNA and genomic DNA revealed that the *CYP2R1* locus contains five exons separated by four introns that together span approximately 15 kilobases of DNA on human chromosome 11p15.2. A series of six oligonucleotide primer pairs were designed and synthesized to allow amplification and sequencing via the PCR of individual exons and their immediate flanking DNAs (Fig. 1). PCR reactions with these oligonucleotide primers and genomic DNA isolated from a normal individual confirmed the predicted CYP2R1 gene structure. For genetic analysis of the CYP27A1 gene, oligonucleotides for amplification of the nine exons were synthesized as described previously (Leitersdorf et al., 1993), optimal PCR conditions for their use were determined.

Genomic DNA from the patient with low 25-hydroxyvitamin D_3 levels and control individuals was extracted and amplified by the PCR using the CYP2R1 and CYP27A1 oligonucleotides, and individual products were subjected to DNA sequence analysis. These experiments revealed this individual is homozygous for a transition mutation (T → C) in exon 2 of the CYP2R1 gene, which is predicted to cause the substitution of a proline for leucine at position 99 (L99P) of the encoded protein (Fig. 2). Leucine 99 is conserved in the CYP2R1 enzymes of the puffer fish, mouse and rat. The T → C change in exon 2 was not detected in the genomic DNAs of 50 control African American subjects, suggesting that the nucleotide change represents a mutation rather than a polymorphism in the CYP2R1 gene. No mutations were detected in the CYP27A1 gene of this subject.

The biochemical consequences of the CYP2R1 L99P mutation for 25-hydroxylation were determined in assays utilizing [^{14}C]vitamin D$_3$ as a substrate (Fig. 3). When cells transfected with a control plasmid DNA (CMV) were incubated with this radiolabeled substrate, no conversion to the 25-hydroxylated form was detected (*lane 1*). In contrast, expression of the normal CYP2R1 enzyme in the HEK 293 cells led to the formation of 25-hydroxyvitamin D$_3$ (*lane 2*). The CYP2R1 enzyme with the L99P mutation was inactive (*lane 3*), and even after extended phosphorimage analysis showed no ability to 25-hydroxylate the substrate or to produce other products (data not shown).

Because the amount of [^{14}C]vitamin D$_3$ substrate available for further biochemical assays was limiting, we next assessed the consequences of the L99P mutation for CYP2R1 enzyme activity using functional assays. To this end, the abilities of the normal and mutant enzymes to activate the vitamin D receptor were evaluated in three reporter gene systems in which vitamin D receptor response elements were linked to transcription of a luciferase gene. These experiments took advantage of the fact that 25-hydroxyvitamin D$_3$ is a more potent ligand for the vitamin D receptor than is non-hydroxylated vitamin D$_3$ (Cheng et al., 2003). As shown by the data in Fig. 4, when expression vectors specifying either normal or mutant CYP2R1 enzymes were transfected into cultured HEK 293 cells together with DNAs expressing different vitamin D receptors and their responsive genes, only cells expressing the normal CYP2R1 enzyme showed increased transcription from the luciferase gene. The degree of stimulation varied with the system used, with the strongest activation measured for the intact vitamin D receptor and a reporter gene containing three copies of a vitamin D receptor response element (*middle panel*, Fig. 4). Here, the stimulus mediated by CYP2R1-

catalyzed 25-hydroxylation of vitamin D_3 was > 40-fold over background, and no augmentation over baseline was observed with the L99P mutant protein.

The reporter gene experiments shown in Fig. 4 were carried out at single concentrations of vitamin D_3. To determine whether the CYP2R1 enzyme with the L99P mutation was active at higher concentrations of substrate, a dose response curve was generated for the secosteroid. As shown in Fig. 5*A*, increasing the concentration of vitamin D_3 in the medium from zero to 1 x 10^{-6} M led to an increase in luciferase gene expression of approximately 14-fold. When the L99P CYP2R1 enzyme was present, no stimulation over that in mock-transfected cells was observed. The stimulus detected in the control cells at higher vitamin D_3 concentrations is attributable to endogenous CYP2R1 and CYP27A1 activities in the HEK 293 cells (Cheng et al., 2003).

A hallmark feature that distinguishes the microsomal CYP2R1 from the mitochondrial CYP27A1 is that the CYP2R1 enzyme 25-hydroxylates both vitamin D_3 and vitamin D_2 whereas CYP27A1 only 25-hydroxylates vitamin D_3 (Cheng et al., 2003; Guo et al., 1993; Holmberg et al., 1986). The capacity of the CYP2R1 enzyme with the L99P mutation to 25-hydroxylate vitamin D_2 is shown in Fig. 5*B*. As expected, the normal enzyme utilized this plant-derived secosteroid as a substrate, producing a ligand that activated the vitamin D receptor. The mutant enzyme was far less active but at the higher concentrations of vitamin D_2 added to the medium (> 7.5 x 10^{-7} M), did provide a greater stimulus than that observed in mock-transfected cells. Similar modest stimulation was observed in three separate experiments. Together, the data shown in Fig. 5 suggested that the L99P CYP2R1

enzyme was incapable of hydroxylating vitamin D_3 but retained residual activity against vitamin D_2.

DISCUSSION

The current data on mutation of the CYP2R1 enzyme are of interest from two points of view. First, they identify the microsomal CYP2R1 as a biologically important human vitamin D 25-hydroxylase, and second, they reveal the molecular basis of a new human genetic disease, selective 25-hydroxyvitamin D_3 deficiency.

At the enzyme level, it has been difficult to identify the biologically relevant vitamin D 25-hydroxylase for several reasons, including the existence of multiple candidate enzymes and the possibility of redundancy and compensation. Early studies indicated that 25-hydroxylase activity is present in both mitochondrial and microsomal subcellular fractions (Bhattacharyya and DeLuca, 1974; Bjorkhem and Holmberg, 1978; Madhok and DeLuca, 1979) and that the two enzymes exhibit different biochemical properties with respect to substrate affinity and capacity (Bjorkhem et al., 1980; Fukushima et al., 1976). The mitochondrial enzyme was purified (Dahlback and Wikvall, 1988; Wikvall, 1984) and following the cloning of its cDNA (Andersson et al., 1989), revealed to be the CYP27A1 cytochrome P450 that is also responsible for the 27-hydroxylation of sterol intermediates in bile acid synthesis (Russell, 2003). Shortly thereafter, mutations in the encoding gene located on human chromosome 2 were reported in patients with the cholesterol storage disorder cerebrotendinous xanthomatosis (Cali et al., 1991; Skrede et al., 1986). The finding of normal vitamin D metabolism in these subjects raised the redundancy issue (Bjorkhem et al., 2001).

Several different P450s were considered as candidates for the microsomal enzyme based on in vitro vitamin D 25-hydroxylase activity. One was the CYP2D25 enzyme purified from pig liver (Hosseinpour and Wikvall, 2000); however, this protein is not well conserved among species, as would be expected for an important vitamin D biosynthetic enzyme, and the closest human homologue (CYP2D6) does not have 25-hydroxylase activity (Hosseinpour and Wikvall, 2000). Furthermore, a molecular analysis by another group of the human CYP2D6 in the patient studied here failed to find mutations in the gene (Lin et al., 2003). Another candidate gene encoding the CYP3A4 enzyme also is normal in this individual (unpublished data). The rat CYP2C11 is a vitamin D 25-hydroxylase present in males only (Andersson et al., 1983), and the fact that there is no known sexual dimorphism in vitamin D signaling means that this enzyme is unlikely to play a major biosynthetic role.

A fourth candidate for the microsomal enzyme is CYP2R1, which was identified in 2003 (Cheng et al., 2003). CYP2R1 is preferentially expressed in the liver, is not sexually dimorphic, is highly conserved among species ranging from fish to human, and is equally active in the 25-hydroxylation of both vitamin D_2 and vitamin D_3 (Cheng et al., 2003). These characteristics indicate that CYP2R1 is a biologically important vitamin D 25-hydroxylase, and the current data provide genetic evidence to support this assignment. CYP2R1 may be unique in fulfilling this role as the individual studied here has a normal CYP27A1 gene, and presumably normal enzyme activity, which were unable to compensate for the loss of CYP2R1. Whether the CYP27A1 enzyme plays any role as a vitamin D 25-hydroxylase remains moot; however, it is interesting to note that this subject responded to treatment with vitamin D and did have low levels of 1α,25-hydroxyvitamin D (Casella et al., 1994)

suggesting that an alternate but non-essential pathway for the formation of 25-hydroxyvitamin D must exist.

With regard to human inborn errors, selective 25-hydroxyvitamin D_3 deficiency is a rare autosomal recessive disorder characterized by impaired synthesis of an intermediate in the vitamin D biosynthetic pathway that results in endocrine defects in vitamin D signaling. In the patient studied here, the disease presented as vitamin D-dependent rickets associated with low to normal serum calcium and phosphate levels, elevated serum alkaline phosphatase activity, and most importantly, reduced levels of 25-hydroxyvitamin D. This individual was treated effectively with vitamin D_2 therapy (3000 U/day) (Casella et al., 1994), confirming the absence of end-organ resistance and the presence of a functional vitamin D receptor. The positive response to vitamin D_2 may reflect the residual enzyme activity present with this substrate in the mutant protein (Fig. 5), or conversion by an alternate vitamin D_2 25-hydroxylase (Gupta et al., 2004).

Multiple individuals have been described with selective 1α,25-dihydroxyvitamin D deficiency due to mutations in the gene encoding the CYP27B1 vitamin D 1α-hydroxylase (Kitanaka et al., 2001; Liberman and Marx, 2001). Of the potential cases of selective vitamin D 25-hydroxylase deficiency that have been reported in the literature (Abdullah et al., 2002; Asami et al., 1995; Casella et al., 1994; Lin et al., 2003; Nutzenadel et al., 1995; Zerwekh et al., 1979), we were able to analyze two. The current studies indicate that the subject described by Casella et al. (Casella et al., 1994) has mutations in the CYP2R1 gene. The individual described by Zerwekh et al. (Zerwekh et al., 1979) presented with a complex phenotype that was postulated to be due to mutations in both the vitamin D 25-hydroxylase

and the vitamin D receptor. We sequenced the exons of the CYP2R1 and CYP27A1 genes from this individual and found no mutations in either gene; however, biochemical and molecular analyses confirmed the presence of mutations in the vitamin D receptor gene (Griffin and Zerwekh, 1983; Whitfield et al., 1996).

It is not clear why mutations in the CYP27B1 vitamin D 1α-hydroxylase appear to be more common than those in the CYP2R1 vitamin D 25-hydroxylase. This discrepancy may represent an ascertainment bias as the subject studied here with CYP2R1 mutations had normal levels of circulating 1α,25-dihydroxyvitamin D. For reasons that are usually attributed to dietary supplementation or diminished clearance, many subjects with hereditary defects in calciferol metabolism have low to normal levels of 1α,25-dihydroxyvitamin D (Liberman and Marx, 2001), which may mask mutations in other biosynthetic enzymes. The scarcity of 25-hydroxylase deficiency cases also may reflect genetic polymorphisms that allow alternate pathways to function in some individuals. Along these lines, it is of possible significance that the vitamin D 25-hydroxylase deficient subject identified here was Nigerian. Individuals with dark skin require exposure to sunlight for longer periods of time to generate requisite levels of vitamin D_3 as compared to those with less skin pigmentation and may be more sensitive to impaired synthesis of the vitamin (Bell et al., 1985; Kreiter et al., 2000; Nesby-O'Dell et al., 2002; Norman, 1998). Furthermore, we sequenced exon 2 of the CYP2R1 gene in fifty control subjects from Nigeria (Cooper et al., 2002) and identified one individual who was heterozygous for the L99P mutation. This result suggests that there may be a founder gene effect in Nigeria, a country in which the prevalence of rickets is high

(Thacher et al., 2000). Further studies in patients with selective 25-hydroxyvitamin D deficiency in Nigeria and elsewhere will be necessary to clarify these points.

Figure 1. Structure of the human CYP2R1 gene. The predicted exon-intron structure of the human CYP2R1 gene is shown together with six pairs of oligonucleotides used to amplify and sequence fragments of the DNA. Exon 3 was amplified with primer pair 5, 8 and sequenced with primers 5, 6, 7, and 8. The gene is drawn to scale with the exception of intron 1, which is estimated to be 9.1 kilobases in length. The autosomal location of the gene was deduced from the human genome database (http://www.ncbi.nlm.nih.gov/mapview/maps.cgi?taxid=9606&chr=11).
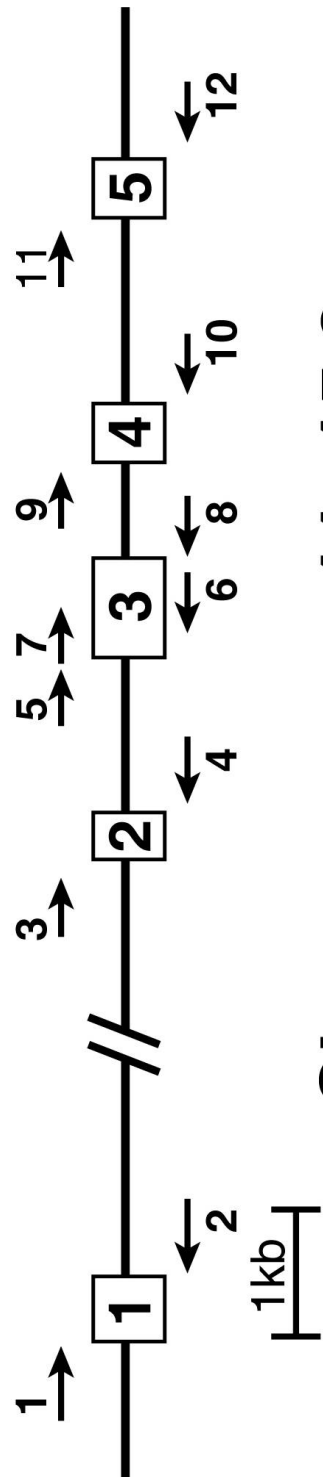
Chromosome 11p15.2

Figure 2. DNA sequence analysis of mutation in CYP2R1 vitamin D 25-hydroxylase. The partial DNA sequence of exon 2 from the CYP2R1 gene is shown from a normal individual (*top panel*), and from an individual with selective 25-hydroxyvitamin D deficiency (*bottom panel*). The codon specifying amino acid 99 is CTT in the normal gene and CCT (*arrow*) in the affected individual. The T → C transition mutation in the second nucleotide causes a change from leucine to proline at residue 99. All other nucleotides in the CYP2R1 gene of the proband were identical to those in normal individuals.

K E C L V H Q

AAGGAATGCCTTGTTCATCAA

Control
Leu99

Exon 2

K E C P V H Q

AAGGAATGCCCTGTTCATCAA
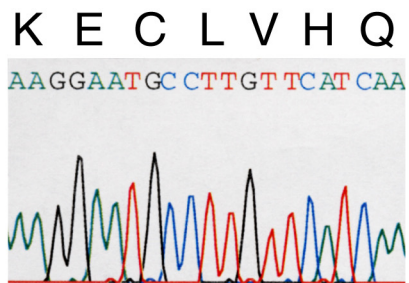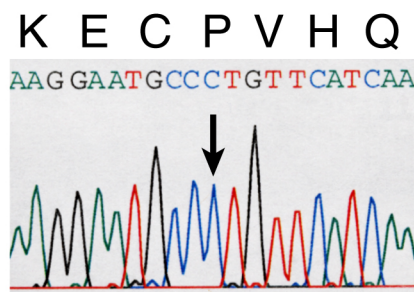
Subject
Leu99Pro

Figure 3. Biochemical assay of CYP2R1 vitamin D 25-hydroxylase enzyme activity. HEK 293 cells were transfected with the indicated expression plasmids for a period of 8-10 h. Thereafter, the medium was made 4.6 x 10^{-7} M in [4-^{14}C-vitamin D_3] and the incubation continued for an additional 96 h. Lipids were extracted from cells and medium into chloroform:methanol (2:1, v/v), and vitamin D metabolites and standards were separated by thin layer chromatography on 150 Å silica gel plates (Whatman, #4855-821) in a solvent system containing cyclohexane:ethyl acetate (3:2, v/v). After development, radioactivity was detected by phosphorimage analysis, and the positions to which authentic vitamin D_3 and 25-hydroxyvitamin D_3 migrated on the plate were determined by staining with iodine.
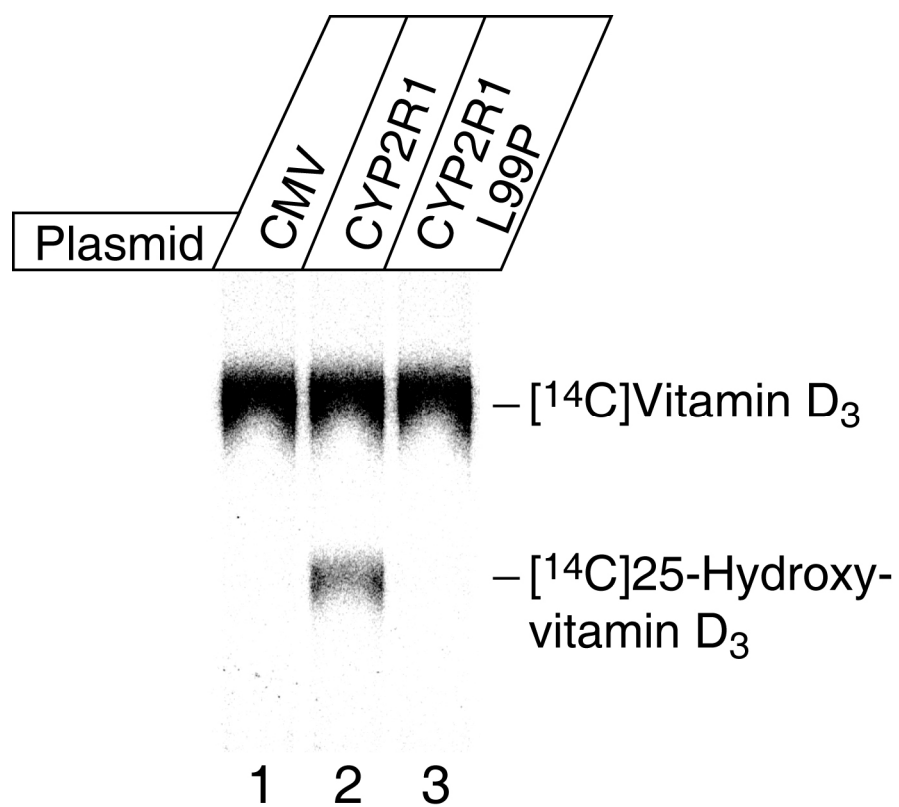
Figure 4. L99P mutation in CYP2R1 causes loss of vitamin D$_3$ activation. Expression vectors encoding no protein (*CMV*), the normal CYP2R1 enzyme (*CYP2R1*), or a version containing a proline substituted for leucine at amino acid 99 (*CYP2R1L99P*), were transfected in triplicate into HEK 293 cells together with the indicated vitamin D receptor-reporter gene systems. The concentrations of vitamin D$_3$ added to the medium ranged from 0.25-1.0 μM. After 16-20 h, cells were lysed and assayed for enzyme activities. Relative luciferase activity was calculated by dividing units of luciferase enzyme activity measured on a luminometer (Dynex MLX) by units of β–galactosidase enzyme activity measured on a spectrophotometer (Dynex Opsys MR). Means ± S.E. of measurement were calculated and plotted in histogram form. The data are representative of two separate experiments carried out on different days.
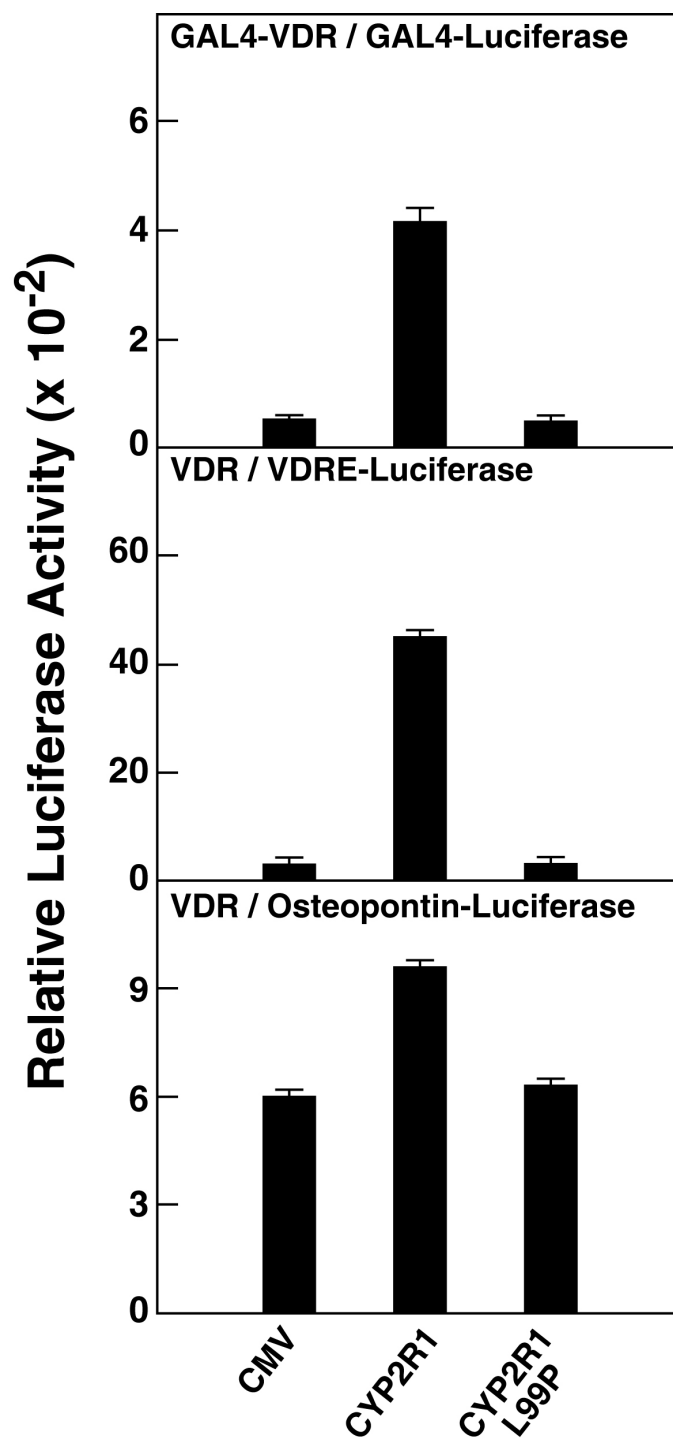
Figure 5. Response of normal and L99P CYP2R1 enzymes to increasing concentrations of vitamin D_3 (*A*) and vitamin D_2 (*B*). The indicated expression plasmids were introduced into HEK 293 cells together with DNAs constituting the VDR/VDRE-Luciferase reporter gene system. After an expression period (8h), different amounts of the two forms of vitamin D were added to the medium and the incubation continued for an additional 16 h. Thereafter, cells were lysed and assayed for luciferase and β–galactosidase enzyme activities. Points on the graphs represent means of triplicate values established at each concentration of secosteroid. These experiments were repeated at least two times each.

A. Relative Luciferase Activity (x10⁻³) vs [Vitamin D₃] x 10⁻⁷ M

Legend:
- ■ CYP2R1
- ● CYP2R1 L99P
- ▲ CMV

B. Relative Luciferase Activity (x10⁻³) vs [Vitamin D₂] x 10⁻⁷ M
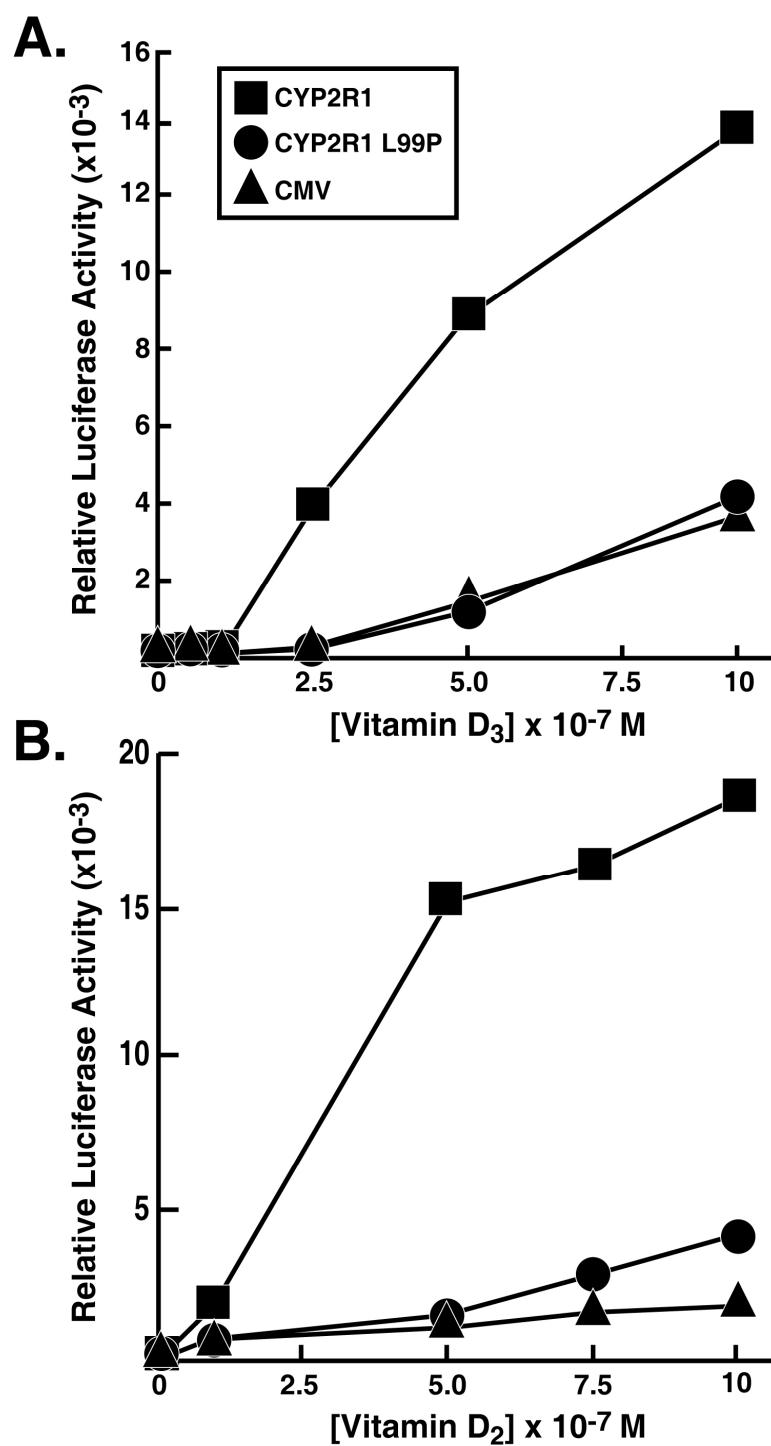
CHAPTER FIVE
IDENTIFICATION OF TWO MAMMALIAN FATTY ACYL-COENZYME A REDUCTASES WITH DIFFERENT SUBSTRATE SPECIFICITIES AND TISSUE DISTRIBUTIONS

INTRODUCTION

Wax esters are abundant neutral lipids that coat the surfaces of plants, insects, and mammals. They are composed of long chain alcohols esterified to fatty acids and have the chemical property of being solid at room temperature and liquid at higher temperatures. Waxes play essential biological roles in preventing water loss, abrasion, and infection, and are produced commercially at levels approaching 3 billion pounds per year for use in polishes, cosmetics, and packaging. In mammals, wax esters compose approximately 30% of sebum and meibum, the oils secreted by the sebaceous and meibomium glands onto the surfaces of the skin and eye, respectively (Downing and Strauss, 1974; Nikkari, 1974a).

Although the enzymes of wax biosynthesis in mammals have not been isolated, the components of the pathway can be inferred from work in plants (Jenks et al., 2002; Kunst and Samuels, 2003) and mammalian tissue extracts (Wykle et al., 1979). As indicated in Scheme 1, two catalytic steps are required to produce a wax monoester, including reduction of a fatty acid to a fatty alcohol and subsequently, the trans-esterification of the fatty alcohol to a fatty acid to produce a wax. The first step is catalyzed by the enzyme fatty acyl-coenzyme A (CoA) reductase, which uses the reducing equivalents of NAD(P)H to convert a fatty acyl-CoA into a fatty alcohol. cDNAs specifying fatty acyl-CoA reductases have been

identified in the jojoba plant (Metz et al., 2000), the silkworm moth (Moto et al., 2003), wheat (Wang et al., 2002), and in a microorganism (Reiser and Somerville, 1997); however, the biochemical properties and subcellular localizations of these enzymes have not been reported.

Fatty alcohols have two metabolic fates in mammals; incorporation into ether lipids or incorporation into waxes. Ether lipids account for ~20% of phospholipids in the human body and are synthesized in membranes by a pathway involving at least seven enzymes (Nagan and Zoeller, 2001). The second step of this pathway is catalyzed by the enzyme 1-acyldihydroxy acetone phosphate synthase, which exchanges an *sn-1* fatty acid in ester linkage to dihydroxyacetone phosphate with a long chain fatty alcohol to form an alkyl ether intermediate. Once produced, ether lipids are precursors for platelet activating factor, for cannabinoid receptor ligands, and for essential membrane components in cells of the reproductive and nervous systems (Munn et al., 2003; Nagan and Zoeller, 2001).

In the current study a bioinformatics approach was used to identify mouse and human cDNAs encoding two fatty acyl-CoA reductase isozymes designated FAR1 and FAR2. The biochemical properties and subcellular localizations of recombinant FAR enzymes expressed in cultured mammalian and insect cells were defined, and tissue distributions were delineated. An accompanying study reports the isolation and characterization of a wax synthase enzyme that catalyzes the second step of the mammalian wax biosynthesis pathway (Cheng and Russell, 2004a).

MATERIALS AND METHODS

Bioinformatics and cDNA Cloning – Fatty acyl-CoA reductase protein sequences from the jojoba plant (*Simmondsia chinensis*, (Metz et al., 2000)), and the silkworm moth (*Bombyx mori*, (Moto et al., 2003)), were compared to those in the protein database using the program BLASTP (Altschul, 1997) to identify potential mouse and human reductase sequences. Two proteins with approximately 30% sequence identity to the plant and insect enzymes were identified and cDNAs for each were obtained. A mouse fatty acyl-CoA reductase 1 cDNA (mFAR1, IMAGE clone 3495305, GenBank™/EBI Data Bank Accession number BC007178) in the pCMV•SPORT6 vector was obtained from the Mammalian Gene Collection (IRAV) (Invitrogen, Carlsbad, CA). A mouse fatty acyl-CoA reductase 2 cDNA (mFAR2, IMAGE clone 6809131, GenBank™/EBI Data Bank Accession number BC055759) in the pYX-Asc vector was obtained from Open Biosystems (Huntsville, AL). The cDNA insert in this plasmid was released by digestion with the restriction enzymes *Eco*RI and *Not*I, purified by agarose gel electrophoresis and extraction (Qiaquik Gel Extraction kit, Qiagen, Valencia, CA), and ligated into the pCMV6 vector (GenBank™/EBI Data Bank accession number AF239250).

A human fatty acyl-CoA reductase 1 cDNA (hFAR1, nucleotides 134-5358 of GenBank™/EBI Data Bank Accession number AY600449) in the pCMV6-XL6 vector was purchased from Origene Technologies (Rockville, MD). A human fatty acyl-CoA reductase 2 cDNA (hFAR2, IMAGE clone 4732586) in the pDNR-LIB vector was obtained from Invitrogen. The cDNA insert in this plasmid was released by digestion with the restriction

enzymes *Eco*RI and *Xho*I and then treated with the Klenow fragment of *E. coli* DNA polymerase I and the four deoxynucleoside triphosphates to generate blunt ends. The engineered hFAR2 cDNA insert (nucleotides 62-2235 of GenBank™/EBI Data Bank Accession number BC022267) was purified by gel electrophoresis and extraction (Qiaquik Gel Extraction kit) and ligated into the *Sma*I site of the pCMV6 vector. DNA sequence analysis confirmed the identity and structure of the hFAR2 cDNA.

Construction of FLAG Epitope Tagged Expression Plasmids - An expression plasmid (pCMV•SPORT6-FLAG-mFAR1) encoding a FLAG epitope tagged version of the mouse FAR1 protein was assembled as follows. The mFAR1 cDNA was amplified from the pCMV•SPORT6-mFAR1 template described above by the polymerase chain reaction (PCR) using the oligonucleotide primers, 5'-GTACCTGTCGACCCACCATGGATTACAAGGATGACGACGATAAGAGACAAGTCT GGATGGTTTCAATCC-3' and 5'-ATTATGCGGCCGCGGTCTTCAGTATCTCATAGTGCTG

-3'. The DNA was digested with the restriction enzymes *Sal*I and *Not*I and ligated into the pCMV•SPORT6 vector (Invitrogen). The mFAR1 encoded by the resulting plasmid has the FLAG epitope (amino acid sequence DYKDDDDK) at the amino terminus.

An expression plasmid (pCMV•SPORT6-FLAG-mFAR2) encoding a FLAG epitope tagged version of the mouse FAR2 protein was assembled as follows. The mFAR2 cDNA was amplified from the pCMV6-mFAR2 template described above by the PCR using the oligonucleotide primers, 5'-

GTACCTGTCGACCCACCATGGATTACAAGGATGACGACGATAAGATGTCCATGA
TCGCAGCTTTCTAC-3' and 5'-ATTATGCGGCCGCTGTTCTTAGACCTTGAGTGTGCTG-3'. The DNA product was digested with the restriction enzymes *Sal*I and *Not*I and ligated into the pCMV•SPORT6 vector (Invitrogen). This engineering placed the FLAG epitope at the amino terminus of the encoded mouse fatty acyl-CoA reductase 2 protein.

Baculovirus Expression Vectors – A baculovirus recombinant donor plasmid with the mouse FAR1 cDNA in the pFastBac HTC vector (Invitrogen) was constructed. The mFAR1 cDNA insert in the vector pCMV•SPORT6-mFAR1 described above was released by digestion with the restriction enzymes *Sal*I and *Not*I, purified by agarose gel electrophoresis and QiaQuik Gel Extraction, and ligated into pFastBAC HTC.

A mouse FAR2 cDNA baculovirus recombinant donor plasmid was constructed by amplifying the cDNA from the pCMV6-mFAR2 plasmid using the oligonucleotide primers 5'-GCCTATGTCGACGAACCATACAGGAACGGAGGAATC-3' and 5'-ATTATGCGGCCGCGTATCTGAGGTTCCAGATGATGGG-3'. The resulting DNA product was digested with the restriction enzymes *Sal*I and *Not*I and ligated into pFastBAC HTC.

A baculovirus donor plasmid containing the mouse Δ^4-3-oxosteroid 5β-reductase cDNA (nucleotides 48-1053 of GenBank™/EBI Data Bank accession number BC018333) was constructed as follows. First, hepatic cDNA was amplified via the polymerase chain reaction using the oligonucleotide primers 5'-CAGAAGCTTCAGATTCTTCTCTACG-3'

and 5'-TGTTCAGTATTCGTCATGAAATGGG-3'.   Second, the resulting cDNA product
was ligated into the TOPO TA vector (Invitrogen) and propagated in *E. coli.*   Third, the
cDNA insert in this plasmid was excised by digestion with the restriction enzyme *Eco*RI,
purified by agarose gel electrophoresis and the Qiaquik gel extraction kit, and then ligated
into the pFastBAC HTC vector.

Following construction of the donor plasmids, infectious *Autographica californica*
nuclear polyhedrosis baculovirus stocks were generated and titrated in *Spodoptera frugiperda*
(Sf9) cells using the Bac-to-Bac Baculovirus Expression System kit (Invitrogen).

Preparation of Bovine Serum Albumin (BSA)-Conjugated Fatty Acids – Decanoic acid
(C10:0), lauric acid (C12:0), myristic acid (C14:0), palmitic acid (C16:0), stearic acid
(C18:0), oleic acid (C18:1), linoleic acid (C18:2), γ-linolenic acid (C20:3), and arachidonic
acid (C20:4) were purchased from Sigma Chemical Co. (St. Louis, MO), dissolved in ethanol
at a concentration of 62 mM, and then precipitated by the addition of 5 M NaOH to a final
concentration of 0.25 M.   The ethanol was evaporated under a stream of N_2 gas and
precipitated fatty acids were resuspended in 4 ml 0.9% (w/v) NaCl.   An aliquot (4.16 ml) of
24% (w/v) BSA dissolved in H_2O was added and the solution stirred at approximately 80 °C
for 10 min.   Thereafter, 0.9% NaCl was added to bring the total volume to 10 ml.   The
resulting stocks contained 5 mM fatty acid, 0.5% (w/v) NaCl, and 10% (w/v) BSA.   [1-
^{14}C]palmitic acid and [1-^{14}C]oleic acid dissolved in ethanol were purchased from Perkin-
Elmer (Boston, MA).   [1-^{14}C]decanoic acid, [1-^{14}C]lauric acid, [1-^{14}C]myristic acid, [1-
^{14}C]palmitic acid, [1-^{14}C]stearic acid, [1-^{14}C]oleic acid, [1-^{14}C]γ-linolenic acid, and [1-

^{14}C]arachidonic acid dissolved in ethanol were purchased from American Radiolabeled Chemicals (St. Louis, MO). An aliquot of radiolabeled fatty acid was dried under a stream of N_2 gas and resuspended in the corresponding 5 mM solution of unlabelled fatty acid made as above to generate a stock containing 5 mM BSA-conjugated fatty acid and 0.36 to 0.4 mM [1-^{14}C]-labeled conjugated fatty acid.

FAR Enzyme Assay In Transfected 293 Cells - On day 0, human embryonic kidney (HEK) 293 cells (American Type Culture Collection CRL number 1573) were plated at a density of 4×10^5 cells per 60-mm dish in low-glucose Dulbecco's Modified Eagle's Medium (DMEM) supplemented with 10% (v/v) fetal calf serum, 100 units/ml of penicillin, and 100 μg/ml streptomycin sulfate. On day 2, cells were transfected with 3.5 μg of a plasmid mixture containing 0.5 μg of pVA1 and 3 μg of either pCMV•SPORT6-mFAR1, pCMV6-XL6-hFAR1, pCMV6-mFAR2, or pCMV6-hFAR2 expression plasmid using the FuGENE6 reagent. Approximately 23 h after transfection, the cell medium was aspirated and replaced with 2.25 ml of fresh DMEM medium supplemented with 33.3 μM BSA-conjugated palmitic acid and 2.4 μM of BSA-conjugated [1-^{14}C]palmitic acid. After a further 24 h of incubation, cells were washed once with phosphate buffered saline (PBS), harvested with a rubber policeman into 2 ml of PBS, and utilized for thin layer chromatography (TLC) as described below.

FAR Enzyme Assay In Baculovirus-Infected Sf9 Cells - Sf9 cells were plated on day 0 at a density of 2.5×10^6 cells per 60 mm dish in Sf-900 II SFM medium (Invitrogen).

Approximately 4 h after plating, the medium was replaced with Sf-900 medium supplemented with 50 units/ml of penicillin, and 50 μg/ml streptomycin sulfate, and the cells were infected with recombinant baculovirus at a multiplicity of infection (MOI) of 5-10 for 26 h. Thereafter, the medium was replaced with 2 ml of plating medium supplemented with 37.5 μM BSA-conjugated fatty acids and 2.7-3 μM of BSA-conjugated [1-^{14}C]fatty acids, and the infected cells were returned to the incubator for an additional 28 h. The cells were washed with 2 ml of PBS and then scraped into 2 ml of PBS using a rubber policeman prior to analysis by TLC.

Thin Layer Chromatography – Fatty acid metabolites in transfected or infected cells harvested into 2 ml of PBS were extracted into 8 ml of chloroform:methanol (2:1, v/v). The organic layer was dried under a stream of nitrogen and the lipid residue was resuspended in 50 μl of hexane and spotted on pre-scored 150 Å silica gel plates (Whatman, Clifton, NJ). Metabolites were resolved by chromatography in one of two solvent systems. Solvent system 1 involved development for 30 min in hexane:ether:formic acid (65:35:2, v/v/v). Solvent system 2 employed development for 30 min in hexane, followed by drying of the plate in air for 15 min, and a second development for 40 min in toluene. Radiolabeled metabolites on the plates were detected either by exposure to Biomax MR film (Kodak) or phosphorimaging using Fuji BAS-TR2040 screens (Fuji Medical Systems, Tokyo, Japan) and the Storm 820 imaging system (Amersham Biosciences, Piscataway, NJ). Lipid standards were purchased from Sigma Chemical Co., dissolved in ethanol (palmitic acid, stearic acid, hexadecanol, octadecanol, 1-oleoyl-rac-glycerol, 1,3-diolein, and glyceryl trioleate) or

chloroform (dipalmitin and glyceryl tripalmitate) at final concentrations of 10 mM, and aliquots of 5 μl were chromatographed on the plates in lanes adjacent to those containing radiolabeled lipids. Standards were visualized by spraying the TLC plates with a 0.1% (w/v) of 2', 7'-dichlorofluorescein in ethanol followed by examination under ultraviolet light (Touchstone, 1992).

Preparation of Sf9 Cell Membranes - On day 0 of an experiment, Sf9 cells were inoculated at a density of 500,000 cells/ml in 120-ml Sf-900 II SFM medium. On day 1, the cultures were infected at an MOI of 2.0 - 4.0 with the indicated recombinant baculovirus and cultured an additional 48 h. Cells were collected by centrifugation at 1000g for 5 min at 4 °C in a desk-top centrifuge, and the cell pellets were washed once with 30-ml of PBS. Cell pellets were resuspended in 3-ml of hypotonic lysis buffer (10 mM Hepes-KOH, pH 7.6, 1.5 mM $MgCl_2$, 10 mM KCl, 1 mM EDTA, pH 8.0, 1 mM EGTA, pH 8.0), incubated on ice for 10 min, and then lysed by passage through a 23 gauge needle 20 times. The nuclei were removed by centrifugation at 1000g for 5 min at 4 °C, and the resulting supernatant was centrifuged at 130,000g for 30 min at 4 °C in a TLA100.4 rotor in a Tl-100 ultracentrifuge (both from Beckman Coulter, Inc., Fullerton, CA). The membrane pellets were resuspended in the assay buffer (0.3 M sucrose, 0.1 M Tris-HCl, pH 7.4, 1 mM EDTA).

Assay of Cofactor Preference – FAR enzyme activity was measured in a volume of 500 μl of 0.3 M sucrose, 0.1 M Tris-HCl, pH 7.4, 1 mM EDTA, 2.5 mM dithiothreitol, 5 mM $MgCl_2$, 0.8 mg/ml BSA, 98 μM palmitoyl-CoA, 7 μM [1-^{14}C]palmitoyl-CoA (Perkin Elmer), and 2.5

mM β-NADPH or β-NADH. Aliquots (75 μg) of Sf9 cell membrane protein isolated from cells infected with either baculovirus expressing the steroid 5β-reductase or the mFAR1 enzyme were added and the reaction incubated at 37 °C for 30 min. The reaction was stopped by addition of 100 μl of 6 N HCl, 0.9 ml of PBS was added to each tube, and lipids were extracted into 6 ml of chloroform:methanol (2:1, v/v). TLC on dried and resuspended lipids was performed as described above.

Assay of Palmitoyl-CoA vs. Palmitic Acid Preference - These experiments were done as described under "Assay for Cofactor Preference" except that the reaction mixtures contained 2.5 mM β-NADPH, and either 98 μM palmitoyl-CoA and 7 μM [1-^{14}C]palmitoyl-CoA (obtained from Perkin Elmer), or 2.9 μM of BSA-conjugated [1-^{14}C]palmitic acid and 40 μM BSA-conjugated palmitic acid with or without 1 mM ATP and 100 μM coenzyme A. Aliquots (75 μg) of Sf9 cell membrane protein isolated from cells infected with either baculovirus expressing the steroid 5β-reductase or the mFAR1 enzyme were added to the mixture, and the tube was incubated at 37 °C for 30 min. The reaction was stopped by addition of 100 μl 6 N HCl and the lipids were separated by TLC as described above.

Immunocytochemistry - On day 0 of an experiment, Chinese hamster ovary (CHO)-K1 cells (American Type Culture Collection no. CCL-61) were plated at a density of 1 x 10^5 cells in 6-well dishes containing 22-mm^2 glass cover slips in DMEM/Ham's F-12 (50:50 mix) medium supplemented with 5% fetal calf serum (v/v), 100 units/ml penicillin, and 100 μg/ml streptomycin sulfate. On day 1, cells were transfected with 1 μg of plasmid DNA

(either pCMV6, pCMV•SPORT6-FLAG-mFAR1, or pCMV•SPORT6-FLAG-mFAR2) using the FuGENE6 reagent. After 18 h, cells were washed twice with ice cold Dulbecco's PBS, and then fixed in methanol at -20 °C for 10 min. Cells were washed three times with ice cold PBS, and then incubated in a blocking solution (PBS containing 1% (w/v) BSA (Sigma, catalog #A-2153)) for 9 h at 4 °C. Cells were incubated with primary antibodies, (SKL rabbit polyclonal antibody (Gould et al., 1990) at 1:1000 dilution and/or FLAG M2 mouse monoclonal antibody (Sigma) at 1:2500 dilution) for 8 h at 4 °C. The cells were then rinsed three times for 5 min each in PBS containing 0.1 (w/v) BSA, and incubated for 1 h with secondary antibodies (Alexa Fluor 568 goat anti-rabbit IgG (Molecular Probes, Inc., Eugene, OR, catalog #A-11036) and/or Alexa Fluor 488 goat anti-mouse IgG (Molecular Probes, catalog #A-11001)) both at 1:500 dilution in PBS containing 0.1% (w/v) BSA. Cells were rinsed three times with PBS 0.1% BSA, twice with PBS, and then twice with deionized-distilled H_2O. The cover slips were mounted on a glass slide using a ProLong Antifade Kit (Molecular Probes), and then examined using a 63×1.3 NA PlanApo objective on a Model 510 Laser Scanning Confocal microscope (Carl Zeiss, Inc., Göttingen, Germany).

Real Time PCR - Total RNA was prepared from mouse tissues using RNA STAT-60 (Tel-Test, Friendswood, TX). Aliquots (100 μg) of RNA were treated with deoxyribonuclease I (RNAse-free, Ambion, Inc., Austin, TX). cDNA synthesis was initiated from 2 μg of deoxyribonuclease I-treated RNA using random hexamer primers and Taqman Reverse Transcription Reagents (Applied Biosystems, Foster City, CA). For each of the real time PCR reactions, which were carried out in triplicate, cDNA synthesized from 20 ng of

deoxyribonuclease I-treated RNA was mixed with 2X SYBR Green PCR Master Mix (Applied Biosystems). Samples were analyzed on an Applied Biosystems PRISM 7900HT Sequence Detection System. Oligonucleotide primer sequences used in these experiments were: mFAR1 mRNA, 5'-TTAATGTTTATGCTCAAAACCTAGTGAAC-3' and 5'-CCCCTTCCTACCCTTTGCA-3', mFAR2 mRNA, 5'-CCCGACAAAACTAATTTAAACTCACTAA-3' and 5'-GCTTGGTGCTGCCTTTCTCT-3', and cyclophilin mRNA, 5'-TGGAGAGCACCAAGACAGACA-3' and 5'-TGCCGGAGTCGACAATGAT-3'.

RESULTS

The sequences of two eukaryotic fatty acyl-CoA reductase enzymes were used as probes of the mammalian database. The first, from the jojoba plant *Simmondsia chinensis*, (Metz et al., 2000), identified two mouse and human proteins with approximately 30% sequence identity. The second fatty acyl-CoA reductase sequence was from the silk worm moth *Bombyx mori* (Moto et al., 2003). A search for orthologs of this insect enzyme in the mammalian database revealed the same two mouse and human proteins as did searches with the plant enzyme sequence, again with low sequence identity. The fact that the plant, insect, mouse, and human sequences shared the same short regions of amino acid identity (Fig. 1) suggested that the mammalian enzymes were potential fatty acyl-CoA reductases. The two enzymes were tentatively named mouse (m) and human (h) fatty acyl-CoA reductase 1 and 2 (FAR1 and FAR2).

Comparisons between cDNA sequences and genomic DNA revealed that the mouse FAR1 enzyme was encoded by a gene on chromosome 7F1 and contained at least 13 exons and 12 introns. The mouse FAR2 gene on chromosome 6G3 contained at least 12 exons and 11 introns. The structures of the two genes were similar, both in overall size and in the positions of the introns, ten of which interrupted the coding portions of the enzymes at the same positions (*black triangles*, Fig. 1). Two introns in the FAR1 gene were located in the 5'-noncoding portion of the transcribed mRNA and the FAR2 gene contained one intron in this region. The human FAR1 and FAR2 genes contained at least 12 exons and 11 introns

and were present on autosomes (FAR1 = chromosome 11p15.2; FAR2 = chromosome 12p11.23).

The amounts of FAR1 and FAR2 mRNAs were determined in different tissues of the mouse by real time PCR (Fig. 2). The FAR1 mRNA had the broadest distribution, being present at readily detectable levels (C_T = 16 to 28) in the twenty tissues or cell lines examined (Fig. 2, *left panel*). The tissue with the highest level of FAR1 mRNA was the preputial gland (C_T = 16.8), a specialized sebaceous gland located near the tail of the animal. In contrast to the FAR1 mRNA, the FAR2 mRNA was present at generally lower levels in a smaller number of tissues. The two highest expressing tissues were the eyelid (C_T = 21.3) and skin (C_T = 23.2) (Fig. 2, *right panel*). An abundance of FAR2 mRNA in these tissues is consistent with a wax synthesis role for this reductase isozyme in the meibomium glands of the eyelid and the sebaceous glands of the skin. Both FAR1 and FAR2 mRNAs are present at high levels in the brain where large quantities of ether lipids are synthesized. RNA blotting experiments indicated an abundant FAR1 mRNA of 4.2 kilobases (kb) in the preputial gland together with a minor species of 3.8 kb. Similarly, an abundant FAR2 mRNA of 2.7 kb was detected in eyelid RNA along with minor species of 1.7 and 3.3 kb (data not shown).

Complementary DNAs encoding mouse and human FAR1 and FAR2 were cloned into mammalian expression vectors as described in "Experimental Procedures". Expression of FAR1 and FAR2 cDNAs in HEK 293 cells resulted in the conversion of BSA-conjugated [^{14}C]palmitate into [^{14}C]hexadecanol (Fig. 3, *lanes 2-5*), whereas transfection of a vector lacking a cDNA insert did not produce hexadecanol (*lane 1*), indicating that HEK 293 cells

have negligible levels of endogenous fatty acyl-CoA reductase activity. Several conclusions were reached from these results. First, the putative mammalian FAR cDNAs identified by bioinformatics encoded bona fide fatty acyl-CoA reductases. Second, there are two fatty acyl-CoA reductase isozymes in the mouse and human as well as other mammalian genomes (see Discussion). Third, comparisons of the results in Fig. 3, *lanes 2* and *3* to those in *lanes 4* and *5* indicated that the expressed mouse and human FAR1 enzymes were more active than the corresponding FAR2 enzymes in transfected HEK 293 cells. Immunoblotting experiments with epitope-tagged FAR proteins expressed in these cells suggested that the relative levels of the two enzymes were similar (data not shown).

In an effort to overcome the discrepancy between the FAR1 and FAR2 enzyme activities, the mouse cDNAs were recombined into baculovirus expression vectors as described in "Experimental Procedures". FAR1 and FAR2 expressing viruses produced higher levels of enzyme activity in intact insect cells compared to those obtained in HEK 293 cells but the levels of FAR1 enzyme activity in the Sf9 cells remained approximately 5- to 10-fold higher than those of FAR2 despite equivalent levels of expression (data not shown). These results suggested that the difference in activity between the recombinant FAR1 and FAR2 enzymes reflected an intrinsic property of the proteins and was not due to an anomaly between the mammalian and insect cell expression systems. For these reasons the two expression systems were used interchangeably in subsequent experiments to characterize FAR1 and FAR2.

Centrifugation experiments with cell lysates from FAR1 baculovirus-infected Sf9 cells showed that reductase enzyme activity sedimented with the membrane fraction. Assays

with membrane preparations showed that enzyme activity with palmitoyl-CoA substrate was optimal over a range of magnesium (3-32 mM) and KCl (0-200 mM) concentrations, and between pH 7.0 and 8.0. When the assay buffer had a pH greater than 8.0, considerable non-enzymatic conversion of fatty acyl-CoA to fatty alcohol was observed. No inhibition of FAR1 activity was detected in the presence of excess product (0.5 mM hexadecanol). Based on these findings, the standard FAR1 enzyme assay was performed in a buffer of pH 7.4 containing 3.0 mM $MgCl_2$ and 0 mM KCl for 30 min at $37^{\circ}C$.

In contrast to the results obtained with membranes from FAR1 expressing cells, FAR2 enzyme activity was lost upon lysis of either baculovirus infected Sf9 cells or transfected HEK293 cells (data not shown). FAR2 enzyme activity was not detected with the inclusion of different fatty acid substrates, NAD(P)H cofactors, or detergents in the assay buffer, and variations in the ionic conditions or in the incubation time failed to resuscitate FAR2 enzyme activity. Thus, we were only able to analyze FAR2 enzyme activity in whole cells.

Fatty acyl-CoA reductases catalyze a concerted reaction in which the thioester bond of the fatty acyl-CoA substrate is cleaved and the resulting fatty acid is reduced to an alcohol by transfer of electrons from an NAD(P)H cofactor (Bishop and Hajra, 1981). A series of experiments were performed to determine the substrate and cofactor utilized by mouse FAR1. As shown by the data in Fig. 4*A*, conversion of palmitate to hexadecanol by membranes from FAR1 baculovirus-infected Sf9 cells required the presence of ATP and CoA in the reaction mixture (*lane 4*). If the preparations were incubated with palmitoyl-CoA, the reaction proceeded in the absence of ATP and CoA (*lane 6*). These results

suggested that FAR1 utilized fatty acyl-CoA esters as substrates instead of free fatty acids. Furthermore, since the synthesis of hexadecanol was approximately the same when palmitoyl-CoA or palmitate plus ATP and CoA were used as substrates, the data indicated the Sf9 cell extracts were saturating for acyl-CoA synthetase enzyme(s) that form the CoA derivatives of fatty acids.

Recombinant mouse FAR1 enzyme also required NADPH as a cofactor (Fig. 4*B*, *lane 7*). No activity was measured when 2.5 mM NADH was substituted in the reaction mixture (*lane 6*), and the inclusion of NADH at this concentration did not inhibit the ability of NADPH to serve as a cofactor (*lane 8*). Membranes prepared from Sf9 cells infected with a baculovirus expressing an unrelated enzyme, steroid 5β-reductase, contained no fatty acyl-CoA reductase activity when these cofactors were present alone or in combination (*lanes 1-4*).

To determine the substrate preferences of the FAR enzymes, Sf9 cells were infected with mouse FAR1 or FAR2 cDNA-containing baculoviruses, or a control virus expressing the mouse steroid 5β-reductase cDNA, and the cells were incubated with BSA-conjugated [^{14}C]fatty acids of different carbon chain length or saturation (Fig. 5). The FAR1 enzyme preferred C16, C18, and C18:1 fatty acids, and was less active against other lipids (*top panel*). With longer exposures of the TLC plate to X-ray film, activity was observed when C10 - C14 substrates were added to the medium. All fatty acids tested were incorporated into monoacylglycerol products by an endogenous insect monoacylglycerol acyltransferase enzyme and to a lesser extent into diacylglycerol products by an endogenous diacylglycerol acyltransferase activity indicating that they gained access to enzymes in the infected cells.

Experiments done with microsomal membranes from FAR1-expressing Sf9 cells produced similar results with respect to fatty acid substrate preference (data not shown).

In contrast to the broad substrate preference of the FAR1 enzyme, the FAR2 enzyme showed a more narrow specificity for fatty acids, acting with partiality towards C16 and C18 lipids (Fig. 5, *middle panel*). Longer exposures of the TLC plate to X-ray film showed weak activity against the shorter saturated fatty acids and C18:2. The control infected cells expressing steroid 5β-reductase did not reduce any of the fatty acids tested although all substrates were incorporated into other lipid products by endogenous enzymes (*lower panel*).

The subcellular localizations of the FAR1 and FAR2 enzymes were determined by immunocytochemistry (Fig. 6). The mouse cDNAs were engineered to contain FLAG epitopes at the amino termini of the encoded proteins and the resulting modified cDNAs cloned into pCMV expression vectors. The introduction of the FLAG epitope did not affect the fatty acyl-CoA reductase activities of the two modified enzymes when the constructs were expressed in HEK 293 cells (data not shown). Transfection of the DNAs into CHO-K1 cells followed by staining with anti-FLAG monoclonal antibody showed that both the FAR1 (Fig. 6, *middle row, panel E*) and FAR2 enzymes (Fig. 6, *lower row, panel H*) localized to peroxisomes distributed throughout the cytoplasm of expressing cells. The identification of these vesicular bodies as peroxisomes was confirmed by co-staining with a polyclonal antiserum directed against a targeting sequence (serine-lysine-leucine, SKL) present in many peroxisomal enzymes (Gould et al., 1990). As seen in Fig. 6 *panels A, D,* and *G*, this antiserum recognized the same type of subcellular organelle in all cells on the cover slip, and when these rhodamine images were merged with the fluorescein images generated with the

anti-FLAG antibody, many peroxisomes in transfected cells were observed to express both

antigens (Fig. 6, *panels F, I*).

DISCUSSION

In the current study, we identify two mammalian fatty acyl-CoA reductase enzymes that convert a variety of fatty acids to fatty alcohols. The two FAR isozymes are approximately 58% identical in sequence and are encoded by genes with similar exon-intron structures located on different chromosomes. FAR1 acts on a broad spectrum of fatty acids of different chain lengths and degrees of saturation, whereas FAR2 prefers saturated C16 and C18 fatty acids as substrates. The FAR enzymes are localized to the peroxisome as judged by immunocytochemistry in transfected cells. The mouse FAR1 mRNA is most abundant in the preputial gland and present at lower levels in many other organs and cells. The highest levels of FAR2 mRNA are detected in tissues that are rich in sebaceous glands (eyelid and skin). The distinct biochemical properties and tissue distributions of the two fatty acyl-CoA reductases suggest that these isozymes perform different functions in lipid metabolism.

Pair-wise sequence comparisons between the mammalian FAR enzymes and the previously defined plant and insect orthologs reveal approximately 30% amino acid identity (Fig. 1). Searches with the mouse protein sequences indicate putative fatty acyl-CoA reductases in many species, including the toad (*Xenopus laevis*, GI28277293), mosquito (*Anopheles gambiae*, e.g., GI31197903, and many others), rat (GI34859004), zebra fish (GI28278322), fruit fly (*Drosophila melanogaster*, e.g., GI24654209 and many others), and nematode (*Caenorhabditis elegans*, GI17570463). The prospective reductases are 33% (mosquito) to 96% (rat) identical in sequence to the mouse FAR enzymes, with identity extending over the complete length of the compared proteins. Homologous sequences

include so-called "male sterility proteins" that are implicated in lipid synthesis and the formation of the pollen cell wall in plants (Aarts et al., 1997), and in the case of wheat, have been shown to have fatty acyl-CoA reductase enzyme activity (Wang et al., 2002).

Comparisons between the known and presumed reductases show that only a small number of amino acids are conserved across species. For example, between mouse, plant and insect proteins, only 61 amino acids (~13%) are identical (Fig. 1). Thirteen of the highly conserved residues are either glycines or prolines, which may play critical structural roles in these proteins. No obvious NADPH cofactor binding or catalysis site was found among the conserved sequences.

The mouse and human FAR1 and FAR2 isozymes are approximately 58% identical in sequence and are encoded by genes of similar structure, suggesting they arose from a common evolutionary precursor via gene duplication. This genetic event is presumably ancient as apparent orthologs for each isozyme are present in several species for which complete genome sequences are available, including the puffer fish (*Fugu rubripes*, FRUP00000132990 and FRUP00000130769) and the rat (XP_215022.2 and NW_047696.1).

The conservation of two isozymes in distantly related species represents one line of evidence that each FAR protein has a different biological function. This idea is further supported by their different fatty acid substrate preferences (Fig. 5), and their differential expression in tissues (Fig. 2). FAR1 is broadly distributed and acts on fatty acids that vary in size and saturation, suggesting that this isozyme plays a general role in the synthesis of fatty alcohols. In contrast, the narrow distribution and substrate preference of the FAR2 isozyme are indicative of a more specialized function. Some support for this division of labor is to be

found in the ether lipids (plasmalogens) of tissues expressing the FAR1 enzyme, which have diverse structures consistent with the production and incorporation of a variety of fatty alcohols into this class of lipids (Nagan and Zoeller, 2001). Furthermore, the fatty alcohol composition of waxes secreted by the sebaceous glands of mouse skin are different from those of the preputial gland (Nikkari, 1974b), which may reflect the differential expression and substrate specificities of the FAR1 and FAR2 enzymes in these tissues.

In the experiments reported here, the FAR1 enzyme was consistently more active in reducing fatty acids than the FAR2 enzyme when assayed in intact cells (e.g., Fig. 3). The reason for this difference was not ascertained but did not appear to be due to discrepancies in expression level as judged by immunoblotting (data not shown), substrate preference (Fig. 5), or differences in subcellular localization (Fig. 6). Furthermore, FAR2 enzyme activity was lost upon lysis of the cells, and could not be preserved or restored by several different treatments. The FAR2 enzyme may require a protein cofactor for activity that is not present in HEK 293 or Sf9 cells. In support of this possibility, a soluble protein identified as a member of the fatty acid binding protein family was reported to enhance reductase activity in extracts of mouse preputial glands (Moore and Snyder, 1982). This effect was shown to be due to the ability of the protein to bind fatty acyl-CoAs, thereby decreasing the effective concentration of the lipid below the critical micelle value and lessening the detergent effects of the substrate. Although BSA was included in all reactions to buffer fatty acyl-CoA concentrations, and no feedback inhibition by substrate was observed with the FAR1 enzyme, we cannot rule out the possibility that FAR2 requires a unique accessory protein for

full activity. Future expression cloning experiments with cDNA libraries from tissues such as the eyelid that express high levels of the FAR2 enzyme may identify a stimulatory factor.

Both the FAR1 and FAR2 enzyme are localized to the peroxisome (Fig. 6), and are found in the pellet fraction of high speed centrifugations suggesting that they are bound to the membrane of this organelle. Hydropathy plots and other sequence analysis programs do not reveal classical transmembrane domain profiles within the reductases thus we do not know whether they are integral membrane proteins or tightly bound to the phospholipid bilayer of the peroxisome. Similarly, it is not immediately evident how the FAR proteins are imported into this organelle as sequence prediction programs that identify peroxisomal proteins (http://mendel.imp.univie.ac.at) do not reveal a type 1 targeting sequence, and visual scanning fails to uncover a conserved type 2 consensus sequence (Sparkes and Baker, 2002).

The presence of FAR enzymes in the peroxisome is consistent with a central role in the production of fatty alcohols for ether lipid biosynthesis. Three of the seven enzymes involved in synthesis of ether lipids are found in this organelle, including akyl-dihydroxyacetone phosphate synthase, which replaces an *sn-1* fatty acid in ester linkage to dihydroxyacetone phosphate with a long chain fatty alcohol to form an alkyl ether intermediate (Nagan and Zoeller, 2001). Co-localization of the reductase and synthase within the peroxisome obviates the need for inter-organellar transport of the fatty alcohol and presumably facilitates the synthesis of ether lipids. In contrast, the synthesis of wax monoesters by the wax synthase enzyme (Scheme 1), which is localized in the endoplasmic reticulum (see accompanying paper) (Cheng and Russell, 2004a), requires transport of the fatty alcohol across two lipid bilayers. Whether the movement of fatty alcohols represents a

controlling step in the synthesis of these and other classes of lipids, and how transport is accomplished, are questions to be answered in future studies.

Scheme 1. The Biochemical Steps of Mammalian Wax Biosynthesis

$$\underset{\substack{\text{Fatty} \\ \text{acyl-CoA}}}{\overset{\overset{\displaystyle O}{\|}}{RCSCoA}} \xrightarrow[\text{NAD(P)H}]{\substack{\text{Fatty acyl-} \\ \text{CoA reductase}}} \underset{\substack{\text{Fatty} \\ \text{alcohol}}}{RCH_2OH} + \underset{\substack{\text{Fatty} \\ \text{acyl-CoA}}}{\overset{\overset{\displaystyle O}{\|}}{RCSCoA}} \xrightarrow[]{\substack{\text{Wax} \\ \text{synthase}}} \underset{\substack{\text{Wax} \\ \text{monoester}}}{\overset{\overset{\displaystyle O}{\|}}{RCH_2OCR'}}$$

$$\underset{\substack{\text{Ether} \\ \text{lipids}}}{} \longrightarrow \underset{\substack{\text{Platelet} \\ \text{activating factor}}}{}$$
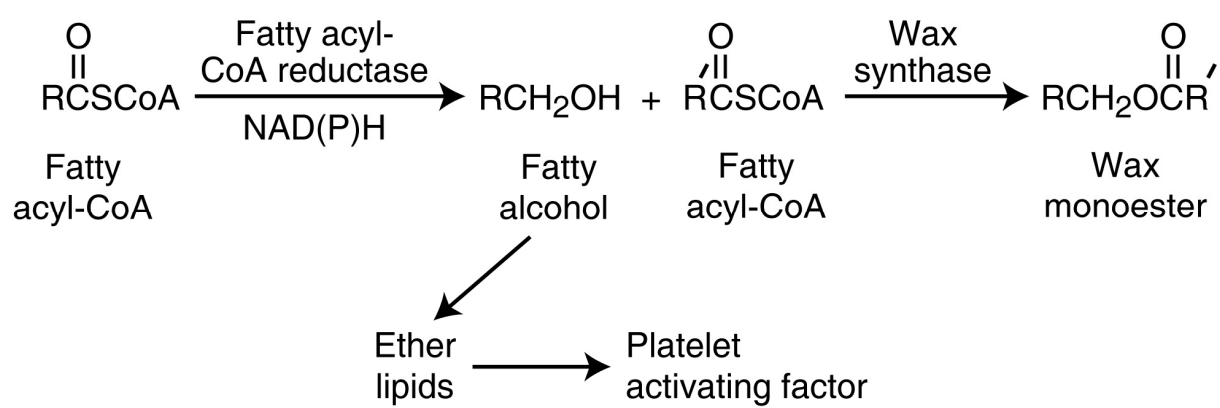
Figure 1. Amino acid sequences of mouse, plant and insect fatty acyl-CoA reductase (FAR) enzymes. *A*, The deduced sequences of the proteins were aligned using the Clustal W (version 1.82) software program with identities indicated by *black boxes*. Amino acids are numbered on the *right*. *Arrowheads* above the mouse FAR1 sequence indicate the positions of 10 introns in the coding portion of the gene. The introns of the FAR2 gene were in the same positions. The GenBank™/EBI Data Bank accession numbers for the mouse FAR1 and FAR2 cDNA sequences are BC007178 and BC055759, respectively. Those for the human FAR1 and FAR2 cDNAs are AY600449

and BC022267, respectively.

```
Mouse FAR1   ----------MVSIPEYYEGKNILLTGATGFLGKVLLEKLLRSCPRVNSVYVLVRQKAGQ  50
Mouse FAR2   ----------MSMIAAFYSNKSILITGATGFLGKVLMEKLFRTSPHLKVIYILVRPKSGQ  50
Insect FAR   MSHNGTLDEHYQTVREFYDGKSVFITGATGFLGKAYVEKLAYSCPGIVSIYILIRDKKGS  60
 Plant FAR   -------MEEMGSILEFLDNKAILVTGATGSLAKIFVEKVLRSQPNVKKLYLLLRATDDE  53


Mouse FAR1   TPQERVE-EILSSKLFDRLRDENPD-----FREKIIAINSELTQPKLALSEE-DKEIIID  103
Mouse FAR2   TLQERVF-QILNSKLFEKVKEVCPN-----VHEKIRPISADLNQRDFAISKE-DVQELLS  103
Insect FAR   NTEERMR-KYLDQPIFSRIKYEHPE-----YFKKIIPISGDITAPKLGLCDE-ERNILIN  113
 Plant FAR   TAALRLQNEVFGKELFKVLKQNLGANFYSFVSEKVTVVPGDITGEDLCLKDVNLKEEMWR  113


Mouse FAR1   STNVIFHCAATVRFNENLRDAVQLNVIATRQLILLAQQMKNLEVFMHVSTAYAYCNRK--  161
Mouse FAR2   CTNIIFHCAATVRFDAHLREAVQLNVTATQQLLLMASQMPKLEAFIHISTAFSNCNLS--  161
Insect FAR   EVSIVIHSAASVKLNDHLKFTLNTNVGGTMKVLELVKEMKNLAMFVYVSTAYSNTSQR--  171
 Plant FAR   EIDVVVNLAATINFIERYDVSLLINTYGAKYVLDFAKKCNKLKIFVHVSTAYVSGEKNGL  173


Mouse FAR1   HIDEVVYP-----------PPVDPKKLID-SLEWMDDGLVNDITPKLIGDR---------  200
Mouse FAR2   HIDEVIYP-----------CPVEPRKIID-SMEWLDDSIIEEITPKLIGDR---------  200
Insect FAR   ILEEKLYP-----------QSLNLNEIQKFAEHYILGKDNDEMIKFIGNH---------  211
 Plant FAR   ILEKPYYMGESLNGRLGLDINVEKKLVEAKINELQAAGATEKSIKSTMKDMGIERARHWG  233


Mouse FAR1   -PNTYIYTKALAEYVVQQEGAKLNVAIVRPSIVGASWKEPFPGWIDNFNGPSGLFIAAGK  259
Mouse FAR2   -PNTYTYTKALGEIVVQQESGNLNVAIVRPSIVGATWQEPFPGWVDNLNGPSGLIIATGK  259
Insect FAR   -PNTYAYTKALAENLVAEEHGEIPTIIIRPSIITASABEPVRGFVDSWSGATAMAAFALK  270
 Plant FAR   WPNVYVFTKALGEMLLMQYKGDIPLTIIRPTIITSTFKEPFPGWVEGVRTIDNVPVYYGK  293


Mouse FAR1   GILRTMRASNNALADLVPVDVVVNTSLAAAWYSGVNRPRNIMVYNCTTGSTNPFHWGEVE  319
Mouse FAR2   GFLRSIKATPMAVADVIPVDTVVNLTIAVGWYTAVHRPKSTLIYHSTSGNLNPCNWYKMG  319
Insect FAR   GWNNIMYSTGEENIDLIPLDYVVNLTLVA--IAKYKPTKEVTVYHVTTSDLNPISIRRIF  328
 Plant FAR   GRLRCMLCGPSTIIDLIPADMVVNATIVAMVAHANQRYVEPVTYHVGSSAANPMKLSALP  353


Mouse FAR1   YHVISTFKRNPLEQAFRRPNVN---LTSN-HLLYHYWIAVSHKAPAFLYDIY-----LRM  370
Mouse FAR2   LQVLATIEKIPFESAFRRPNAD---FTTS-NFTTHYWNTVSHRVPAIIYDFY-----LRL  370
Insect FAR   IKLSEFASKNPTSNAAPFAATT---LLTKQKPLIKLVTFLMQTTPAFLADLW-----MKT  380
 Plant FAR   EMAHRYFTKNPWINPDRNPVHVGRAMVFSSFSTFHLYLTLNFLLPLKVLEIANTIFCQWF  413


Mouse FAR1   TGRSPRMMKTITRLHKAMVFLEYFTSNSWVWNTDNVNMLMNQLNP--EDKKTFNIDVRQL  428
Mouse FAR2   TGRKPRMLKLMNRLLKTISMLEYFINHSWEWSTNNTEMLLSELSP--EDQRVFNFDVRQL  428
Insect FAR   QRKEAKFVKQHNLVVRSRDQLEFFTSQSWLLRCERARVLSAALSD--SDRAVFRCDPSTI  438
 Plant FAR   KGKYMDLKRKTRLLLRLVDIYKPYLFFQGIFDDMNTEKLRIAAKESIVEADMFYFDPRAI  473


Mouse FAR1   HWAEY-IENYCMGTKKYVLNEEMSGLPAARKHLNKLRNIRYGFNTILVILIWRIFIARSQ  487
Mouse FAR2   NWLEY-IENYVLGVKKYLLKEDLAGIPKAKQHLRRLRNIHYLFNTALFIIWRLLIARSQ  487
Insect FAR   DWDQY-LPIYFEGINKHLFKNKL-------------------------------------  460
 Plant FAR   NWEDYFLKTHFPGVVEHVLN---------------------------------------  493


Mouse FAR1   MARNIWYFVVSLCYKFLSYFRASSTMRY 515
Mouse FAR2   MARNVWFFIVSFCYKFISYFRASSTLKV 515
Insect FAR   ---------------------------
 Plant FAR   ---------------------------
```

Figure 2. Tissue distributions of mouse FAR1 and FAR2 mRNAs. The relative levels of each reductase mRNA were determined by real time PCR in the tissues and cell types indicated on the *left* of the figure using cyclophilin mRNA levels as a reference standard. The data for a given FAR mRNA were normalized to the threshold values (C_T) determined in the liver (FAR1 mRNA = 27.4, FAR2 mRNA = 28.0) and then expressed on a $\log_{10}$ scale. This experiment was repeated twice on different days using the same preparations of tissue RNAs, which were isolated from pools of animals (organ samples) or dishes (cell samples).
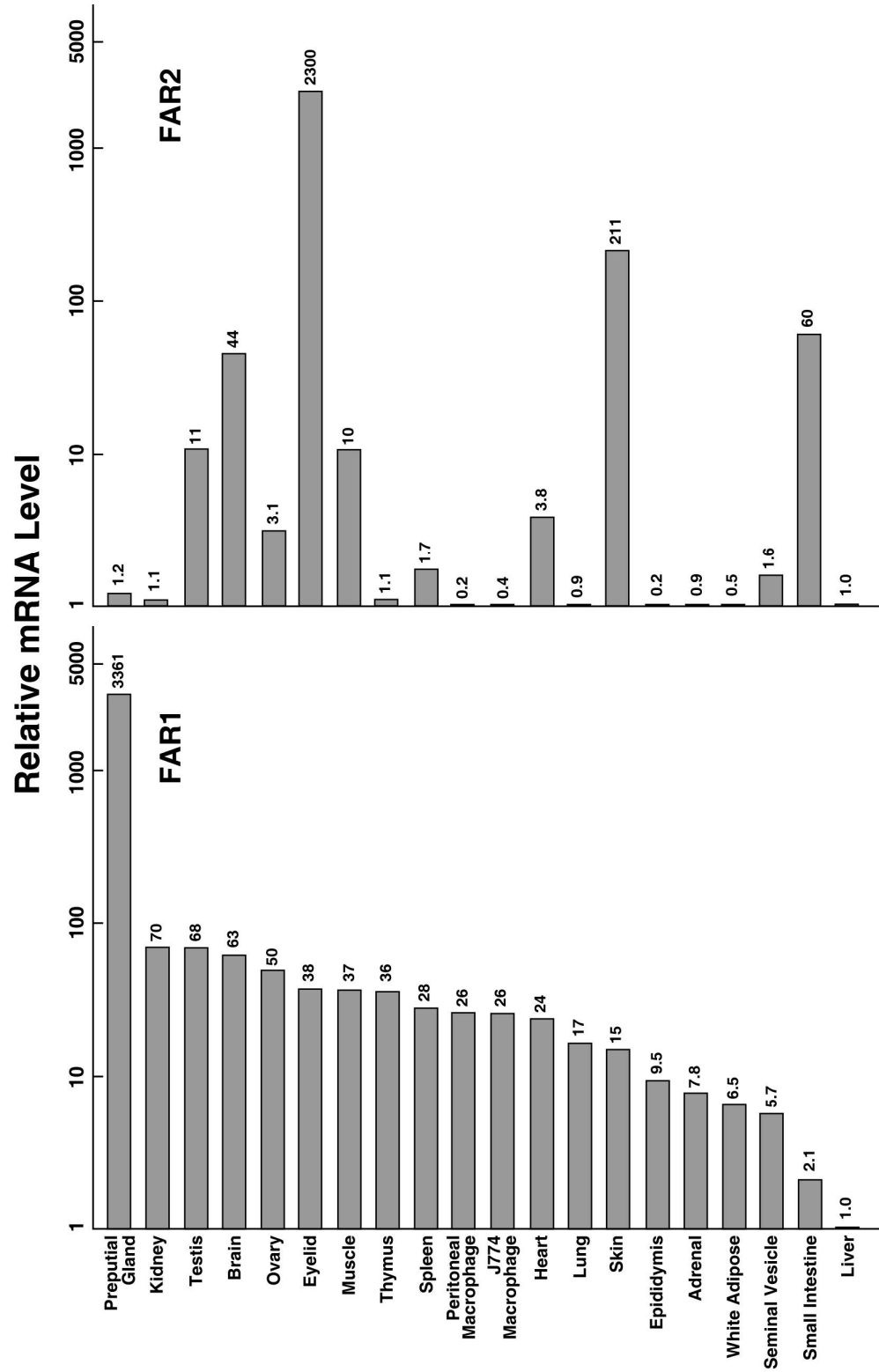
Figure 3. Expression of mouse and human FAR enzymes in HEK 293 cells. Plasmid DNAs encoding the indicated FAR enzymes or a vector alone control (pCMV) were introduced into HEK 293 cells grown in 60-mm dishes. Approximately 24 h after transfection, fresh DMEM medium containing 33.3 μM BSA-conjugated palmitic acid and 2.4 μM BSA-conjugated [1-^{14}C]palmitic acid was added to the cells. After an additional 24 h incubation, cells were washed once with PBS, harvested, and lipids extracted with chloroform/methanol in preparation for TLC. Chromatography on silica gel plates was performed for 0.5 h in Solvent System 1, the silica gel plate was dried in air for 0.25 h, and exposed to Kodak BioMax MR film. The positions to which palmitate and hexadecanol standards migrated to on the TLC plate are indicated on the *right*.
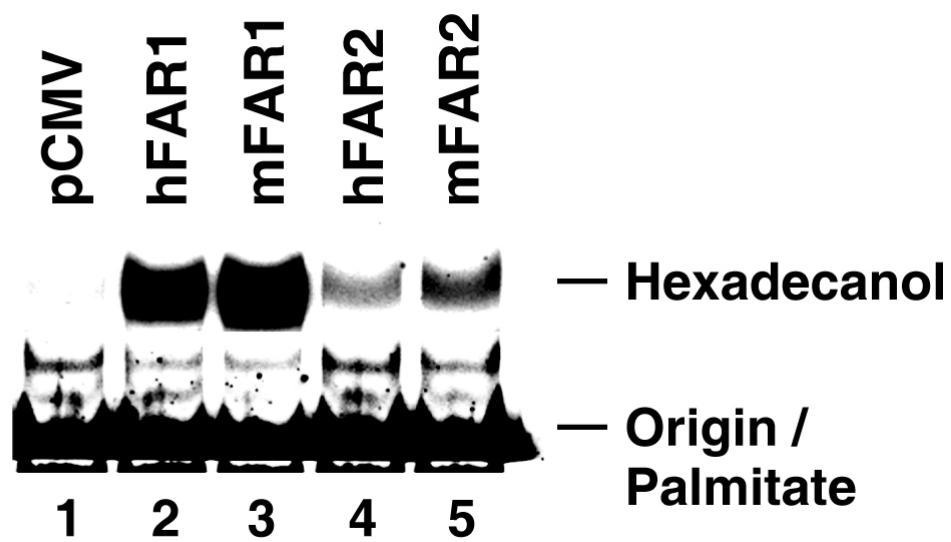
Figure 4. Substrate and cofactor preferences of mouse FAR1 enzyme. *A*, Insect cells (Sf9) in suspension were infected with baculovirus vectors encoding either a control protein (steroid 5β-reductase, *5β-Red*) or the mouse FAR1 enzyme (*mFAR1*) for a period of 48 h at an MOI of 2-4. Cell membranes were prepared as described in "Experimental Procedures", and aliquots (75 μg protein) were incubated for 30 min at 37 °C in a reaction containing 2.5 mM β-NADPH, and either 2.9 μM BSA-conjugated [1-^{14}C]palmitic acid and 40 μM BSA-conjugated palmitic acid, with or without 1 mM ATP and 100 μM coenzyme A, as indicated (*lanes 1-4*), or 98 μM palmitoyl-CoA and 7 μM [1-^{14}C]palmitoyl-CoA (*lanes 5* and *6*).   The reaction was stopped by the addition of 100 μl 6N HCl, lipids were extracted and separated by TLC using Solvent System 2, and radioactivity was detected by exposing the plate to X-ray film. The positions to which palmitate (substrate) and hexadecanol (product) migrated to are shown on the *right*. *B*, Sf9 insect cells were infected with the indicated baculovirus vectors and cell membranes were prepared. Aliquots (75 μg protein) were incubated in reactions containing 98 μM palmitoyl-CoA, 7 μM [1-^{14}C]palmitoyl-CoA, and either 2.5 mM β-NADPH, 2.5 mM β-NADH, or 2.5 mM β-NADPH and 2.5 mM β-NADH, for 30 min at 37°C. Lipids were extracted and analyzed as described in *A*. The experiments of *panels A* and *B* were repeated at least twice on separate days.

A.

	Palmitate				Palmitoyl−CoA	
ATP, CoA	−	−	+	+	−	−
	1	2	3	4	5	6

— Palmitate

— Hexadecanol

5β-Red   mFAR1   5β-Red   mFAR1   5β-Red   mFAR1

B.

	5β-Reductase				mFAR1			
NADH	−	+	−	+	−	+	−	+
NADPH	−	−	+	+	−	−	+	+
	1	2	3	4	5	6	7	8

— Palmitate

— Hexadecanol
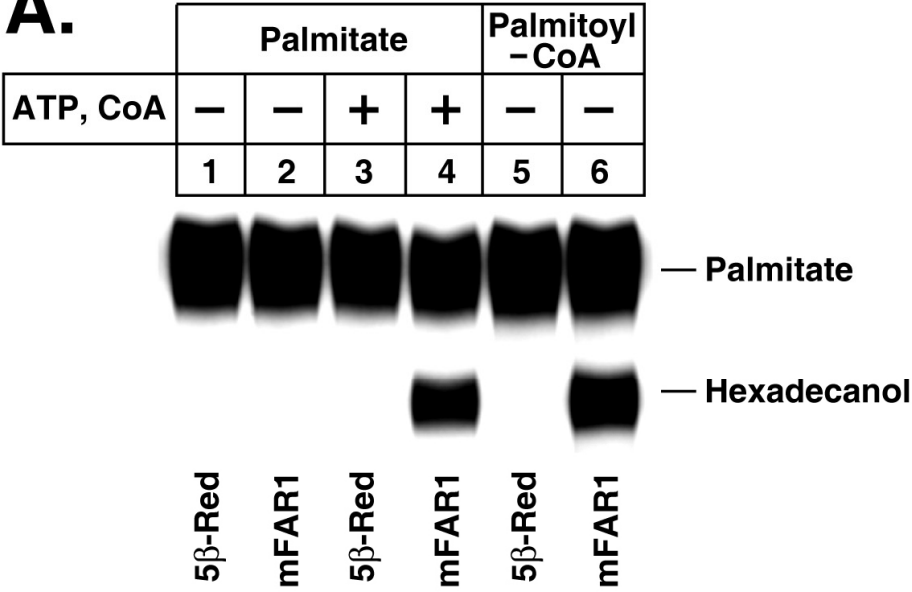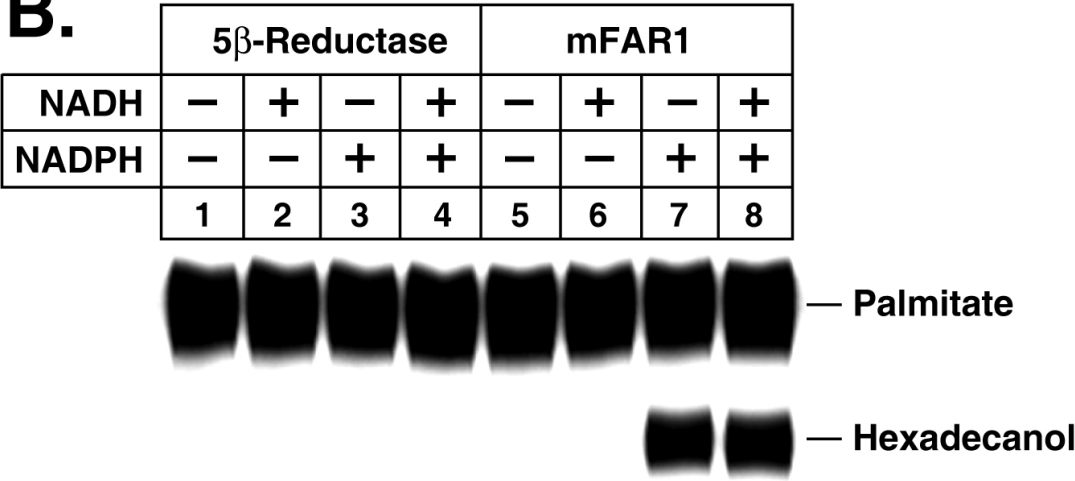
Figure 5. Substrate preferences of mouse FAR1 and FAR2 enzymes. Baculovirus vectors encoding the reductase proteins, or the control protein steroid 5β-reductase, were used to infect adherent Sf9 cells at an MOI of 5-10. Approximately 26 h after infection, intact cells were incubated with the indicated ^{14}C-radiolabeled fatty acids conjugated to BSA. The final concentrations of fatty acids in the medium were 37.5 μM of the unlabeled lipid and 2.7 - 3 μM of the [1-^{14}C]-radiolabeled lipid. The cells were returned to the incubator for an additional 28 h, and thereafter lipids extracted for TLC. The positions to which fatty alcohol (*ROH*), diacylglycerol (*DAG*), and monoacylglycerol (*MAG*) standards migrated to on the plates are indicated on the *right* of the autoradiograms. Several radiolabeled compounds of unknown structure were present in the preparation of radiolabeled γ–linolenic acid (*20:3*) used in these experiments, which were repeated two times.

Fatty Acid	10:0	12:0	14:0	16:0	18:0	18:1	18:2	20:3	20:4

FAR1

ROH
DAG
MAG

FAR2

ROH
DAG
MAG

Steroid 5β-Reductase

ROH
DAG
MAG
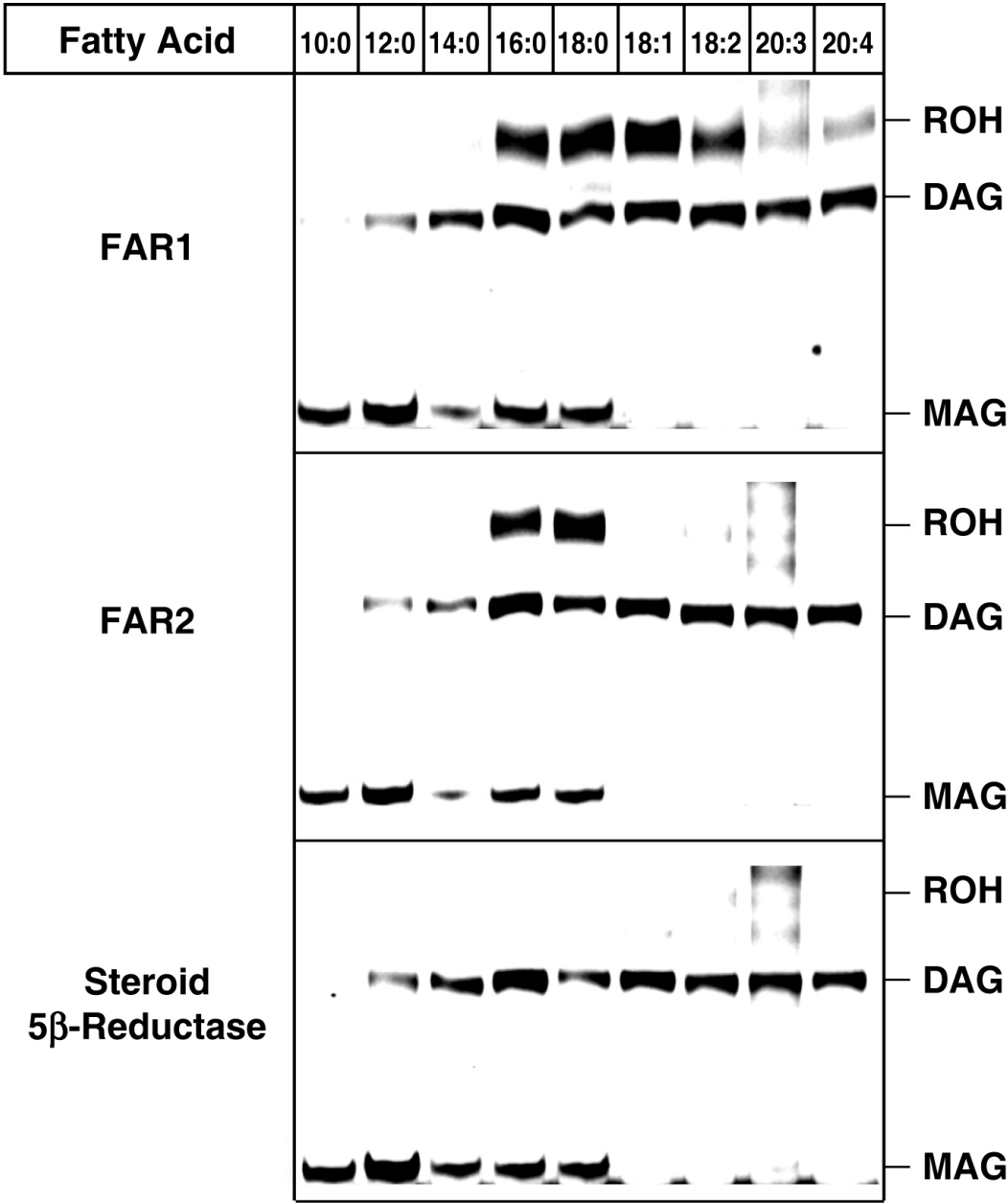
Figure 6. Subcellular localization of mouse FAR1 and FAR2 enzymes. CHO-K1 cells were transfected with the indicated expression vectors encoding nothing (*pCMV6*), FLAG epitope-tagged FAR1 (*FAR1*), or FLAG epitope-tagged FAR2 (*FAR2*) enzymes. After transient expression, cells were fixed, permeabilized, and incubated with a mouse monoclonal antibody directed against the FLAG epitope and a rabbit polyclonal antiserum directed against the SKL epitope of peroxisomal proteins. Panels *A, D, G*: detection of rabbit polyclonal antibodies directed against SKL epitope with rhodamine-conjugated goat anti-rabbit antiserum. Panels *B*, *E*, *H*: detection of FLAG epitope with fluorescein-conjugated goat anti-mouse antiserum. Panels *C*, *F*, *I*: merged images of rhodamine and fluorescein signals. Double indirect immunofluorescence microscopy was performed on a Zeiss 510 Laser Scanning Confocal microscope using a 63 × 1.3 NA PlanApo objective. The FLAG-FAR1 enzyme is detected in the peroxisome (*middle* panels). The FLAG-FAR2 enzyme is present in peroxisomes of cells expressing low levels of the protein, and in the peroxisomes and endoplasmic reticulum of cells expressing high levels of the protein (*lower* panels). The data are representative of two separate experiments.

pCMV

FAR1

FAR2
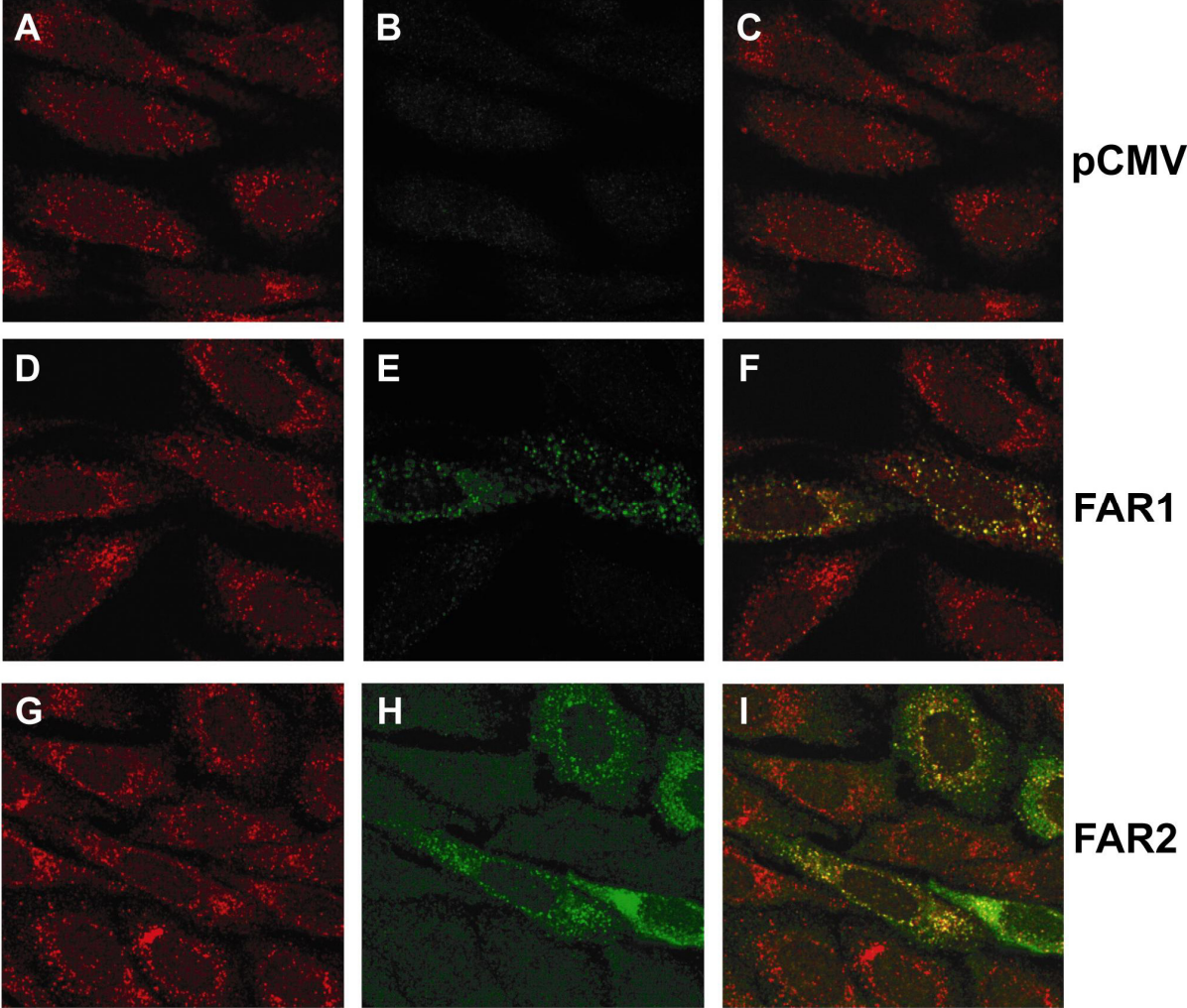
CHAPTER SIX
EXPRESSION CLONING OF MAMMALIAN WAX SYNTHASE CDNAS ENCODING A MEMBER OF THE DIACYGLYCEROL ACYLTRANSFERASE FAMILY

INTRODUCTION

The sebaceous glands produce and exude a lipid-rich secretion termed sebum onto the surface of the skin. Sebaceous glands are found in the dermis of a wide variety of animals but the chemical composition of sebum is distinct in each species, and in some cases, even within a species (Nikkari, 1974a). For example, adult human sebum is principally composed of wax monoesters (25% of total lipids), triglycerides (41%), free fatty acids (16%), and squalene (12%), whereas the composition of mouse fur sebum is wax monoesters (5%), wax diesters (65%), triglycerides (6%), and free and esterified sterols (23%). Within the mouse, the sebum elaborated by the preputial glands, which are specialized sebaceous glands involved in reproduction, has a much higher content of wax monoesters (48%) than fur sebum (Nikkari, 1974a). While much is known concerning the lipid content of sebum, the biosynthesis and functions of this secretion remain largely unfamiliar. Sebum may lubricate the skin and/or contribute to the development of the water barrier. These functions are implied by the role of the meibomian glands, which are modified sebaceous glands in the margin of the eyelid that secrete meibum. Like sebum, meibum is lipid-rich and contains a high percentage of wax monoesters (~35%) (McCulley and Shine, 2002; Nicolaides et al.,

1981). Meibum forms the outer layer of the tear and prevents the evaporation and spreading of the tear film (Driver and Lemp, 1996).

Wax monoesters are a distinctive component of mammalian sebum and meibum. Members of this class of neutral lipids are widely distributed among different organisms and are known to fulfill many biological functions including the prevention of desiccation in insects and plants, sound transmission and/or buoyancy regulation in sperm whales, and energy storage in algae and plankton (Kolattukudy, 1976). Wax monoesters are synthesized by wax synthase enzymes, which conjugate a long chain fatty alcohol to a fatty acyl-CoA via an ester linkage. Wax synthase enzymes and encoding genes are known from the jojoba plant (Lardizabal et al., 2000) and the bacterium *Acinetobacter calcoaceticus* (Kalscheuer and Steinbuchel, 2003). The plant enzyme is exceptionally hydrophobic and is predicted to span the membrane seven to nine times. The protein shares sequence identity with seven *Arabidopsis* genes but does not have an obvious mammalian orthologue. Co-expression of the jojoba wax synthase gene with a fatty acid elongase and a bacterial fatty acyl-CoA reductase leads to the synthesis of large quantities of wax in the seeds of transgenic *Arabidopsis* plants (Lardizabal et al., 2000). The bacterial wax synthase is unrelated to the jojoba wax synthase or to other mammalian proteins in the database but does share sequence identity with proteins specified by several microbial genes (Kalscheuer and Steinbuchel, 2003). It is a bifunctional enzyme, exhibiting wax synthase activity and the ability to form triacylglycerols from diacylglycerol substrates and fatty acyl-CoAs (acyl-CoA:diacylglycerol acyltransferase (DGAT) activity).

In addition to wax monoesters, mice and other species elaborate more complex wax diesters and triesters in fur sebum that are composed of three and four fatty acids/alcohols in ester linkage (Nicolaides, 1965; Sansone and Hamilton, 1969). The biosynthetic enzymes for these lipids are as yet undefined; however, mice deficient in the genes encoding the DGAT1 acyltransferase and stearoyl-CoA desaturase 1 have reduced wax diesters in their fur (Chen et al., 2002; Miyazaki et al., 2002; Miyazaki et al., 2001). These animals also exhibit sebaceous gland atrophy, thus it is not clear whether the reduction in wax diesters in the mutant mice is due to decreased synthesis or secretion of lipid from the deteriorated gland.

In the current study, an expression cloning approach was taken to identify mouse cDNAs encoding wax monoester synthase enzyme activity. A cDNA was identified in a library constructed from sebaceous gland mRNA that specifies a member of the DGAT2/acyl CoA:monoacylglycerol acyltransferase (MGAT) enzyme family with previously unknown function (Cases et al., 2001). Recombinant wax synthase, DGAT, and MGAT proteins were expressed in mammalian and insect cells and their enzyme activities compared. The subcellular localization of the mammalian wax synthase was characterized and its tissue distribution determined by analysis of mRNA by real time polymerase chain reactions. Co-expression in cultured cells of the wax synthase identified here with either of the fatty acyl CoA reductase enzymes reported in the accompanying paper (Cheng and Russell, 2004b) resulted in the synthesis of wax monoesters.

EXPERIMENTAL PROCEDURES

Expression Cloning - A cDNA library was constructed from 5 μg of poly(A)$^+$-enriched mRNA isolated from the preputial glands of male mice using the SuperScript™ Plasmid System for cDNA Synthesis and Cloning (Invitrogen, Carlsbad, CA). cDNA inserts were ligated into the pCMV•SPORT6 vector that had been cleaved with the restriction enzymes *Not*I and *Sal*I, and the resulting DNAs were electroporated into *Escherichia coli* ElectroMAX™ DH10B™ Competent Cells (Invitrogen). A library of approximately 6.8 x 10^6 independent clones was produced in which 95% of the plasmids harbored cDNA inserts with average lengths of ~1.8 kilobases (kb). Aliquots of the ligation mix containing approximately 200 clones were introduced into *E. coli* and plasmid DNA was isolated using the Wizard$^®$ *Plus* Miniprep DNA Purification System (Promega, Madison, WI). Human embryonic kidney (HEK) 293 cells (American Type Culture Collection CRL number 1573) were transfected with pools of cDNAs using the FuGENE6 reagent (Roche, Indianapolis, IN) and assayed for wax synthase activity as described below in the section entitled "*Wax Synthase Enzyme Assay in Transfected Cells*".

Mammalian Expression Plasmids – A pCMV•SPORT6 vector containing the mouse wax synthase cDNA (Genbank™/EBI Data Bank Accession numbers AY611031 and AY611032) was isolated by expression cloning as described above. A human wax synthase cDNA (Genbank™/EBI Data Bank Accession number AY605053) was amplified by the polymerase chain reaction (PCR) from adult human skin Gene Pool™ cDNA (Invitrogen, catalog no.

D8115-01) using the following oligonucleotide primers: 5'-GCCTATGTCGACGGCACAATGCTCTTGCCCTCTAAG-3' and 5'-CCGTTAGGATCCTGAAGGCTACTGGGGATGTCTGTC-3'. The amplified DNA product was digested with the restriction enzymes *Sal*I and *Bam*HI and ligated into the pCMV6 vector (Genbank™/EBI Data Bank accession number AF239250).

A mouse MGAT1 cDNA (nucleotides 1 –1008 of Genbank™/EBI Data Bank accession number AF384162) was amplified by the PCR from random hexamer primed mouse kidney cDNA using the following primers:

5'-GCCTATGTCGACCAGTACCACAAATCCTGCGAAAGG-3' and

5'-ATTATGCGGCCGCGGAGGAAGGAGGTTATTTAAATACC-3'. The amplified DNA product was digested with the restriction enzymes *Sal*I and *Not*I and ligated into the pCMV•SPORT6 vector (Invitrogen) to produce the pCMV•SPORT6-mMGAT1 expression plasmid.

A mouse MGAT2 cDNA (nucleotides 1 – 1016 of Genbank™/EBI Data Bank accession number AY157609) was amplified by the PCR from random hexamer primed mouse kidney cDNA using the following primers: 5'-GCCTATGTCGACAATCCGCAAAGCCCGTGTGTAGAG-3' and

5'-ATTATGCGGCCGCTGGAGACACTTAGCAGAACTCCAG-3'. The amplified DNA product was digested with the restriction enzymes *Sal*I and *Not*I and ligated into the pCMV•SPORT6 vector generating the pCMV•SPORT6-mMGAT2 expression plasmid.

A mouse DGAT1 cDNA (IMAGE clone 3486724, Genbank™/EBI Data Bank Accession number BC003717) in the pCMV•SPORT6 vector was purchased from the

Mammalian Gene Collection (IRAV) (Invitrogen). This plasmid is referred to here as pCMV•SPORT6-mDGAT1.

A mouse DGAT2 cDNA (nucleotides 51-1227 of Genbank™/EBI Data Bank Accession number AF384160) was amplified by the PCR from random hexamer primed mouse liver cDNA using the following primers: 5'-GCCTATGTCGACGGCTTCAGCATGAAGACCCTCATC-3' and 5'-ATTATGCGGCCGCGTCAGTTCACCTCCAGCACCTCAG-3'. The amplified DNA product was digested with the restriction enzymes *Sal*I and *Not*I and ligated into the pCMV•SPORT6 vector (Invitrogen) to make the pCMV•SPORT6-mDGAT2 expression plasmid.

Construction of epitope-tagged expression plasmids - An expression plasmid (pCMV6-FLAG-mWS) encoding a FLAG epitope-tagged version of the mouse wax synthase protein was constructed as follows. The mouse cDNA was amplified from the pCMV•SPORT6-mWS expression plasmid described above by the PCR using the oligonucleotide primers, 5'-GTACCTGTCGACCCACCATGGATTACAAGGATGACGACGATAAGGAGATTCTGG GCACCATGTTCTGG-3' and 5'-ATTATGCGGCCGCTCCAGTGAGGACCAGTCAAGTCAG-3'. The amplified DNA product was digested with the restriction enzymes *Sal*I and *BamH*I and ligated into the pCMV6 vector. The encoded mouse protein has the FLAG epitope (amino acid sequence DYKDDDDK) linked to the amino terminus of the wax synthase enzyme.

The pCMV-Script-FLAG-hDGAT1 plasmid, composed of the human DGAT1 cDNA (nucleotides 245-1895 of Genbank™/EBI Data Bank Accession NM_012079) in the pCMV-Script vector (Stratagene, La Jolla, CA) was a generous gift of Dr. Simon M. Jackson of Tularik, Inc., South San Francisco, CA. The encoded protein has the FLAG epitope tag inserted between amino acids 2 (G) and 3 (R) at the amino terminus of the encoded protein.

An expression construct (pCMV•SPORT6-FLAG-mDGAT2) encoding a FLAG epitope-tagged version of the mouse DGAT2 protein was constructed as follows. A modified DGAT2 cDNA was amplified from the pCMV•SPORT6-mDGAT2 template described above by the PCR using the oligonucleotide primers, 5'-GTACCTGTCGACCCACCATGGATTACAAGGATGACGACGATAAGATGAAGACCCTCATCGCCGCCTAC-3' and 5'-ATTATGCGGCCGCGTCAGTTCACCTCCAGCACCTCAG-3'. The PCR-amplified DNA product was digested with the restriction enzymes *Sal*I and *Not*I and ligated into the pCMV•SPORT6 vector. The encoded DGAT2 protein has the FLAG epitope at the amino terminus.

An expression plasmid (pCMV•SPORT6-FLAG-mMGAT1) encoding a FLAG epitope-tagged version of the mouse MGAT1 protein was constructed as follows. The pCMV•SPORT6-mMGAT1 template described above was used as a template with the oligonucleotide primers, 5'-GTACCTGTCGACCCACCATGGATTACAAGGATGACGACGATAAGAGTCCTCCGGGTAGAACCATGATG-3' and 5'-ATTATGCGGCCGCGGAGGAAGGAGGTTATTTAAATACC-3'. The amplified DNA

product was digested with the restriction enzymes *Sal*I and *Not*I and ligated into the pCMV•SPORT6 vector. The encoded MGAT1 protein has the FLAG epitope linked to the amino terminus.

Wax Synthase Enzyme Assay in Transfected Cells - On day 0 of an experiment, HEK 293 cells were plated at a density of 4 x 10^5 cells per 60-mm dish in low glucose Dulbecco's modified Eagle's Medium (DMEM) supplemented with 10% (v/v) fetal calf serum, 100 units/ml of penicillin, and 100 μg/ml streptomycin sulfate. On day 2, the cells were transfected with the FuGENE6 reagent and 3.5 μg of a mixture of plasmids containing 0.5 μg of pVA1 (Schneider and Shenk, 1987) and 3 μg of pools of mouse preputial gland cDNAs or pCMV6, pCMV•SPORT6-mWS, pCMV6-hWS, pCMV6-FLAG-mWS, pCMV-Script-FLAG-hDGAT1, pCMV•SPORT6-FLAG-mMGAT1, or pCMV•SPORT6-FLAG-mDGAT2 expression plasmid. After 16-20 h, medium was replaced with fresh plating medium supplemented with 2.4 μM [1-^{14}C]hexadecanol (American Radiolabeled Chemicals, St. Louis, MO). After 6-18 h of incubation, cells transfected with individual expression plasmids were washed once with 2 ml phosphate buffered saline (PBS), and scraped into 2 ml of PBS with a rubber policeman. Cells transfected with mouse cDNA pools were scraped directly into the medium with a rubber policeman. Lipid metabolites were extracted from the PBS-cell slurry or the medium-cell slurry with 8 ml of chloroform:methanol (2:1, v/v) and resolved by thin layer chromatography (TLC).

TLC – Separation of lipids was performed as described in the accompanying paper (Cheng and Russell, 2004b) using solvent system 2. Stock solutions (10 mM) of lipid standards purchased from Sigma Chemical Co. (St. Louis, MO) were made as follows: palmitic acid, stearic acid, hexadecanol, octadecanol, 1-oleoyl-rac-glycerol, 1,3-diolein, and glyceryl trioleate were dissolved in ethanol; dipalmitin and glyceryl tripalmitate were dissolved in chloroform; and cholesteryl oleate, cholesteryl palmitate, palmityl palmitate, and stearyl stearate were dissolved in hexane. Aliquots (5 μl) of individual stock solutions were chromatographed on lanes adjacent to those containing radiolabeled cell lipids.

Preparation of HEK 293 cell lysates or membranes - Cells were grown and transfected as described above. Cells were harvested approximately 31 h after transfection by scraping into 2 ml PBS, and then pelleted by centrifugation in a desk-top centrifuge at 1000g for 5 min at 4°C. The cell pellet was washed once by re-suspension in PBS and the cells collected again by centrifugation. Cells were resuspended in Hypotonic Lysis Buffer (10 mM Hepes-KOH, pH 7.6, 1.5 mM $MgCl_2$, 10 mM KCl, 1 mM EDTA, pH 8.0, 1 mM EGTA, pH 8.0) and incubated on ice for 10 min. The swollen cells were lysed by 20 passages through a 23 gauge needle. Nuclei were removed from the cell lysates by centrifugation at 1000g for 5 min at 4°C. Thereafter, 0.1 volume of 2.5 M sucrose, 1 M Tris-HCl, pH 7.4 was added to the supernatant prior to freezing in liquid N_2 and storage at -80° C. In some cases, membranes were prepared by further centrifugation of cell lysates in a Beckman TLA 100.4 rotor in a TL-100 instrument at 130,000g for 30 minutes at 4° C. Membrane pellets were resuspended

in assay buffer (0.3 M sucrose, 0.1 M Tris-HCl, pH 7.4, 1 mM EDTA) , frozen in liquid N_2, and stored at -80° C.

Assay of Fatty Alcohol and Acyl-CoA Preferences – Wax synthase enzyme activity was determined in a volume of 500 μL of 0.3 M sucrose, 0.1 M Tris-HCl, pH 7.4, 1 mM EDTA, 2.5 mM dithiothreitol, 5 mM $MgCl_2$, 0.8 mg/ml BSA, 98 μM palmitoyl-CoA, 7 μM [1-^{14}C]palmitoyl-CoA (Perkin Elmer), and 100 μM of fatty alcohol. The fatty alcohol substrates decanol (C10:0), 11-eicosenol (C20:1), erucyl alcohol (C22:1), nervonyl alcohol (C24:1), and 9,12,15-linolenyl alcohol (C18:3) were purchased from Nu-Check Prep, Inc. (Elysian, MN). The fatty and isoprenoid alcohol substrates: lauryl alcohol (C12:0), tetradecanol (C14:0), cetyl alcohol (C16:0), 1-octadecanol (C18:0), eicosanol (C20:0), palmitoleyl alcohol (C16:1(9)), oleyl alcohol (C18:1(9)), linoleyl alcohol (C18:2(9,12)), geraniol, farnesol, and geranylgeraniol were purchased from Sigma Chem. Co. Fatty acid and isoprenoid alcohol stock solutions were dissolved in ethanol at a concentration of 50 mM. Before use, eicosanol was heated to 55° C to ensure complete resuspension. Aliquots (15-20 μg) of HEK 293 cell membrane protein prepared from cells transfected with either the pCMV6, pCMV•SPORT6-mWS, or pCMV6-hWS plasmids were incubated at 37° C for 25-30 min. The reaction was stopped by addition of 100 μL of 6 N HCl. Following addition of 0.9 ml of PBS to each tube, lipids were extracted into 6 ml of chloroform:methanol (2:1, v/v). TLC of resuspended lipids was performed as described above.

To determine acyl-CoA preference, the above assay conditions were used except 93 μM hexadecanol, 7 μM [1-^{14}C]hexadecanol (Perkin Elmer), and 100 μM of acyl-CoA were

used. The acyl-CoA stocks, including decanoyl-CoA monohydrate (C10:0), lauroyl-CoA lithium salt (C12:0), myristoyl-CoA lithium salt (C14:0), palmitoyl-CoA lithium salt (C16:0), stearoyl-CoA lithium salt (C18:0), palmitoleoyl-CoA lithium salt (C16:1), oleoyl-CoA lithium salt (C18:1), linoleoyl-CoA lithium salt (C18:2), and arachidoyl-CoA monohydrate (C20:4), were purchased from Sigma Chemical Co., and dissolved in 0.01 M sodium acetate, pH 6.0, at a concentration of 10 mM.

Baculovirus Expression Vectors - A baculovirus recombinant donor plasmid with the mouse wax synthase cDNA in the pFastBac HTA vector (Invitrogen) was constructed. The cDNA insert of the pCMV•SPORT6-mWS plasmid described above was released by digestion with the restriction enzymes *Sal*I and *Not*I and ligated into the pFastBac HTA vector. To construct a mouse MGAT2 cDNA donor plasmid, the MGAT2 cDNA was amplified by the PCR from the pCMV·SPORT6-mMGAT2 template described above using the oligonucleotide primers:

5'-GCCTATGTCGACAGCCAGCTCAGCATGGTGGAGTTC-3' and 5'-ATTATGCGGCCGCTGGAGACACTTAGCAGAACTCCAG-3'. The amplified DNA product was digested with *Sal*I and *Not*I and ligated into the pFastBac HTC vector. A mouse DGAT2 donor plasmid was prepared by digesting the pCMV•SPORT6-mDGAT2 plasmid described above with the restriction enzymes *Sal*I and *Not*I to release the cDNA, which was then ligated into pFastBac HTC. A donor plasmid containing the mouse Δ^4-3-oxosteroid 5β-reductase cDNA (nucleotides 48-1053 of Genbank[TM]/EBI Data Bank accession number BC018333) was produced as described (Cheng and Russell, 2004b). Generation of infectious

Autographica californica nuclear polyhedrosis baculovirus stocks from the various donor plasmids was done in *Spodoptera frugiperda* Sf9 cells using the Bac-to-Bac Baculovirus Expression System kit (Invitrogen).

Acyltransferase Enzyme Assay in Baculovirus-Infected Cells - Sf9 cells were plated on day 0 at a density of 9 x 10^5 cells in Sf-900 II SFM media (Invitrogen) in 6-well plates. After letting cells adhere to the plate for approximately 4 h, the medium was replaced with Sf-900 II SFM medium supplemented with 50 units/ml of penicillin and 50 μg/ml streptomycin sulfate, and cells were infected for approximately 50 h with recombinant baculovirus at a multiplicity of infection (MOI) of 1-3. The medium was replaced with 2 ml of fresh plating medium supplemented with 37.5 μM bovine serum albumin (BSA)-conjugated palmitic acid and 2.7 μM of BSA-conjugated [1-^{14}C]palmitic acid (prepared as described in (Cheng and Russell, 2004b)). Cells were incubated with fatty acids for approximately 20 min at room temperature, washed with 2 ml PBS, and then harvested by scraping in 2 ml PBS with a rubber policeman. Lipid metabolites were extracted into 8 ml of chloroform:methanol 2:1 (v/v) and resolved by thin layer chromatography.

Immunoblotting – Cell extracts containing FLAG epitope-tagged proteins were prepared from duplicate plates of transfected HEK 293 cells. Cell extracts containing hexa-histidine-tagged enzymes were harvested from 6-well plates infected with the indicated baculovirus expression vectors. Polyacrylamide gel electrophoresis in the presence of SDS was carried out under standard conditions. Resolved proteins were transferred by electroblotting to

HybondC Extra nitrocellulose membranes (Amersham, Piscataway, NJ). FLAG epitope-tagged proteins were detected by incubation with a 1:1000 dilution of the primary FLAG M2 mouse monoclonal antibody (Sigma Chem. Co.) in a solution of 5% (w/v) powdered milk, 1% (v/v) fetal calf serum, 0.01% (v/v) Tween 20 in PBS, followed by incubation with a 1:7500 dilution of secondary goat anti-mouse horse radish peroxidase-conjugated antibody (Pierce Chem. Co., Rockford IL). Visualization of the peroxidase was performed with enhanced chemiluminescence reagents (Amersham). Hexa-histidine epitope-tagged proteins were detected following the manufacturer's protocol for the Tetra-His HRP Conjugate Kit (Qiagen, Valencia CA).

Immunocytochemistry – Transfection, antibody staining, and imaging were performed as described (Cheng and Russell, 2004b). Chinese hamster ovary (CHO)-K1 cells were transiently transfected with either the pCMV6 or pCMV6-FLAG-mWS plasmids, and then incubated with primary antibodies (anti–calnexin carboxyl terminus rabbit polyclonal antibody (Stressgen, San Diego, CA) at a 1:200 dilution and/or α–FLAG M2 monoclonal antibody (Sigma Chem. Co.) at a 1:500 dilution). Cells were incubated for 1 h with secondary antibodies (Alexa Fluor 568 goat anti-rabbit IgG (Molecular Probes, Eugene, OR) and/or Alexa Fluor 488 goat anti-mouse IgG (Molecular Probes) at a 1:500 dilution.

Real Time PCR – cDNA synthesis and real time PCR reactions were performed as described in (Cheng and Russell, 2004b). Male human adult skin total RNA was obtained from

Stratagene (catalog #735031). Oligonucleotide primers used to amplify the mouse wax synthase cDNA were:

5'-AGTTTTTGTCTTTTTCCCCTGAGA-3' and 5'-CTTGCTGCTAATGCTTTCATGAA-3'. Oligonucleotide primers used to amplify the human wax synthase cDNA were: 5'-TCTTTGCAGCTACTGGTGAGATAGTC-3' and 5'-TTGTCCATTGTTTTCCTCAATGC-3'.

Reconstitution of Wax Biosynthetic Pathway – Enzyme activities were measured in a volume of 500 μl of 0.3 M sucrose, 0.1 M Tris-HCl, pH 7.4, 1 mM EDTA, 2.5 mM dithiothreitol, 5 mM $MgCl_2$, 0.8 mg/ml BSA, 2.5 mM β-NADPH, 2.5 mM β-NADH, 1 mM ATP, 100 μM CoA, 2.9 μM of BSA-conjugated [1-^{14}C]palmitic acid, and 40 μM BSA-conjugated palmitic acid. Aliquots (400 μg protein) of lysates from 293 cells transfected with pCMV6, pCMV•SPORT6-mFAR1, pCMV•SPORT6-mWS, or pCMV•SPORT6-mFAR1 plus pCMV•SPORT6-mWS plasmids were assayed. Alternatively, lysate (200 μg protein) from HEK 293 cells transfected with pCMV•SPORT6-mFAR1 was mixed with the same amount of lysate from cells transfected with the pCMV•SPORT6-mWS and added to the assay mix. All reactions were incubated at 37° C for 30 min and then stopped by the addition of 100 μl of 6 N HCl. Thereafter, 0.9 ml of PBS was added to each tube and lipids were extracted with 6 ml of chloroform:methanol 2:1 (v/v). TLC on resuspended lipids was performed as described above.

RESULTS

The mouse preputial gland is a bilateral sebaceous gland that flanks the reproductive tract and is enriched in wax esters (48% of total lipid content, (Nikkari, 1974a)). Membrane preparations from the gland were found to contain abundant wax synthase activity as judged by the conversion of hexadecanol and [^{14}C]palmitate to the wax monoester cetylpalmitate (see below). This source of enzyme activity was used in preliminary experiments to identify a solvent system that resolved waxes from other classes of neutral lipids on TLC plates and to optimize in vitro conditions for wax synthesis. An expression cloning strategy to isolate cDNAs encoding the wax synthase enzyme(s) was designed thereafter. Poly(A)$^{+}$-enriched RNA was isolated from preputial glands and a library consisting of approximately 6.8 x 10^{6} independent cDNA clones was made.   Plasmid DNA was prepared from pools of approximately 200 cDNAs, transfected into HEK 293 cells, and the formation of wax esters from [1-^{14}C]hexadecanol was monitored in the culture medium and cells by TLC. Several positive pools of cDNAs were identified, and two of these pools were progressively subdivided by repeated rounds of bacterial transformation, cell transfection, and assay until single cDNAs were obtained (Fig. 1*A*). DNA sequence analysis indicated that the two cDNAs encoded the same protein but differed from each other in sequences present in the untranslated regions. One cDNA (GenBank^{TM}/EBI Accession Number AY611031) contained a 272 nucleotide insert at the 3'-terminus that was not present in the second cDNA and that presumably reflected an alternate polyadenylation site in the gene. The second cDNA

(GenBank™/EBI Accession Number AY611032) contained a 24 nucleotide sequence at the 5'-terminus that was not present in the first cDNA.

Humans do not have a direct counterpart to the mouse preputial gland, the tissue from which the wax synthase cDNAs were isolated; however, database searches indicated the presence of a skin mRNA encoding a putative human wax synthase. Based on this information, a cDNA specifying the human protein was isolated by reverse transcriptase-PCR from skin mRNA. Transfection of an expression vector containing this cDNA into HEK 293 cells followed by incubation with [1-^{14}C]hexadecanol led to the synthesis of wax esters (Fig. 1*B*), confirming that the human cDNA encoded a bona fide wax synthase.

The deduced amino acid sequences of the mouse and human wax synthase enzymes are shown in Figure 2*A*. The proteins are the same length (333 amino acids) and share 84% sequence identity. Comparison of the cDNA sequences with those of genomic DNAs reveals that the mouse wax synthase gene is located on the X chromosome, band C3, and contains at least seven exons spanning ~10.3 kb (Fig. 2*B*). The human wax synthase gene is located in a syntenic region of the X chromosome, band q13.1, and is predicted to have an identical exon-intron structure encompassing ~8.2 kb (Fig. 2*B*).

Database searches with the mouse and human wax synthase sequences indicated that they were members of the acyltransferase family of enzymes involved in neutral lipid synthesis. This group of proteins includes the acyl-CoA:cholesterol acyltransferases 1 and 2 (ACAT 1 and ACAT2), the DGAT1 and DGAT2 enzymes, and the MGAT1 and MGAT2 enzymes (Buhman et al., 2001). Sequence identities between acyltransferase family members and the wax synthase are shown in Figure 2*C*. These data indicate that the wax

synthase is most closely related to the MGAT1, MGAT2, and DGAT2 proteins, and they raise the questions of whether the acyltransferases have wax synthase enzyme activity or the wax synthase has acyltransferase activity.

To answer these questions, we first established the fatty acyl-CoA and fatty alcohol substrate preference of the mouse wax synthase enzyme expressed in HEK 293 cells. Membranes from transfected cells were found to contain optimum enzyme activity with hexadecanol and [1-^{14}C]palmitoyl-CoA substrates when the assay buffer had a pH between 7-8, magnesium concentrations between 0-3 mM, and ionic strengths between 0-200 mM KCl. At pH values greater than 8, substantial non-enzymatic formation of wax esters as well as other undefined lipid metabolites was observed. Magnesium at concentrations higher than 3 mM inhibited wax synthase activity. Standard incubation times and temperatures were fixed at 37° C and 30 min, respectively, which represented conditions where only a small percentage of input substrates were converted into product.

The alcohol preference of the mouse wax synthase was determined by incubating membrane preparations containing the enzyme with fatty alcohols of different carbon chain lengths and saturation together with [^{14}C]palmitoyl-CoA (Fig. 3*A*). Of 13 fatty alcohols tested, the rank order of preference was saturated fatty alcohols > monounsaturated fatty alcohols = polyunsaturated fatty alcohols. As a general rule, the longer the fatty alcohol the less well it was utilized as a substrate by the wax synthase enzyme (Fig. 3*A*, compare C:10 to C20:0, and C16:1 to C24:1). Squalene, a polyisoprenoid containing six isoprenoid units, is an abundant constituent of sebum (Nikkari, 1974a), and for this reason various isoprenols were tested as wax synthase substrates. The data of Fig. 3*A* showed that the mouse wax

synthase incorporated 10, 15, and 20 carbon isoprenoid alcohols into wax monoesters but not as efficiently as the C16:0 fatty alcohol, hexadecanol.

The acyl-CoA substrate preference of the mouse wax synthase enzyme was examined by incubating acyl-CoAs of different carbon chain length and saturation with [1-^{14}C]hexadecanol (Fig. 4*B*). Fewer acyl-CoA substrates were available than fatty alcohol substrates, but among those tested the wax synthase enzyme preferred shorter chain fatty acids (compare C10:0 to C18:0 or C20:0). As with the fatty alcohols, the enzyme did not discriminate between monounsaturated and polyunsaturated fatty acyl-CoA substrates under the conditions of the assay. In experiments not shown, membranes derived from HEK 293 cells expressing the human wax synthase enzyme displayed similar substrate preferences for fatty alcohols, isoprenoid alcohols, and acyl-CoAs as those of the recombinant mouse enzyme.

We next tested whether the MGAT and DGAT members of the acyltransferase family had wax synthase enzyme activity. Mouse cDNAs for MGAT1, MGAT2, and DGAT2, and a human DGAT1 cDNA were engineered to encode a FLAG epitope tag at the amino terminus of each enzyme. Control transfection experiments with these cDNAs in HEK 293 cells indicated that the addition of the FLAG epitope tag reduced the acyltransferase activity of the MGAT2 enzyme but had no effects on the activities of the other three enzymes. The wax synthase activity in intact cells expressing the three acyltransferases not affected by the FLAG tag is shown in Fig. 5*A*. The MGAT1 and DGAT1 wax synthase activities were approximately 5-fold higher than background levels detected in mock transfected cells, whereas the DGAT2 activity was approximately 12.5-fold over background. Although

measurable, these activities were less than that for the wax synthase enzyme, which was >100-fold over background (Fig. 5*A*). Immunoblotting of cell lysates from duplicate dishes in the transfection experiment showed that the FLAG epitope-tagged MGAT1, DGAT1, DGAT2, and wax synthase proteins were expressed at similar levels (Fig. 5*A*).

To circumvent the inactivation of the MGAT2 enzyme by the FLAG epitope, the cDNA was engineered to contain a hexa-histidine epitope and then cloned into a baculovirus expression vector. For comparison purposes, the DGAT2 cDNA was engineered in a similar fashion. The data shown in Fig. 5*B* revealed that the MGAT2 enzyme possessed detectable wax synthase activity that appeared to be higher than that of the DGAT2 enzyme; however, comparison of the amount of recombinant protein in the infected cells showed that the MGAT2 enzyme is expressed at levels that are approximately five-fold higher than those of DGAT2 (Fig. 5*B*). As with the experiment in the HEK 293 cells, the amount of wax monoester formed in cells infected with a baculovirus containing the wax synthase cDNA were much greater than either the MGAT2 or DGAT2 enzymes regardless of the amount of protein expressed in the Sf9 cells. Control experiments with uninfected cells or those infected with a virus expressing steroid 5β-reductase (a control enzyme without acyltransferase activity) showed no endogenous wax production (Fig. 5*B*). We concluded from the experiments shown in Figure 5 that the rank order of wax synthase activity among the various acyltransferase enzymes was wax synthase $\gg$ DGAT2 $>$ MGAT2 $=$ MGAT1.

The subcellular localization of the mouse wax synthase protein was determined by immunocytochemistry (Fig. 6). In these experiments, CHO-K1 cells were transfected with either a plasmid encoding a FLAG epitope-tagged mouse wax synthase or a plasmid lacking

194

a cDNA, and then prepared for immunofluorescence microscopy. Staining with a fluorescein-labeled secondary antiserum recognizing the anti-FLAG monoclonal antibody indicated that the wax synthase was present in the endoplasmic reticulum (Fig. 6*E*). This assignment was supported by co-localization of the enzyme with calnexin (Fig. 6*F*), an integral membrane protein of the endoplasmic reticulum (Fig. 6*A, C, D*). No immunofluorescent signal corresponding to the FLAG epitope was detected in mock-transfected cells (Fig. 6*B*).

Waxes are components of sebum and meibum, the oils secreted by sebaceous glands to coat the external surfaces of the organism. Based on this function, we anticipated that the highest levels of wax synthase mRNA in the mouse would be present in the preputial gland, skin, and eyelid. The real time PCR data of Fig. 7 show that this expected distribution was observed, and that several additional tissues contained measurable levels of wax synthase mRNA, including thymus and spleen. RNA blotting experiments showed that the major wax synthase mRNA in the preputial gland is approximately 1.4 kilobases in length and that a second minor transcript of about 2.9 kb is also present in this tissue (data not shown). Oligonucleotide primers for the human wax synthase mRNA generated a threshold value (C_T) of 26.4 when total RNA from male skin was used as a template, indicating that the wax synthase gene is transcribed in the human dermis.

In a final series of experiments, the mammalian wax biosynthetic pathway was reconstituted in cultured HEK 293 cells by co-expressing cDNAs encoding mouse fatty acyl-CoA reductase 1 (FAR1) (Cheng and Russell, 2004b) and wax synthase. When membranes from co-transfected cells were incubated with BSA-conjugated [^{14}C]palmitate, both

radiolabeled fatty alcohol and wax monoester were produced (Fig. 8, *lane 4*). Similarly, when equal amounts of membranes from cells transfected individually with the FAR1 or wax synthase cDNAs were mixed together, both the fatty alcohol and the wax were synthesized (*lane 5*). In control experiments, mock transfected cells produced little of either product (*lane 1*), while membranes from cells transfected with the FAR1 cDNA produced hexadecanol but no wax (*lane 2*), and those transfected with the wax synthase made neither product due to the absence of an endogenous fatty acyl-CoA reductase (*lane 3*). Similar results were obtained in intact cells when either FAR1 or FAR2 and wax synthase cDNAs were transfected into HEK 293 cells (data not shown).

DISCUSSION

We report the cDNA cloning and characterization of a mammalian wax synthase that catalyzes the formation of ester bonds between fatty alcohols and fatty acyl-CoAs to form wax monoesters. The wax synthase belongs to a small family of enzymes termed acyltransferases that participate in neutral lipid synthesis. Recombinant wax synthase utilizes a range of fatty alcohol and fatty acyl-CoA substrates and is more active in wax monoester synthesis than in cholesteryl ester, diacylglycerol, or triacylglycerol synthesis. Conversely, acyltransferase family members that share significant sequence identity with the wax synthase, including the MGAT1, MGAT2, and DGAT2 enzymes, exhibit modest wax monoester synthesis activity. When expressed in HEK 293 cells, the wax synthase localizes to the endoplasmic reticulum. Wax synthase mRNA is most abundant in tissues that are rich in sebaceous glands, including the eyelid and preputial gland, and is less plentiful in other tissues. Co-expression of fatty acyl-CoA reductase and wax synthase enzymes in naïve cells leads to the reconstitution of a wax biosynthetic pathway.

Several lines of evidence suggest that the wax synthase enzyme identified in this study plays a biologically relevant role in the synthesis of wax monoesters in mammals. First, the wax synthase is related in sequence to several members of a family of enzymes that synthesize the major classes of neutral lipids. The acyltransferase enzymes include ACAT1 and ACAT2 that produce cholesteryl esters, MGAT1 and MGAT2 that produce diacylglycerols, and DGAT1 and DGAT2 that produce triacylglycerols. Among acyltransferases, the wax synthase is most closely related to the MGAT1, MGAT2, and

DGAT2 enzymes, and shares little more than random sequence identity with the ACAT1, ACAT2, and DGAT1 enzymes (Fig. 2*C*). While the more closely related enzymes have measurable wax synthase activities, these are at least an order of magnitude less than that of the wax synthase enzyme (Fig. 4). Under the conditions utilized here, we were unable to demonstrate significant acyltransferase enzyme activity associated with the recombinant wax synthase (Fig. 5), nor did the wax synthase have detectable ACAT activity (e.g., Fig. 1). Thus, unlike the bacterial wax synthase enzyme from *Acinetobacter calcoaceticus*, which has both wax synthase and DGAT activity (Kalscheuer and Steinbuchel, 2003), the mammalian counterpart appears to be largely a wax synthase. These results suggest that following the genetic event leading to the formation of the primordial wax synthase gene in the mammalian lineage, the specificity of the encoded enzyme evolved to specialize in the formation of wax esters at the expense of other neutral lipids. This specialization may reflect the localization of the wax synthase gene on the X chromosome as genes on the sex chromosomes are subject to different selective pressures from those on autosomes (Brown and Greally, 2003).

A second line of support indicating the potential biological importance of the wax synthase comes from comparisons between the fatty acids and alcohols present in waxes of mouse sebum to the substrate preferences of the recombinant enzyme. The fatty acids of waxes isolated from the preputial gland are present in the following order of abundance: C16:1>C18:1>C16:0>C20:0>C14:0, and the fatty alcohol moiety is predominantly C16:0 (Snyder and Blank, 1969). Each of these fatty acids or alcohols are utilized as substrates by the mouse enzyme in vitro (Fig. 3*A*, 3*B*), and presumably are in vivo as well. Despite this correlation, additional factors must influence the wax composition of sebum, including the

substrate preferences of the fatty acyl-CoA reductases, intracellular lipid transport proteins, and fatty acid synthesis enzymes. These inputs may explain the absence of short chain fatty acids (e.g., C10:0 and C12:0) from sebum waxes even though these lipids are excellent substrates for the wax synthase in vitro.

In addition to straight chain fatty alcohols and acids, the wax synthase incorporated several polyisoprenols into waxes (Fig. 3*C*), and was active in the formation of retinol esters (S. Andersson, unpublished results). Polyisoprenoid-containing waxes have not been reported in sebum and meibum surveys of mammals (Nicolaides, 1965; Nicolaides et al., 1981; Nikkari, 1974a; Sansone and Hamilton, 1969), thus it is not clear whether these lipids are synthesized in vivo. Nevertheless, if they were, the recurring branched chains and unsaturation of the isoprenoid moieties would be expected to confer unique physiochemical and perhaps biochemical properties on this class of waxes. It also remains undetermined whether the formation of retinol esters by the wax synthase is biologically relevant.

The preponderance of wax synthase mRNA in the preputial gland and eyelid is a third indication that a major function of the encoded enzyme is the synthesis of wax monoesters. The preputial gland of the mouse contains large quantities of wax monoesters (Nikkari, 1974a), as does the meibomian gland of the cow (Nicolaides et al., 1981), and coincident with this lipid composition, these tissues in the mouse have the highest levels of wax synthase mRNA (Fig. 7). Similarly, human sebum is composed of ~25% wax monoesters and the wax synthase mRNA is detectable in this tissue by real time PCR. Inasmuch as mRNA levels equate with expression of the enzyme, and activity assays with membranes from the mouse preputial gland suggest this is the case (Fig. 8), these data place the wax

synthase in the appropriate tissues for a role in sebaceous gland lipid synthesis. The wax synthase mRNA also is present in several other organs, notably the thymus and spleen, which suggests that waxes may be produced in non-dermal locations.

A fourth line of evidence that speaks to the biological role of the wax synthase is the ability to reconstitute the wax biosynthetic pathway in cells by co-expression of the fatty acyl-CoA reductase 1 and wax synthase enzymes (Fig. 8). This result signifies that as in plants (Jenks et al., 2002; Kunst and Samuels, 2003), the minimum number of enzymes required for wax monoester synthesis in mammals is two. Furthermore, the localization of the fatty acyl-CoA reductase enzymes in the peroxisome (Cheng and Russell, 2004b) and the wax synthase in the endoplasmic reticulum (Fig. 6), indicates the existence of transport systems that facilitate the movement of substrates and products of the pathway between these organelles. The proteins involved in this intracellular transport are presumably present in HEK 293 and Sf9 cells given the synthesis of waxes by these cell types (e.g., Fig. 4). A separate transport system may move waxes out of the cell as the products of the pathway were not secreted into the medium. The deposition of sebum in mammals is accomplished by lysis of lipid-laden sebocytes in a process termed holocrine secretion (Thody and Shuster, 1989), whereas in plants, waxes are secreted without cell lysis (Kunst and Samuels, 2003). The proteins involved in wax secretion in plants have not been identified but it may be possible to isolate these using expression cloning in mammalian cells and an assay that screens for the presence of wax in the culture medium.

The reconstitution of the mammalian wax biosynthetic pathway in cultured cells suggests that it may be possible to assemble a bioreactor for the production of wax

---

monoesters of defined chemical composition. Wax monoesters are an important constituent of cosmetics, polishes, and coatings, which presently are isolated by laborious methods from natural sources such as the jojoba plant (candelilla wax), Brazilian palm tree (carnauba wax), sheep wool (lanolin), or honey bee (beeswax). While a majority of the three billion pounds of wax produced each year is derived from petroleum in the form of paraffins, which are mixtures of normal and iso-alkanes, the properties of these chemically-manufactured paraffins are different from those of wax monoesters. The development of cell lines that express the fatty acyl-CoA reductase and wax synthase cDNAs, perhaps coupled with a wax transport system to allow secretion of the wax into the medium, might provide an alternate source of wax esters for commercial purposes.

201

Figure 1. *A*, Expression cloning of wax synthase cDNAs from mouse preputial gland. A cDNA library was prepared from male preputial gland mRNA and divided into pools of ~200 cDNAs each. Plasmid DNA from individual pools was combined with pVA1 plasmid (to increase expression from the expression plasmids, (Schneider and Shenk, 1987)), and introduced via the FuGENE6 reagent (Roche) into HEK 293 cells. [1-^{14}C]hexadecanol was added to the medium 16-20 h later, and after a further incubation of 6-18 h, the cells were harvested by scraping into the medium. Lipid metabolites were extracted from the slurry with into chloroform:methanol (2:1, v/v) and resolved by TLC. An autoradiogram prepared by exposure of the TLC plate to Kodak BioMax MR film for 72 h is shown. *Lane 1*, radiolabeled lipids from mock-transfected cells; *lane 2*, lipids synthesized in cells transfected with a 200-member cDNA pool encoding wax synthase activity; *lane 3*, lipids synthesized from a sub-pool of 20 cDNAs derived from the pool analyzed in lane 2; *lane 4*, lipids from cells transfected with a single positive cDNA derived from the sub-pool of lane 3. The positions to which cholesteryl esters and a wax monoester standard (cetyl palmitate) migrated to on the plate are shown on the *right*. Only the portion of the autoradiogram containing radiolabeled cholesteryl and wax esters is shown. *B*, Expression of mouse and human wax synthase enzyme activities in HEK 293 cells. Expression vectors encoding nothing (*pCMV*, *lane 1*), the human wax synthase enzyme (*hWS, lane 2*), or the mouse wax synthase enzyme (*mWS, lane 3*) were introduced into HEK 293 cells by transfection. Subsequent assay for wax ester synthesis was carried out as described in *A*.

A. cDNA Pool Size — Mock, 200, 20, — | Cholesteryl esters, Wax esters | lanes 1 2 3 4

B. pCMV, hWS, mWS | Cholesteryl esters, Wax esters | lanes 1 2 3
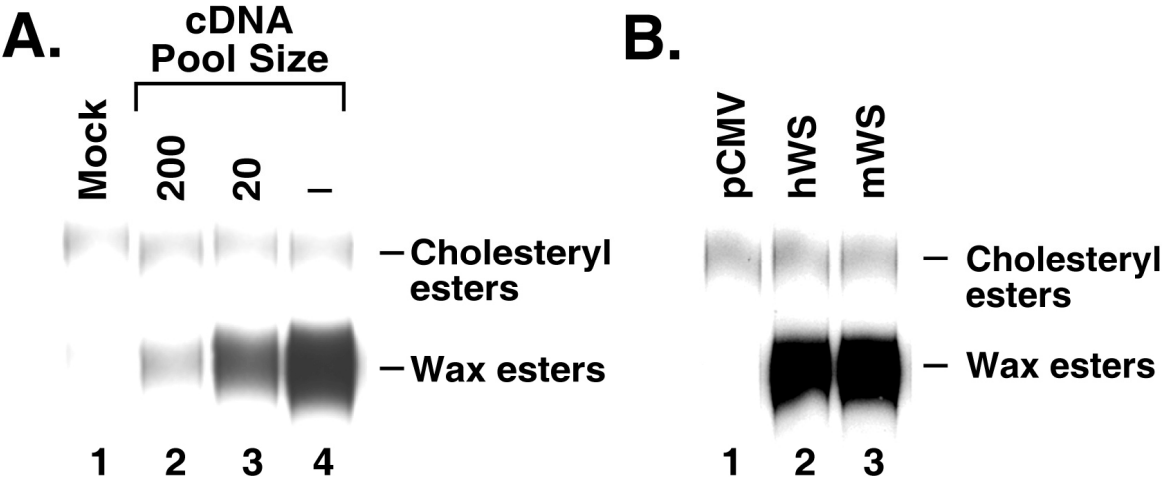
Figure 2. Comparison of mouse and human wax synthases. *A*, The deduced sequences of the human (*hWS*) and mouse (*mWS*) wax synthase proteins are aligned with identities between the two enzymes indicated by *black boxes*. Amino acids are numbered on the *right*. *Arrowheads* above the alignment indicate the positions of introns in the encoding genes. *Dots* indicate every tenth amino acid residue. The GenBank™/EBI Data Bank accession number for the human wax synthase cDNA sequence is AY605053 and for the mouse are AY611031 and AY611032. *B*, Structures and chromosomal locations of the human and mouse wax synthase genes. Exons are indicated by *boxes* and introns by *connecting lines*. Amino acids encoded at the beginning and end of the protein are indicated *above* the gene schematic. The structures of the gene and their chromosomal locations were deduced by comparing the sequences of the cloned cDNAs to those of genomic DNAs (GenBank™/EBI Data Bank accession number HsX_11826_33.52 for human gene and MmX_78942_32 for mouse gene). *C*, Amino acid sequence identities between mouse acyltransferase enzymes. The percent sequence identity between the indicated family members was deduced by pair wise comparisons using the BLASTP 2.2.6 program.

A.

```
                          •                              ▼  •
hWS  M L L P S K K D L K T A L D  V F A V  F Q W  S F  S A L  L  I T T      30
mWS  M F W P T K K D L K T A M E  V F A L  F Q W  A L  S A L  V  I V T

           •                    •              •
     T V I  A V N L Y L V V F T  P  Y W P V T V L  I  L T W L A F D W       60
     T V I  I V N L Y L V V F T  S  Y W P V T V L  M  L T W L A F D W

              ▼    •                                            ▼ •
     K T P Q  R G G R R F T C V R H  W R L W K H Y S D Y F P L K  L        90
     K T P E  R G G R R F T C V R K  W R L W K H Y S D Y F P L K  M

              •              •                •
     L K T H  D I C P S  R N Y I L V C H P H G L  F A H G W  F G H F       120
     V K T K  D I S P D  R N Y I L V C H P H G L  M A H S C  F G H F

           •                •                  •
     A T E A S  G F S K  I  F P G I T P Y  I  L T L G A F F W  M  P F L    150
     A T D T T  G F S K  T  F P G I T P Y  M  L T L G A F F W  V  P F L

                    ▼   •                        •                  •
     R E Y V M S T G A  C S V S R S S  I  D F L L T H  K G T G N M  V      180
     R D Y V M S T G S  C S V S R S S  M  D F L L T Q  K G T G N M  L

         •                •                •
     I  V V I G G L A E C R Y S  L P G S  S T L  V L K N R S  G F V R      210
     V  V V V G G L A E C R Y S  T P G S  T T L  F L K K R Q  G F V R

              ▼  •                 •                   •
     M  A L Q H G V  P L I P A Y A F G E T D L Y D Q H I F T P G G         240
     T  A L K H G V  S L I P A Y A F G E T D L Y D Q H I F T P G G

                 •              •                  •
     F V N R F Q K W F Q  S  M V H I Y P C A F Y G R G  F  T K N S W       270
     F V N R F Q K W F Q  K  M V H I Y P C A F Y G R G  L  T K N S W

                      ▼  •              •                •
     G L L P Y S  R  P V T T I  V G E P L P M  P K I E N P S Q  E I V      300
     G L L P Y S  Q  P V T T V  V G E P L P L  P K I E N P S E  E I V

              •                •                  •
     A K Y H T L Y I D A L R K L F D Q H K T K F G I S E T Q E L           330
     A K Y H T L Y I D A L R K L F D Q H K T K F G I S E T Q E L

     E  I  I   333
     V  I  V
```

B.

C.

	ACAT1	ACAT2	DGAT1	DGAT2	MGAT1	MGAT2
Wax Synthase	13.8%	15.9%	13.2%	46.5%	38.7%	40.5%

Figure 3. Substrate preferences of the mouse wax synthase enzyme. Aliquots (15-20 µg) of

HEK 293 membrane protein prepared from cells expressing the mouse wax synthase enzyme

were incubated with the indicated radiolabeled and unlabeled lipids at 37° C for 25-30 min.

Reactions were stopped by acidification and lipids extracted for TLC analysis as described in

"*Experimental Procedures*". The radiolabeled lipids used in these reactions are incorporated

into multiple products by endogenous enzymes and for this reason only the portion of the

autoradiogram containing wax esters is shown. *A*, Fatty alcohol substrates. Individual fatty

alcohols tested are designated by chain length and number of unsaturated bonds (e.g., 10:0 is

decanol, which has ten carbons and zero double bonds; 18:3 is 9,12,15 linolenyl alcohol,

which has eighteen carbons and three double bonds). *B*, Fatty acyl-CoA substrates. Fatty

acyl groups are designated by chain length and number of unsaturated bonds. *C*, Isoprenol

substrates. C_{10}, farnesol, C_{15}, geraniol, C_{20}, geranylgeraniol, *C16:0*, hexadecanol control.

The results shown in *panels A-C* are typical of those obtained in at least two separate

experiments carried out on different days using recombinant mouse and human wax

synthases.

A.

[14C]Palmitoyl-CoA	+	+	+	+	+	+	+	+	+	+	+	+	+	+
Fatty Alcohol	—	10:0	12:0	14:0	16:0	18:0	20:0	16:1	18:1	20:1	22:1	24:1	18:2	18:3

Wax esters

B.

[14C]Hexadecanol	+	+	+	+	+	+	+	+	+	+	+
Fatty Acyl-CoA	—	10:0	12:0	14:0	16:0	18:0	20:0	16:1	18:1	18:2	20:4

Wax esters

C.

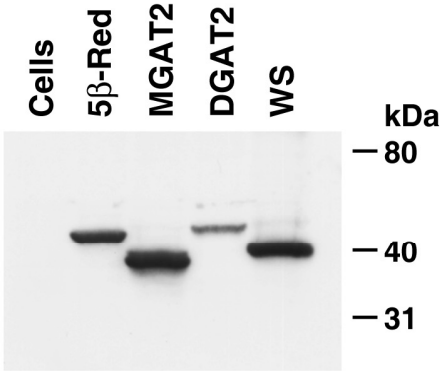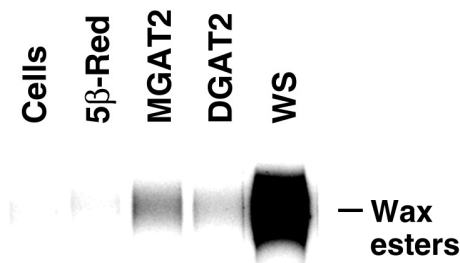| [14C]Palmitoyl-CoA	+	+	+	+	+
Substrate	—	C_{10}	C_{15}	C_{20}	16:0

Wax esters

Figure 4. Wax synthase activity of acyltransferase family members. *A*, HEK 293 cells were transfected with expression plasmids encoding the indicated acyltransferase enzymes modified to contain FLAG epitopes and then assayed for the synthesis of wax esters following addition of [^{14}C]hexadecanol to the culture medium (*top panel*). The positions to which cholesteryl and wax esters migrated to on the TLC plate are indicated on the *right* of the autoradiogram. To determine relative expression levels of the acyltransferase enzymes, cell lysates were prepared from duplicate dishes and subjected to immunoblotting using a monoclonal antibody directed against the FLAG epitope (*bottom panel*). The positions to which protein standards of known molecular weight migrated to on the SDS-polyacrylamide gel are indicated on the *right* of the lumigram. *B*, Insect Sf9 cells were infected with baculovirus vectors encoding the indicated acyltransferase or control enzyme (steroid 5β-reductase, *5β-Red*) modified to contain a hexa-histidine epitope and then assayed for the synthesis of wax esters as described in *A* (*top panel*). Endogenous levels of ACAT enzyme activity are low in Sf9 cells and thus the formation of cholesteryl esters in the infected cells was not detected in the exposure shown. Cell lysates from duplicate dishes were subjected to immunoblotting using a monoclonal antibody directed against the hexa-histidine epitope (*bottom panel*). The results shown are representative of at least two experiments performed on different days.

A. HEK 293 Cells

pCMV | MGAT1 | DGAT1 | DGAT2 | WS

— Cholesteryl esters

— Wax esters

MGAT1 | DGAT1 | DGAT2 | WS | kDa

—80

—40

—31

Anti-FLAG

B. Sf9 Cells

Cells | 5β-Red | MGAT2 | DGAT2 | WS

— Wax esters

Cells | 5β-Red | MGAT2 | DGAT2 | WS | kDa

—80

—40

—31
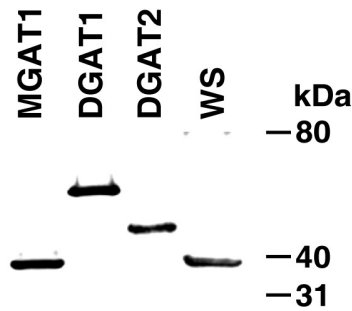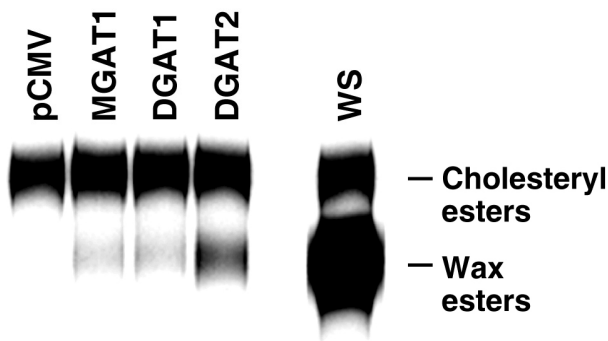
Anti-His

Figure 5. Acyltransferase activity of wax synthase enzyme. Insect Sf9 cells were infected with baculovirus vectors encoding the mouse wax synthase (*WS*), indicated acyltransferase, or control enzyme (steroid 5β-reductase, *5β-Red*), each modified to contain a hexa-histidine epitope, and then assayed for the synthesis of diacylglycerols and triacylglycerols following the addition of BSA-conjugated [^{14}C]palmitate to the culture medium (*top panel*). Only a product of unknown structure was detected in uninfected cells (*Cells*), whereas those infected with the control steroid 5β-reductase virus synthesized this product and an enhanced level of triacylglycerols. Cells infected with the MGAT2 expressing virus produced elevated levels of diacylglycerols, which were further converted into triacylglycerols, and those infected with the DGAT2-expressing virus produced elevated levels of triacylglycerols. No increase in acyltransferase activity was detected in cells infected with the wax synthase expressing virus. To determine relative expression levels of the various enzymes, cell lysates from duplicate dishes were subjected to immunoblotting using a monoclonal antibody directed against the hexa-histidine epitope (*bottom panel*). The MGAT2 and wax synthase enzymes were expressed at higher levels than the steroid 5β-reductase and DGAT2 enzymes. The results shown in panels *A* and *B* are typical of those obtained in three different experiments.

Sf9 Cells

Cells 5β-Red MGAT2 DGAT2 WS

— Triacylglycerols

— Palmitate

— Diacylglycerols
— Unknown

Cells 5β-Red MGAT2 DGAT2 WS

kDa
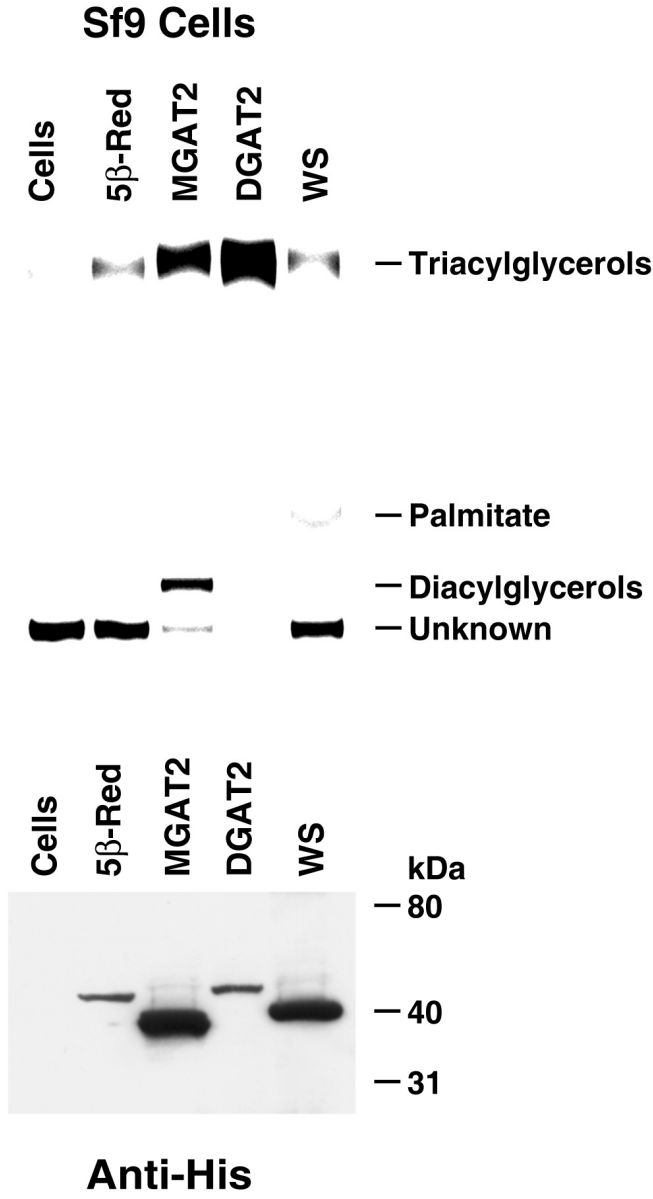— 80

— 40

— 31

Anti-His

Figure 6. Subcellular localization of mouse wax synthase enzyme. CHO-K1 cells were transfected with the indicated expression vectors encoding nothing (*pCMV*) or a FLAG epitope-tagged wax synthase (*Wax Synthase*) enzyme. After transient expression, cells were fixed, permeabilized, and incubated with a rabbit polyclonal antiserum directed against the endoplasmic reticulum protein calnexin (*Anti-Calnexin*) and a mouse monoclonal antibody directed against the FLAG epitope (*Anti-FLAG*). Panels *A, D*: detection of rabbit polyclonal antibodies directed against calnexin with rhodamine-conjugated goat anti-rabbit antiserum. Panels *B, E*: detection of FLAG epitope with fluorescein-conjugated goat anti-mouse antiserum. Panels *C, F*: merged images of rhodamine and fluorescein signals. Double indirect immunofluorescence microscopy was performed on a Zeiss 510 Laser Scanning Confocal microscope using a 63 × 1.3 NA PlanApo objective. Both the calnexin and FLAG-wax synthase enzymes are detected in endoplasmic reticulum membranes of CHO cells. These data are representative of two separate experiments.

A B C pCMV
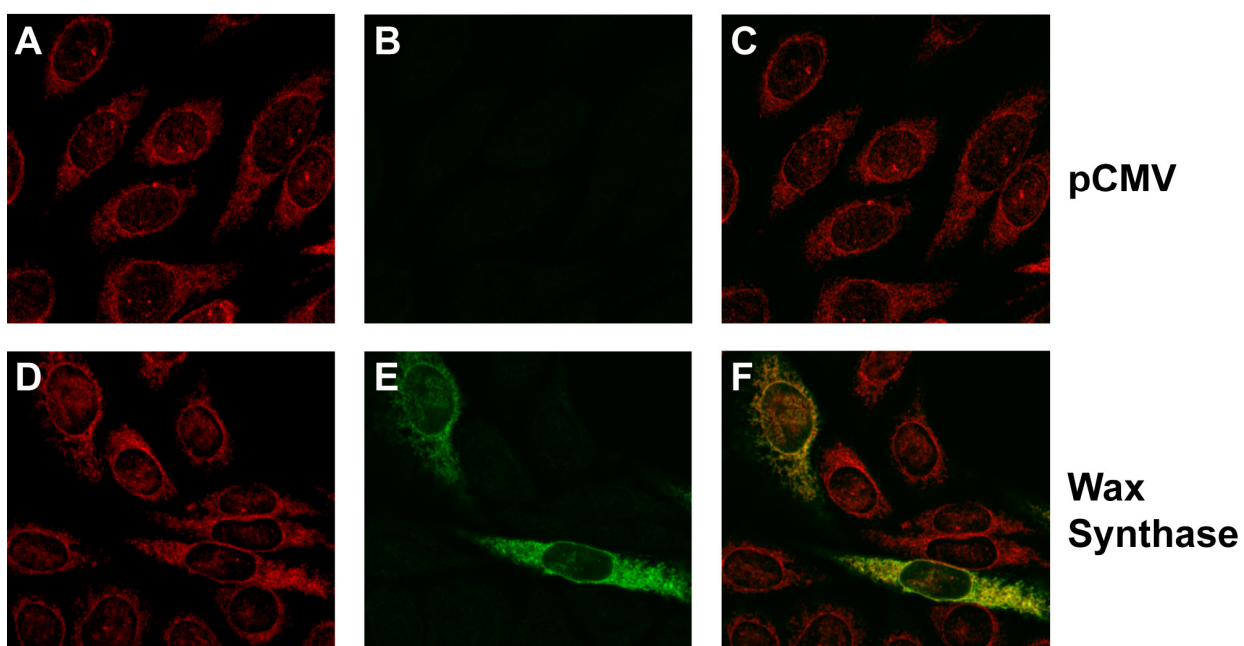
D E F Wax Synthase

213

Figure 7. Tissue distributions of mouse wax synthase mRNA. The relative levels of wax synthase mRNA were determined by real time PCR in the tissues and cell types indicated on the *left* of the figure using cyclophilin mRNA levels as a reference standard. The data were then normalized to the threshold values (C_T) determined in the liver ($C_T = 29.2$) and then expressed on a $\log_{10}$ scale. This experiment was repeated twice using the same preparations of tissue RNAs isolated from pools of animals (organ samples) or dishes (macrophage samples).
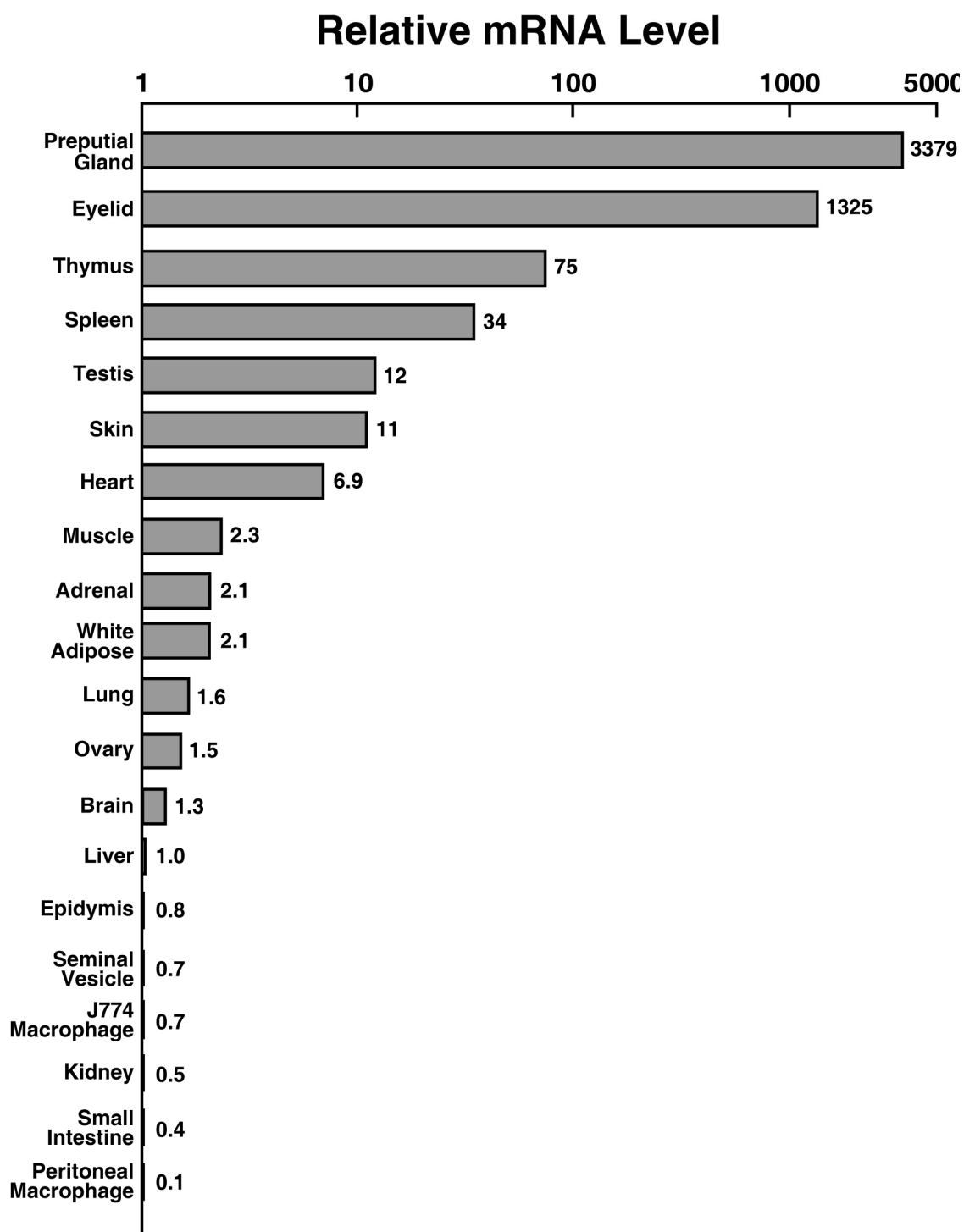
Relative mRNA Level

Figure 8. Reconstitution of mammalian wax biosynthetic pathway in cell lysates of transfected HEK 293 cells. The indicated plasmid DNAs were introduced into HEK 293 cells by transfection and allowed to express for two days. Cellular membranes were isolated and the conversion of BSA-conjugated [^{14}C]palmitate into lipids was determined. *Lane 1*, mock-transfected cells synthesized an unknown product and triacylglycerols. *Lane 2*, cells expressing fatty acyl CoA-reductase 1 (*FAR1*) produced these same two products and hexadecanol. *Lane 3*, cells expressing wax synthase (*WS*) produced only the two background lipids, indicating the near absence of fatty acyl-CoA reductase activity in HEK 293 cells. *Lane 4*, cells transfected with the fatty acyl-CoA reductase 1 and wax synthase cDNAs produced the two background lipids, hexadecanol, wax esters, and an additional lipid of unknown structure. *Lane 5*, the mixing of equal amounts of membranes derived from cells transfected individually with the fatty acyl-CoA reductase 1 and wax synthase cDNAs resulted in the production of the background lipids plus hexadecanol and wax esters. *Lane 6*, positive control showing synthesis of hexadecanol and wax esters by membranes from mouse preputial glands. This experiment was performed in various guises many times.
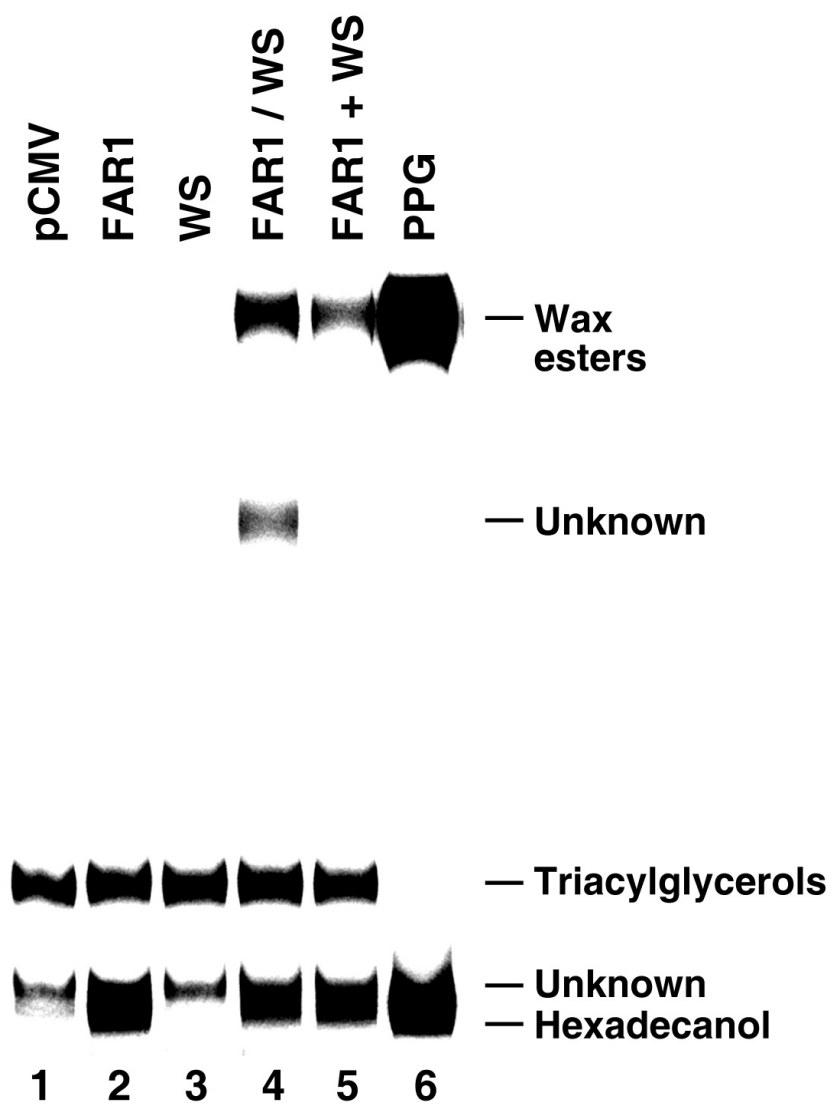
BIBLIOGRAPHY

Aarts, M. G. M., Hodge, R., Kalantidis, K., Florack, D., Wilson, Z. A., Mulligan, B. J., Stiekema, W. J., Scott, R., and Pereira, A. (1997). The *Arabidopsis MALE STERILITY 2* protein shares similarity with reductases in elongation/condensation complexes. Plant J *12*, 615-623.

Abdullah, M. A., Salhi, H. S., Bakry, L. A., Okamoto, E., Abomelha, A. M., Stevens, B., and Mousa, F. M. (2002). Adolescent rickets in Saudi Arabia: a rich and sunny country. J Pediatr Endocrin Metab *15*, 1017-1025.

Altschul, S. F., Madden, T.L., Schaffer, A.A., Zhang, J., Zhang, Z., Miller, W., and Lipman, D.J. (1997). Gapped BLAST and PSI-BLAST: a new generation of protein database programs. Nuc Acids Res *25*, 3389-3402.

Andersson, S., Davis, D. L., Dahlback, H., Jornvall, H., and Russell, D. W. (1989). Cloning, structure, and expression of the mitochondrial cytochrome P-450 sterol 26-hydroxylase, a bile acid biosynthetic enzyme. J Biol Chem *264*, 8222-8229.

Andersson, S., Holmberg, I., and Wikvall, K. (1983). 25-Hydroxylation of C27-steroids and vitamin D3 by a constitutive cytochrome P-450 from rat liver microsomes. J Biol Chem *258*, 6777-6781.

Andersson, S., and Jornvall, H. (1986). Sex differences in cytochrome P-450-dependent 25-hydroxylation of C27-steroids and vitamin D3 in rat liver microsomes. J Biol Chem *261*, 16,932-916,936.

Asami, T., Kawasaki, T., and Uchiyama, M. (1995). Unique form of rickets with low serum 25-hydroxyvitamin D in normally nourished children. Acta Paediatr Jpn *37*, 182-188.

Barletta, F., Freedman, L. P., and Christakos, S. (2002). Enhancement of VDR-mediated transcription by phosphorylation: Correlation with increased interaction between VDR and DRIP205, a subunit of the VDR-interacting protein coactivator complex. Mol Endocrinol *16*, 301-314.

Beckman, M. J., Tadikonda, P., Werner, E., Prahl, J., Yamada, S., and DeLuca, H. F. (1996). Human 25-hydroxyvitamin D3-24-hydroxylase, a multicatalytic enzyme. Biochemistry *35*, 8465-8472.

Bell, N. H., Greene, A., Epstein, S., Oexmann, M. J., Shaw, S., and Shary, J. (1985). Evidence for alteration of the vitamin D-endocrine system in blacks. J Clin Invest *76*, 470-473.

Bhattacharyya, M. H., and DeLuca, H. F. (1974). Subcellular location of rat liver calciferol-25-hydroxylase. Arch Biochem Biophys *160*, 58-62.

Bishop, J. E., and Hajra, A. K. (1981). Mechanism and specificity of formation of long chain alcohols by developing rat brain. J Biol Chem *256*, 9542-9550.

Bjorkhem, I., Boberg, K. M., and Leitersdorf, E. (2001). Inborn errors in bile acid biosynthesis and storage of sterols other than cholesterol. In The Metabolic and Molecular Bases of Inherited Disease., C. R. Scriver, A. L. Beaudet, W. S. Sly, D. Valle, B. Childs, K. W. Kinzler, and B. Vogelstein, eds. (New York, McGraw-Hill, Inc.), pp. 2961-2988.

Bjorkhem, I., and Holmberg, I. (1978). Assay and properties of a mitochondrial 25-hydroxylase active on vitamin D3. J Biol Chem *253*, 842-849.

Bjorkhem, I., Holmberg, I., Oftebro, H., and Pedersen, J. I. (1980). Properties of a reconstituted vitamin D$_3$ 25-hydroxylase from rat liver mitochondria. J Biol Chem *255*, 5,244-245,249.

Blunt, J. W., DeLuca, H. F., and Schnoes, H. K. (1968). 25-Hydroxycholecalciferol. A biologically active metabolite of vitamin D. Biochem *7*, 3317-3322.

Borst, P., and Elferink, R. O. (2002). Mammalian ABC transporters in heath and disease. Annu Rev Biochem *71*, 537-592.

Bove, K., Daugherty, C. C., Tyson, W., Heubi, J. E., Balistreri, W. F., and Setchell, K. D. R. (2000). Bile acid synthetic defects and liver disease. Pediatr Develop Pathol *3*, 1-16.

Brown, C. J., and Greally, J. M. (2003). A stain upon the silence: genes escaping X inactivation. Trends Genet *19*, 432-438.

Buhman, K. K., Chen, H. C., and Farese Jr., R. V. (2001). The enzymes of neutral lipid synthesis. J Biol Chem *276*, 40369-40372.

Bull, L. N., van Eijk, M. J. T., Pawlikowska, L., DeYoung, J. A., Juijn, J. A., Liao, M., Klomp, L. W. J., Lomri, N., Berger, R., Scharschmidt, B. F.*, et al.* (1998). A gene encoding a P-type ATPase mutated in two forms of hereditary cholestasis. Nat Genet *18*, 219-224.

Cali, J. J., Hsieh, C., Francke, U., and Russell, D. W. (1991). Mutations in the bile acid biosynthetic enzyme sterol 27-hydroxylase underlie cerebrotendinous xanthomatosis. J Biol Chem *266*, 7779-7783.

Casella, S. J., Reiner, B. J., Chen, T. C., Holick, M. F., and Harrison, H. E. (1994). A possible defect in 25-hydroxylation as a cause of rickets. J Pediatr *124*, 929-932.

Cases, S., Stone, S. J., Zhou, P., Yen, E., Tow, B., Lardizabal, K. D., Voelker, T., and Farese, R. V., Jr. (2001). Cloning of DGAT2, a second mammalian diacylglycerol acyltransferase, and related family members. J Biol Chem *276*, 38870-38876.

Chawla, A., Repa, J. J., Evans, R. M., and Mangelsdorf, D. J. (2001). Nuclear receptors and lipid physiology: Opening the X-files. Science *294*, 1866-1870.

Chen, H. C., Smith, S. J., Tow, B., Elias, P. M., and Farese, J., R. V. (2002). Leptin modulates the effects of acyl CoA:diacylglycerol acyltransferase deficiency on murine fur and sebaceous glands. J Clin Invest *109*, 175-181.

Chen, K. S., Prahl, J. M., and DeLuca, H. F. (1993). Isolation and expression of human 1,25-dihydroxyvitamin D3 24-hydroxylase cDNA. Proc Natl Acad Sci U S A *90*, 4543-4547.

Cheng, J. B., Motola, D. L., Mangelsdorf, D. J., and Russell, D. W. (2003). De-orphanization of cytochrome P450 2R1, a microsomal vitamin D 25-hydroxylase. J Biol Chem *278*, 38,084-038,093.

Cheng, J. B., and Russell, D. W. (2004). Mammalian wax biosynthesis: I. Identification of two fatty acyl-Coenzyme A reductases with different substrate specificities and tissue distributions. J Biol Chem *279*, 37,789-37,797.

Cheng, J. B., and Russell, D. W. (2004). Mammalian wax biosynthesis: II. Expression cloning of wax synthase cDNAs encoding a member of the acyltransferase enzyme family. J Biol Chem *279*, 37,798-37,807.

Cho, H. P., Nakamura, M., and Clarke, S. D. (1999a). Cloning, expression, and fatty acid regulation of the human Delta-5 desaturase. J Biol Chem *274*, 37335-37339.

Cho, H. P., Nakamura, M. T., and Clarke, S. D. (1999b). Cloning, expression, and nutritional regulation of the mammalian Delta-6 desaturase. J Biol Chem *274*, 471-477.

Choi, M., Yamamoto, K. R., Itoh, T., Makishima, M., Mangelsdorf, D. J., Moras, D., DeLuca, H. F., and Yamada, S. (2003). Interaction between vitamin D receptor and vitamin D ligands. Two-dimensional alanine scanning mutagenesis analysis. Chem Biol *10*, 261-270.

Clayton, P. T., Leonard, J. V., Lawson, A. M., Setchell, K. D., Andersson, S., Egestad, B., and Sjovall, J. (1987). Familial giant cell hepatitis associated with synthesis of 3α, 7α-dihydroxy-and 3β, 7α, 12α-trihydroxy-5-cholenoic acids. J Clin Invest *79*, 1031-1038.

Cooper, R. S., Luke, A., Zhu, X., Kan, D., Adeyemo, A., Rotimi, C., Bouzekri, N., Ward, R., and Rorimi, C. (2002). Genome scan among Nigerians linking blood pressure to chromosomes 2, 3, and 19. Hypertension *40*, 629-633.

Dahlback, H., and Wikvall, K. (1988). 25-Hydroxylation of vitamin D_3 by a cytochrome P-450 from rabbit liver mitochondria. Biochem J *252*, 207-213.

Daugherty, C. C., Setchell, K. D. R., Heubi, J. E., and Balistreri, W. F. (1993). Resolution of liver biopsy alterations in three siblings with bile acid treatment of an inborn error of bile acid metabolism (Δ^4-3-oxosteroid 5β-reductase deficiency). Hepatology *18*, 1096-1101.

de Vet, E., Ijlst, L., Oostheim, W., Wanders, R. J., and van den Bosch, H. (1998). Alkyl-dihydroxyacetonephosphate synthase - Fate in peroxisome biogenesis disorders and identification of the point mutation underlying a single enzyme deficiency. J Biol Chem *273*, 10296-10301.

de Vet, E., van den Broek, B. T., and van den Bosch, H. (1997). Nucleotide sequence of human alkyl-dihydroxyacetonephosphate synthase cDNA reveals the presence of a peroxisomal targeting signal 2. Biochim Biophys Acta *1346*, 25-29.

de Vree, J. M., Jacquemin, E., Sturm, E., Cresteil, D., Bosma, P. J., Aten, J., Deleuze, J. F., Desrochers, M., Burdelski, M., Bernard, O.*, et al.* (1998). Mutations in the MDR3 gene cause progressive familial intrahepatic cholestasis. Proc Natl Acad Sci USA *95*, 282-287.

Dean, M., Hamon, Y., and Chimini, G. (2001). The human ATP-binding cassette (ABC) transporter superfamily. J Lipid Res *42*, 1007-1017.

Demay, M. (1999). Inherited Defects of Vitamin D Metabolism. In Vitamin D : molecular biology, physiology, and clinical applications, M. F. Holick, ed. (Totowa, Humana Press), pp. 307-316.

Downing, D. T., and Strauss, J. S. (1974). Synthesis and composition of surface lipids of human skin. J Investig Dermatol *62*, 228-244.

Driver, P. J., and Lemp, M. A. (1996). Meibomian gland dysfunction. Survey Opthamol *40*, 343-367.

Edelson, P. J., Zweibel, R., and Cohn, Z. A. (1975). The pinocytic rate of activated macrophages. J Exp Med *142*, 1150-1164.

Fraser, D. R., and Kodicek, E. (1970). Unique biosynthesis by kidney of a biologically active vitamin D metabolite. Nature *228*, 764-766.

Fukushima, M., Susuki, Y., Tohira, Y., Nishi, Y., Susuki, M., Sasaki, S., and Suda, T. (1976). 25-Hydroxylation of 1α-hydroxyvitamin D_3 in vivo in the perfused rat liver. FEBS Lett *65*, 211-214.

Furster, C., Zhang, J., and Toll, A. (1996). Purification of a 3β-hydroxy-Δ^5-C_{27}-steroid dehydrogenase from pig liver microsomes active in major and alternative pathways of bile acid synthesis. J Biol Chem *271*, 20903-20907.

Garabedian, M., and Ben-Mekhbi, H. (1999). Rickets and Vitamin D Deficiency. In Vitamin D : molecular biology, physiology, and clinical applications, M. F. Holick, ed. (Totowa, Humana Press), pp. 273-286.

Gibbs, R. A., Weinstock, G. M., Metzker, M. L., Muzny, D. M., Sodergren, E. J., Scherer, S., Scott, G., Steffen, D., Worley, K. C., Burch, P. E*., et al.* (2004). Genome sequence of the Brown Norway rat yields insights into mammalian evolution. Nature *428*, 493-521.

Gould, S. J., Krisans, S., Keller, G. A., and Subramani, S. (1990). Antibodies directed against the peroxisomal targeting signal of firefly luciferase recognize multiple mammalian peroxisomal proteins. J Cell Biol *110*, 27-34.

Graham, S. E., and Peterson, J. A. (2002). Sequence alignments, variabilities, and vagaries. Meth Enzymol *357*, 15-28.

Griffin, J. E., and Zerwekh, J. E. (1983). Impaired stimulation of 25-hydroxyvitamin D-24-hydroxylase in fibroblasts from a patient with vitamin D-dependent rickets, type II. J Clin Invest *72*, 1190-1199.

Gunning, P., Ponte, P., Okayama, H., Engel, J., Blau, H., and Kedes, L. (1983). Isolation and characterization of full-length cDNA clones for human α−, β−, and γ-actin mRNAs: Skeletal but not cytoplasmic actins have an amino-terminal cysteine that is subsequently removed. Mol Cell Biol *3*, 787-795.

Guo, Y.-D., Strugnell, S. A., Back, D. W., and Jones, G. (1993). Transfected human liver cytochrome P-450 hydroxylates vitamin D analogs at different side-chain positions. Proc Natl Acad Sci U S A *90*, 8668-8672.

Gupta, R. P., Hollis, B. W., Patel, S. B., Patrick, K. S., and Bell, N. H. (2004). CYP3A4 is a human vitamin D 25-hydroxylase. J Bone Mineral Res *19*, 680-688.

Gutierrez, A., Grunau, A., Paine, M., Munro, A. W., Wolf, C. R., Roberts, G. C., and Scrutton, N. S. (2003). Electron transfer in human cytochrome P450 reductase. Biochem Soc Trans *31*, 497-501.

Haussler, M. R., Myrtle, J. F., and Norman, A. W. (1968). The association of a metabolite of vitamin D_3 with intestinal mucosa chromatin in vivo. J Biol Chem *243*, 4055-4064.

Haussler, M. R., and Norman, A. W. (1969). Chromosomal receptors for a vitamin D metabolite. Proc Natl Acad Sci U S A *62*, 155-162.

Holick, M. F. (1999). Noncalcemic Actions of 1,25-Dihydroxyvitamin D_3 and Clinical Implications. In Vitamin D : molecular biology, physiology, and clinical applications, M. F. Holick, ed. (Totowa, Humana Press), pp. 207-216.

Holick, M. F., Schnoes, H. K., DeLuca, H. F., Suda, T., and Cousins, R. J. (1971). Isolation and identification of 1,25-dihydroxycholecalciferol. A metabolite of vitamin D active in the intestine. Biochem *10*, 2799-2804.

Holmberg, I., Berlin, T., Ewerth, S., and Bjorkhem, I. (1986). 25-Hydroxylase activity in subcellular fractions from human liver. Evidence for different rates of mitochondrial hydroxylation of vitamin D2 and D3. Scand J Clin Lab Invest *46*, 785-790.

Hosseinpour, F., and Wikvall, K. (2000). Porcine microsomal vitamin D(3) 25-hydroxylase (CYP2D25). Catalytic properties, tissue distribution, and comparison with human CYP2D6. J Biol Chem *275*, 34,650-634,655.

Ichimaya, H., Nazer, H., Gunasekaran, T., Clayton, P., and Sjovall, J. (1990). Treatment of chronic liver disease caused by 3β-hydroxy-Δ^5-C_{27}-steroid dehydrogenase deficiency with chenodeoxycholic acid. Arch Dis Childhood *65*, 1121-1124.

Itoh, S., Yoshimura, T., Iemura, O., Yamada, E., Tsujikawa, K., Kohama, Y., and Mimura, T. (1995). Molecular cloning of 25-hydroxyvitamin D-3 24-hydroxylase (Cyp-24) from mouse kidney: its inducibility by vitamin D-3. Biochim Biophys Acta *1264*, 26-28.

Jacquemin, E. (2000). Progressive familial intrahepatic cholestasis. Genetic basis and treatment. Clin Liver Dis *4*, 753-763.

Jacquemin, E., Gerhardt, M., Cresteil, D., Fabre, M., Taburet, A. M., Hadchouel, M., Trivin, F., Setchell, K. D. R., and Bernard, O. (2001). Long-term effects of bile acid therapy in children with defects ofprimary bile acid synthesis:3β-hydroxy-C_{27}-steroid-dehydrogenase/isomerase and Δ^4-3-oxosteroid 5β-reductase deficiencies. (Dordrecht, Kluwer Academic Publishers).

Jacquemin, E., Setchell, K. D. R., O'Connell, N. C., Estrada, A., Maggiore, G., Schmitz, J., Hadchouel, M., and Bernard, O. (1994). A new cause of progressive intrahepatic cholestasis: 3β-hydroxy-C_{27}-steroid dehydrogenase/isomerase deficiency. J Pediatrics *125*, 379-384.

Jelinek, D. F., Andersson, S., Slaughter, C. A., and Russell, D. W. (1990). Cloning and regulation of cholesterol 7α-hydroxylase, the rate limiting enzyme in bile acid biosynthesis. J Biol Chem *265*, 8190-8197.

Jenks, M. A., Eigenbrode, S. D., and Lemieux, B. (2002). Cuticular waxes of *Arabidopsis*. (American Society of Plant Biologists, Rockville, MD).

Jones, G., Strugnell, S. A., and DeLuca, H. F. (1998). Current understanding of the molecular actions of vitamin D. Physiol Rev *78*, 1193-1231.

Kalscheuer, R., and Steinbuchel, A. (2003). A novel bifunctional wax ester synthase/acyl-CoA:diacylglycerol acyltransferase mediates wax ester and triacylglycerol biosynthesis in *Acinetobacter calcoaceticus* ADP1. J Biol Chem *278*, 8075-8082.

Kato, S. (2001). Vitamin D 1α-hydroxylase knockout mice as a hereditary rickets animal model. Endocrinology *142*, 2734-2735.

Kawauchi, H., Sasaki, J., Adachi, T., Hanada, K., Beppu, T., and Horinouchi, S. (1994). Cloning and nucleotide sequence of a bacterial cytochrome P-450$_{VD25}$ gene encoding vitamin D-3 25-hydroxylase. Biochim Biophys Acta *1219*, 179-183.

Kitanaka, S., Takeyama, K., Murayama, A., and Kato, S. (2001). The molecular basis of vitamin D-dependent rickets type I. Endocr J *48*, 427-432.

Kitanaka, S., Takeyama, K., Murayama, A., Sato, T., Okamura, K., Nogami, M., Hasegawa, Y., Niimi, H., Yanagisawa, J., Tanaka, T., and Kato, S. (1998). Inactivating mutations in the 25-hydroxyvitamin D_3 1α-hydroxylase gene in patients with pseudovitamin D-deficiency rickets. N Engl J Med *338*, 681-682.

Kleene, K. C. (2001). A possible meiotic function of the peculiar patterns of gene expression in mammalian spermatogenic cells. Mech Develop *106*, 3-23.

Kolattukudy, P. E. (1976). Chemistry and Biochemistry of Natural Waxes (Amsterdam, Elsevier).

Kreiter, S. R., Schwartz, R. P., Kirkman, H. N., Charlton, P. A., Calikoglu, A. S., and Davenport, M. L. (2000). Nutritional rickets in African American breast-fed infants. J Pediatr *137*, 153-157.

Kunst, L., and Samuels, A. L. (2003). Biosynthesis and secretion of plant cuticular wax. Prog Lipid Res *42*, 51-80.

Lardizabal, K. D., Metz, J. G., Sakamoto, T., Hutton, W. C., Pollard, M. R., and Lassner, M. W. (2000). Purification of a jojoba embryo wax synthase, cloning of its cDNA, and production of high levels of wax in seeds of transgenic Arabidopsis. Plant Physiol *122*, 645-655.

Lehmann, J. M., Kliewer, S. T., Moore, L. B., Smith-Oliver, T. A., Oliver, B. B., Su, J., Sundseth, S. S., Winegar, D. A., Blanchard, D. E., Spencer, T. A., and Willson, T. M. (1997). Activation of the nuclear receptor LXR by oxysterols defines a new hormone response pathway. J Biol Chem *272*, 3137-3140.

Leitersdorf, E., Reshef, A., Meiner, V., Levitzki, R., Schwartz, S. P., Dann, E. J., Berkman, N., Cali, J. J., Klapholz, L., and Berginer, V. M. (1993). Frameshift and splice-junction mutations in the sterol 27-hydroxylase gene cause cerebrotendinous xanthomatosis in jews of Moroccan origin. J Clin Invest *91*, 2488-2496.

Liberman, U. A., and Marx, S. J. (2001). Vitamin D and other calciferols. In The Metabolic & Molecular Bases of Inherited Disease, C. R. Scriver, A. L. Beaudet, W. S. Sly, D. Valle, B. Childs, K. W. Kinzler, and B. Vogelstein, eds. (New York, McGraw-Hill), pp. 4223-4240.

Li-Hawkins, J., Lund, E. G., Bronson, A. D., and Russell, D. W. (2000). Expression cloning of an oxysterol 7α-hydroxylase selective for 24-hydroxycholesterol. J Biol Chem *275*, 16543-16549.

Lin, C. J., Wijesuriya, S. D., Abdullah, M. A., Casella, S. J., and Miller, W. L. (2003). Lack of mutations in CYP2D6 and CYP27 in patients with apparent deficiency of vitamin D 25-hydroxylase. Mol Genet Metab *80,* 469-472.

Lu, T. T., Makishima, M., Repa, J. J., Schoonjans, K., Kerr, T. A., Auwerx, J., and Mangelsdorf, D. J. (2000). Molecular basis for feedback regulation of bile acid synthesis by nuclear receptors. Mol Cell *6,* 507-515.

Lund, E. G., Guileyardo, J. M., and Russell, D. W. (1999). cDNA cloning of cholesterol 24-hydroxylase, a regulator of cholesterol homeostasis in the brain. Proc Natl Acad Sci USA *96*, 7238-7243.

Lund, E. G., Kerr, T. A., Sakai, J., Li, W.-P., and Russell, D. W. (1998). cDNA cloning of mouse and human cholesterol 25-Hydroxylases, polytopic membrane proteins that synthesize a potent oxysterol regulator of lipid metabolism. J Biol Chem *273*, 34316-34348.

Luong, A., Hannah, V. C., Brown, M. S., and Goldstein, J. L. (2000). Molecular characterization of human acetyl-CoA synthetase, an enzyme regulated by sterol regulatory element-binding proteins. J Biol Chem *275*, 26458-26466.

Madhoc, T. C., and DeLuca, H. F. (1979). Characteristics of the rat liver microsomal enzyme system converting cholecalciferol into 25-hydroxycholecalciferol. Biochem J *184*, 491-499.

Madhok, T. C., and DeLuca, H. F. (1979). Characteristics of the rat liver microsomal enzyme system converting cholecalciferol into 25-hydroxycholecalciferol. Evidence for the participation of cytochrome p-450. Biochem J *184*, 491-499.

Makishima, M., Lu, T. T., Xie, W., Whitfield, G. K., Domoto, H., Evans, R. M., Haussler, M. R., and Mangelsdorf, D. J. (2002). Vitamin D receptor as an intestinal bile acid sensor. Science *296*, 1313-1316.

Masumoto, O., Ohyama, Y., and Okuda, K. (1988). Purification and characterization of vitamin D 25-hydroxylase from rat liver mitochondria. J Biol Chem *263*, 14,256-214,260.

McCulley, J. P., and Shine, W. E. (2002). Meibomian gland and tear film lipids: structure, function, and control. Adv Exp Med Biol *506*, 373-378.

McDonnell, D. P., Mangelsdorf, D. J., Pike, J. W., Haussler, M. R., and O'Malley, B. W. (1987). Molecular cloning of complementary DNA encoding the avian receptor for vitamin D. Science *235*, 1214-1217.

McKenna, N. J., Lanz, R. B., and O'Malley, B. W. (1999). Nuclear receptor coregulators: cellular and molecular biology. Endocr Rev *20*, 321-344.

Metz, J. G., Pollard, M. R., Anderson, L., Hayes, T. R., and Lassner, M. W. (2000). Purification of a jojoba embryo fatty acyl-coenzyme A reductase and expression of its cDNA in high erucic acid rapeseed. Plant Physiol *122*, 635-644.

Miyazaki, M., Gomez, F. E., and Ntambi, J. M. (2002). Lack of stearoyl-CoA desaturase-1 function induces a palmitoyl-CoA Δ6 desaturase and represses the stearoyl-CoA desaturase-3 gene in the preputial gland of the mouse. J Lipid Res *43*, 2146-2154.

Miyazaki, M., Jacobson, M. J., Man, W. C., Cohen, P., Asilmaz, E., Friedman, J. M., and Ntambi, J. M. (2003). Identification and characterization of murine SCD4, a novel heart-specific stearoyl-CoA desaturase isoform regulated by leptin and dietary factors. J Biol Chem *278*, 33904-33911.

Miyazaki, M., Man, W. C., and Ntambi, J. M. (2001). Targeted disruption of stearoyl-CoA desaturase 1 gene in mice causes atrophy of sebaceous and meibomian glands and depletion of wax esters in the eyelid. J Nutr *131*, 2260-2268.

Miyazaki, M., and Ntambi, J. M. (2003). Role of stearoyl-coenzyme A desaturase in lipid metabolism. Prostaglandins Leukot Essent Fatty Acids *68*, 113-121.

Moon, Y. A., and Horton, J. D. (2003). Identification of two mammalian reductases involved in the two-carbon fatty acyl elongation cascade. J Biol Chem *278*, 7335-7343.

Moon, Y. A., Shah, N. A., Mohapatra, S., Warrington, J. A., and Horton, J. D. (2001). Identification of a mammalian long chain fatty acyl elongase regulated by sterol regulatory element-binding proteins. J Biol Chem *276*, 45358-45366.

Moore, C., and Snyder, F. (1982). Regulation of acyl coenzyme A reductase by a heat-stable cytosolic protein during preputial gland development. Arch Biochem Biophys *214*, 500-504.

Mooser, V., Scheer, D., Marcovina, S. M., Wang, J., Guerra, R., Cohen, J., and Hobbs, H. H. (1997). The Apo(a) gene is the major determinant of variation in plasma Lp(a) levels in African Americans. Am J Hum Genet *61*, 402-417.

Moto, K., Yoshiga, T., Yamamoto, M., Takahashi, S., Okano, K., Ando, T., Nakat, T., and Matsumoto, S. (2003). Pheromone gland-specific fatty-acyl reductase of the silkmoth, *Bombyx mori*. Proc Natl Acad Sci U S A *100*, 9156-9161.

Munn, N. J., Arnio, E., Liu, D., Zoeller, R. A., and Liscum, L. (2003). Deficiency in ethanolamine plasmalogen leads to altered cholesterol transport. J Lipid Res *44*, 182-192.

Nagan, N., and Zoeller, R. A. (2001). Plasmalogens: biosynthesis and functions. Prog Lipid Res *40*, 199-229.

Nelson, D. R. (2003). Comparison of P450s from human and fugu: 420 million years of vertebrate P450 evolution. Arch Biochem Biophys *409*, 18-24.

Nelson, D. R., Koymans, L., Kamataki, T., Stegeman, J. J., Feyereisen, R., Waxman, D. J., Waterman, M. R., Gotoh, O., Coon, M. J., Estabrook, R. W*., et al.* (1996). P450 superfamily: update on new sequences, gene mapping, accession numbers and nomenclature. Pharmacogenetics *6*, 1-42.

Nesby-O'Dell, S., Scanlon, K. S., Cogswell, M. E., Gillespie, C., Hollis, B. W., Looker, A. C., Allen, C., Doughertly, C., Gunter, E. W., and Bowman, B. A. (2002). Hypovitaminosis D prevalence and determinants among African American and white women of reproductive age: third National Health and Nutrition Examination Survey. Am J Clin Nutr *76*, 187-192.

Nicolaides, N. (1965). Skin lipids II. Lipid class composition of samples from various species and anatomical sites. J Am Oil Chem Soc *42*, 691-702.

Nicolaides, N., Kaitaranta, J. K., and Rowdan, T. N. (1981). Meibomian gland studies: comparison of steer and human lipids. Invest Opthamol Vis Sci *20*, 522-536.

Nikkari, N. (1974a). Comparative chemistry of sebum. J Invest Dermatol *62*, 257-267.

Nikkari, T. (1974b). Comparitive chemistry of sebum. J Invest Dermatol *62*, 257-267.

Norman, A. W. (1998). Sunlight, season, skin pigmentation, vitamin D, and 25-hydroxyvitamin D: integral components of the vitamin D endocrine system. Am J Clin Nutr *67*, 1108-1110.

Nutzenadel, W., Mehls, O., and Klaus, G. (1995). A new defect in vitamin D metabolism. J Pediatr *126*, 676-677.

Nykjaer, A., Dragnun, D., Walther, D., Vorum, H., Jacobsen, C., Herz, J., Melsen, F., Christensen, E. I., and Willnow, T. E. (1999). An endocytic pathway essential for renal uptake and activation of the steroid 25-(OH) vitamin D$_3$. Cell *96*, 507-515.

Ofman, R., Hettema, E. H., Hogenhout, E. M., Caruso, U., Muijsers, A. O., and Wanders, R. J. A. (1998). Acyl-CoA : dihydroxyacetonephosphate acyltransferase: cloning of the human cDNA and resolution of the molecular basis in rhizomelic chondrodysplasia punctata type 2. Hum Mol Genet *7*, 847-853.

Ohyama, Y., Noshiro, M., and Okuda, K. (1991). Cloniing and expression of cDNA encoding 25-hydroxyvitamin D3 24-hydroxylase. FEBS Lett *278*, 195-198.

Omdahl, J. L., Morris, H. A., and May, B. K. (2002). Hydroxylase enzymes of the vitamin D pathway: Expression, function, and regulation. Annu Rev Nutr *22*, 139-166.

Omura, T. (1999). Forty years of cytochrome P450. Biochem Biophys Res Commun *266*, 690-698.

Peterson, J. A., and Graham, S. E. (1998). A close family resemblance: the importance of structure in understanding cytochromes P450. Structure *6*, 1079-1085.

Ponchon, G., and DeLuca, H. F. (1969). The role of the liver in the metabolism of vitamin D. J Clin Invest *48*, 1273-1279.

Ponchon, G., Kennan, A. L., and DeLuca, H. F. (1969). "Activation" of vitamin D by the liver. J Clin Invest *48*, 2032-2037.

Prescott, S. M., Zimmerman, G. A., and McIntyre, T. M. (1990). Platelet-Activating Factor. J Biol Chem *265*, 17381-17384.

Reiser, S., and Somerville, C. (1997). Isolation of mutants of *Acinetobacter calcoaceticus* deficient in wax ester synthesis and complementation of one mutation with a gene encoding a fatty acyl coenzyme A reductase. J Bacteriol *179*, 2969-2975.

Repa, J. J., Lund, E. G., Horton, J. D., Leitersdorf, E., Russell, D. W., Dietschy, J. M., and Turley, S. D. (2000). Disruption of the sterol 27-hydroxylase gene in mice results in hepatomegaly and hypertriglyceridemia: reversal by cholic acid feeding. J Biol Chem *275*, 39,685-639,692.

Rosen, C. J. (1999). Vitamin D and Bone Health in Adults and the Elderly. In Vitamin D : molecular biology, physiology, and clinical applications, M. F. Holick, ed. (Totowa, Humana Press), pp. 287-305.

Rosen, H., Reshef, A., Maeda, N., Lippoldt, A., Shpizen, S., Triger, L., Eggertsen, G., Bjorkhem, I., and Leitersdorf, E. (1998). Markedly reduced bile acid synthesis but maintained levels of cholesterol and vitamin D metabolites in mice with disrupted sterol 27-hydroxylase gene. J Biol Chem *273*, 14805-14812.

Russell, D. W. (2003). The enzymes, regulation, and genetics of bile acid synthesis. Annu Rev Biochem *72*, 137-174.

Saarem, K., and Pedersen, J. L. (1985). 25-Hydroxylation of 1α-hydroxyvitamin D-3 in rat and human liver. Biochim Biophys Acta *840*, 117-126.

Sambrook, J., and Russell, D. W. (2000). Molecular Cloning: A Laboratory Manual., 3rd edn (Plainview, NY, Cold Spring Harbor Laboratory Press).

Sambrook, J., and Russell, D. W. (2001). Molecular Cloning: A Laboratory Manual., 3rd edn (Plainview, NY, Cold Spring Harbor Laboratory Press).

Sansone, G., and Hamilton, J. G. (1969). Glyceryl ether, wax ester and triglyceride composition of the mouse preputial gland. Lipids *4*, 435-440.

Schneider, R. J., and Shenk, T. (1987). Impact of virus infection on host cell protein synthesis. Ann Rev Biochem *56*, 317-332.

Schwarz, M., Lund, E. G., Lathe, R., Bjorkhem, I., and Russell, D. W. (1997). Identification and characterization of a mouse oxysterol 7α-hydroxylase cDNA. J Biol Chem *272*, 23995-24001.

Schwarz, M., Lund, E. G., and Russell, D. W. (1998). Two 7α-hydroxylase enzymes in bile acid biosynthesis. Current Opinion Lipidol *9*, 1-6.

Schwarz, M., Lund, E. G., Setchell, K. D. R., Kayden, H. J., Zerwekh, J. E., Bjorkhem, I., Herz, J., and Russell, D. W. (1996). Disruption of cholesterol 7α-hydroxylase gene in mice. J Biol Chem *271*, 18024-18031.

Schwarz, M., Wright, A. C., Davis, D. L., Nazer, H., Bjorkhem, I., and Russell, D. W. (2000). Expression cloning of 3β-hydroxy-Δ^5-C$_{27}$-steroid oxidoreductase gene of bile acid synthesis and its mutation in progressive intrahepatic cholestasis. J Clin Invest *106*, 1175-1184.

Setchell, B. P., and Waites, G. M. H. (1975). The blood-testis barrier. In Handbook of Physiology, R. O. Greep, and E. B. Astwood, eds. (Washington, D. C., American Physiological Society).

Setchell, K. D., Suchy, F. J., Welsh, M. B., Zimmer-Nechemias, L., Heubi, J., and Balistreri, W. F. (1988). Δ^4-3-oxosteroid 5β-reductase deficiency described in identical twins with neontal hepatitis. A new inborn error in bile acid synthesis. J Clin Invest *82*, 2148-2157.

Setchell, K. D. R., Balistreri, W. F., Piccoli, D. A., and Clerici, C. (1990). Oral bile acid therapy in the treatment of inborn errors in bile acid synthesis associated with liver disease. In Bile Acids as Therapeutic Agents: From Basic Science to Clinical Practice, G. Paumgartner, A. Stiehl, and W. Gerok, eds. (Dordrecht, Kluwer), pp. 367-373.

Setchell, K. D. R., and O'Connell, N. C. (1994). Inborn Errors of Bile Acid Metabolism. In Liver Disease in Children, F. J. Suchy, ed. (St. Louis, Mosby), pp. 835-851.

Setchell, K. D. R., and O'Connell, N. C. (2001). Disorders of bile acid synthesis and metabolism: A metabolic basis for liver disease. In Liver Disease in Children, F. J. Suchy, R. J. Sokol, and W. F. Balistreri, eds. (Philadelphia, Lippincott Williams & Wilkins), pp. 701-734.

Setchell, K. D. R., Schwarz, M., O'Connell, N. C., Lund, E. G., Davis, D. L., Lathe, R., Thompson, H. R., Tyson, R. W., Sokol, R. J., and Russell, D. W. (1998). Identification of a new inborn error in bile acid synthesis: mutation of the oxysterol 7α-hydroxylase gene causes severe neonatal liver disease. J Clin Invest *102*, 1690-1703.

Simoni, R. D., Hill, R. L., and Vaughan, M. (2002). Classics. J Biol Chem *277*, e8-9.

Skrede, S., Bjorkhem, I., Kvittingen, E. A., Buchmann, M. S., Lie, S. O., East, C., and Grundy, S. (1986). Demonstration of 26-hydroxylation of C27-steroids in human skin fibroblasts, and a deficiency of this activity in cerebrotendinous xanthomatosis. J Clin Invest *78*, 729-735.

Snyder, F., and Blank, M. L. (1969). Relationships of chain lengths and double bond locations in O-alkyl, O-alkyl-1-eny, acyl, and fatty alcohol moieties in preputial glands of mice. Arch Biochem Biophys *130*, 101-110.

Sparkes, I. A., and Baker, A. (2002). Peroxisome biogenesis and protein import in plants, animals and yeasts: enigma and variations? Mol Membr Biol *19*, 171-185.

Strautnieks, S. S., Bull, L. N., Knisely, A. S., Kocoshis, S. A., Dahl, N., Arnell, H., Sokal, E., HDahan, K., Childs, S., Ling, V.*, et al.* (1998). A gene encoding a liver-specific ABC transporter is mutated in progressive familial intrahepatic cholestasis. Nat Genet *20*, 233-238.

Su, P., Rennert, H., Shayiq, R. M., Yamamoto, R., Zheng, Y., Addya, S., Strauss, J. F., III, and Avadhani, N. G. (1990). A cDNA encoding a rat mitochondrial cytochrome p450

catalyzing both the 26-hydroxylation of cholesterol and 25-hydroxylation of vitamin D3: Gonadotropic regulation of the cognate mRNA in ovaries. DNA Cell Biol *9*, 657-665.

Tai, M. H., Chirala, S. S., and Wakil, S. J. (1993). Roles of Ser(101), Asp(236), and His(237) in Catalysis of Thioesterase-Ii and of the C-Terminal Region of the Enzyme in Its Interaction with Fatty-Acid Synthase. Proc Natl Acad Sci U S A *90*, 1852-1856.

Takeyama, K., Kitanaka, S., Sato, T., Kobori, M., Yanagisawa, J., and Kato, S. (1997). 25-Hydroxyvitamin D3 1α-hydroxylase and vitamin D synthesis. Science *277*, 1827-1830.

Thacher, T. D., Fischer, P. R., Pettifor, J. M., Lawson, J. O., Isichei, C. O., and Chan, G. M. (2000). Case-control study of factors associated with nutritional rickets in Nigerian children. J Pediatr *137*, 367-373.

Thai, T. P., Heid, H., Rackwitz, H. R., Hunziker, A., Gorgas, K., and Just, W. W. (1997). Ether lipid biosynthesis: isolation and molecular characterization of human dihydroxyacetonephosphate acyltransferase. Febs Letters *420*, 205-211.

Thody, A. J., and Shuster, S. (1989). Control and function of sebaceous glands. Physiol Rev *69*, 383-416.

Touchstone, J. C. (1992). Practice of Thin Layer Chromotography, Third edn (New York, John Wiley & Sons).

Trauner, M., Meier, P. J. M., and Boyer, J. L. (1998). Molecular pathogenesis of cholestasis. New England J Med *339*, 1217-1227.

Tvrdik, P., Westerberg, R., Silve, S., Asadi, A., Jakobsson, A., Cannon, B., Loison, G., and Jacobsson, A. (2000). Role of a new mammalian gene family in the biosynthesis of very long chain fatty acids and sphingolipids. J Cell Biol *149*, 707-717.

Usui, E., Noshiro, M., and Okuda, K. (1990). Molecular cloning of cDNA for vitamin D_3 25-hydroxylase from rat liver mitochondria. FEBS Lett *262*, 135-138.

Wakil, S. J., Stoops, J. K., and Joshi, V. C. (1983). Fatty-Acid Synthesis and Its Regulation. Annu Rev Biochem *52*, 537-579.

Wallis, J. G., Watts, J. L., and Browse, J. (2002). Polyunsaturated fatty acid synthesis: what will they think of next? Trends Biochem Sci *27*, 467-473.

Wang, A., Xia, Q., Xia, W., Dumonceaux, T., Zou, J., Datla, R., and Selvaraj, G. (2002). Male gametophyte development in bread wheat (*Triticum aestivum* L.): molecular, cellular, and biochemical analyses of a sporophytic contribution to pollen wall ontogeny. Plant J *30*, 613-623.

Whitfield, G. K., Selznick, S. H., Haussler, C. A., Hsieh, J.-C., Galligan, M. A., Jurutka, P. W., Thompson, P. D., Lee, S. M., Zerwekh, J. E., and Haussler, M. R. (1996). Vitamin D receptors from patients with resistance to 1,25-dihydroxyvitamin D_3: point mutations confer reduced transactivation in response to ligand and impaired interaction with retinoid X receptor heterodimeric partner. Mol Endocrinol *10*, 1617-1631.

Wikvall, K. (1984). Hydroxylations in biosynthesis of bile acids. J Biol Chem *259*, 3800-3804.

Willy, P. J., Umesono, K., Ong, E. S., Evans, R. M., Heyman, R. A., and Mangelsdorf, D. J. (1995). LXR, a nuclear receptor that defines a distinct retinoid response pathway. Genes Dev *9*, 1033-1045.

Witzleben, C. L., Piccoli, D. A., and Setchell, K. D. R. (1992). Case 3. A new category of causes of intrahepatic cholestasis. J Pediatr Path *12*, 269-274.

Wykle, R. L., Malone, B., and Snyder, F. (1979). Acyl-CoA reductase specificity and synthesis of wax esters in mouse preputial gland tumors. J Lipid Res *20*, 890-896.

Yamasaki, T., Izumi, S., Ide, H., and Ohyama, Y. (2004a). Identification of a Novel Rat Microsomal Vitamin D3 25-Hydroxylase. J Biol Chem *279*, 22848-22856.

Yamasaki, T., Izumi, S., Ide, H., and Ohyama, Y. (2004b). Identification of a novel rat microsomal vitamin D_3 25-hydroxylase. J Biol Chem *279*, in press.

Zehnder, D., Bland, R., Walker, E. A., Bradwell, A. R., Howie, A. J., Hewison, M., and Stewart, P. M. (1999). Expression of 25-hydroxyvitamin D_3-1α-hydroxylase in the human kidney. J Am Soc Nephrol *10*, 2465-2473.

Zerwekh, J. E., Glass, K., Jowsey, J., and Pak, C. Y. (1979). An unique form of osteomalacia associated with end organ refractoriness to 1,25-dihydroxyvitamin D and apparent defective synthesis of 25-hydroxyvitamin D. J Clin Endocrinol Metab *49*, 171-175.

Zhang, M. Y., Wang, X., Wang, J. T., Compagnone, N. A., Mellon, S. H., Olson, J. L., Tenehouse, H. S., Miller, W. M., and Portale, A. A. (2002). Dietary phosphorous

transcriptionally regulates 25-hydroxyvitamin D-1α-hydroxylase gene expression in the

proximal renal tubule. Endocrinology *143*, 587-595.

Ziegler, G. A., Vonrhein, C., Hanukoglu, I., and Schulz, G. E. (1999). The structure of

adrenodoxin reductase of mitochondrial P450 systems: Electron transfer for steroid

biosynthesis. J Mol Biol *289*, 981-99

VITAE

Jeffrey Binyan Cheng was born in Washington D.C., on September 15, 1975, the son of Chi-Miin Cheng and Michael Cheng. After completing his work at Northgate High School, Walnut Creek, California in 1993, he entered the University of California at Berkeley. He received the degree of Bachelor of the Arts with a major in Molecular and Cell Biology from UC Berkeley in May, 1997. The following year he was employed as a research associate in the laboratory of Dr. Kathleen Collins at UC Berkeley. In July, 1998 he entered the Medical Scientist Training Program at the University of Texas Southwestern Medical Center at Dallas. As a member of the Genetics and Development graduate program, he conducted his dissertation research in the laboratory of David W. Russell, Ph.D.

Permanent Address: 2600 Cole Ave. #324
                        Dallas, TX 75204